

Decarbonizing Brazil's Power Sector: High-Resolution Simulation and Lifecycle Emissions Analysis of a 100% Renewable Grid

Gabriel Fonseca Oliveira Roma - 61427

Trabalho realizado sob a orientação de
Prof^ª Dr. Ângela Paula Ferreira
Prof. Dr. Géremi Gilson Dranka

Mestrado em Engenharia Eletrotécnica e de Computadores

2024-2025

Decarbonizing Brazil's Power Sector: High-Resolution Simulation and Lifecycle Emissions Analysis of a 100% Renewable Grid

Dissertação de Mestrado

Mestrado em Engenharia Eletrotécnica e de Computadores

Escola Superior de Tecnologia e Gestão

Gabriel Fonseca Oliveira Roma - 61427

2024-2025

A Escola Superior de Tecnologia e de Gestão não se responsabiliza pelas opiniões expressas neste relatório.

Declaro que o trabalho descrito neste relatório é da minha autoria e é da minha vontade que o mesmo seja submetido a avaliação.

Gabriel Fonseca Oliveira Roma - 61427

Dedicatória

Dedico este trabalho à minha família, que sempre acreditou em mim e me ajudou a seguir em frente nos momentos difíceis — especialmente ao meu pai Celso, à minha mãe Joseane e ao meu irmão Daniel.

Agradecimentos

Agradeço a minha amiga Joesili pela sua ajuda na revisão, ao professor Géremi e à professora Ângela pelo apoio durante todo o processo e, principalmente, por acreditarem em mim mesmo nos momentos em que eu duvidei.

Resumo

À medida que o mundo acelera os esforços para combater as alterações climáticas, a transição para sistemas eléctricos totalmente renováveis tornou-se um objectivo crucial, especialmente para economias emergentes. Este trabalho explora a viabilidade de um sistema eléctrico 100% renovável no Brasil até 2050, através de simulações de alta resolução utilizando o modelo EnergyPLAN e uma Avaliação do Ciclo de Vida (ACV) probabilística das tecnologias renováveis consideradas. Ferramentas tradicionais de planeamento energético e estratégias nacionais de longo prazo tendem a subestimar ou ignorar as emissões indirectas de gases com efeito de estufa (GEE) associadas ao ciclo de vida das tecnologias renováveis — incluindo construção, fabrico, manutenção e desmantelamento —, que podem alterar significativamente o perfil ambiental dos cenários futuros. Assim, são necessárias abordagens integradas de modelação que combinem simulações detalhadas com análises ambientais robustas. A metodologia adoptada inclui modelação operacional horária baseada nas projecções do Plano Nacional de Energia (PNE 2050) e a construção de um Ano Meteorológico Típico (TMY) para representar perfis realistas de geração. Foi elaborado um inventário detalhado de emissões indirectas de GEE para centrais hidroeléctricas, eólicas, solares fotovoltaicas, biomassa e nucleares, complementado por uma simulação de Monte Carlo para capturar incertezas. Os resultados indicam que uma rede 100% renovável poderá ainda emitir, em média, 30,8 MtCO₂eq/ano devido às emissões indirectas. A inclusão de sistemas combinados de armazenamento energético poderá reduzir as necessidades de importação de electricidade de 19,87 TWh para 8,8 TWh, aumentando a capacidade do sistema para lidar com a variabilidade sazonal. Estes resultados reforçam a viabilidade técnica da transição e evidenciam a importância do investimento estratégico em armazenamento e da contabilização ambiental rigorosa.

Palavras-chave: energia renovável, planeamento energético, avaliação do ciclo de vida, simulação de Monte Carlo.

Abstract

As the world accelerates efforts to combat climate change, transitioning to fully renewable electricity systems has become a critical objective, particularly for emerging economies. This work explores the possibility of a 100% renewable electricity system in Brazil by 2050 through high-resolution simulations using the EnergyPLAN model and a probabilistic Life Cycle Assessment (LCA) of renewable technologies. Traditional energy planning tools and national strategies often underestimate or overlook indirect GHG emissions across life cycles—construction, manufacturing, maintenance, and decommissioning—which can significantly alter the environmental profile of future scenarios. Integrated modelling approaches are thus needed to ensure the path to decarbonization is both technically feasible and environmentally robust. The methodology includes hourly operational modelling based on projections from the National Energy Plan (PNE 2050) and the construction of a Typical Meteorological Year (TMY) to reflect realistic generation profiles. A detailed inventory of indirect GHG emissions for hydropower, wind, solar PV, biomass, and nuclear was assembled, and a Monte Carlo simulation was performed to capture uncertainty. Results show that a fully renewable grid could still emit 30.8 MtCO₂eq/year due to indirect emissions. The inclusion combined energy storage systems could drop imports needs from 19.87 TWh to 8.8 TWh, enhancing the system’s ability to manage seasonal variability. These findings underscore the technical feasibility of a 100% renewable grid in Brazil, while also highlighting the importance of strategic investments in storage infrastructure and the need for robust environmental accounting. The study concludes that a successful transition will require coordinated public policy, improved demand forecasting, and ongoing evaluation of both technical constraints and environmental trade-offs.

Keywords: renewable energy, energy planning, life cycle assessment, Monte Carlo simulation.

Contents

1	Introduction	1
2	Theoretical Background	8
2.1	The Brazilian Electricity System and Long-Term Planning	8
2.1.1	Historical Evolution and Renewable Energy Sources	8
2.1.2	Energy Planning Instruments (PNE 2050 & PDE)	8
2.1.3	Demand Projections and Strategic Scenarios	9
2.2	PNE 2050: Assumptions, Strategies, and the 100% Renewable Scenario	11
2.2.1	Strategic Methodology and Governance Principles	11
2.2.2	Energy System Structure and Key Assumptions	12
2.2.3	Renewable Technology Pathways and Systemic Challenges	13
2.3	Energy System Modelling Approaches and Tools	15
2.4	The EnergyPLAN Model	18
2.4.1	Data Input Structure	19
2.4.2	Dispatch Priorities and Internal Logic	20
2.5	EnergyPLAN Electricity Dispatch Model	20
2.5.1	Must-Run Generation Sources	20
2.5.2	Variable Renewable Energy Sources Generation	21
2.5.3	Energy Storage Dynamics	21
2.5.4	Thermal Power Plant Activation	22
2.5.5	Cross-Border Electricity Exchange	22
2.6	Life Cycle Assessment and Carbon Footprint	23
2.7	Deterministic versus Probabilistic analysis	23
2.8	Monte Carlo Method	25
2.8.1	Monte Carlo Simulation for Emissions Modelling	26

3	Methodology	28
3.1	Research Design and Methodological Framework	28
3.2	EnergyPLAN’s model validation	31
3.2.1	Methodology of Model Validation	31
3.3	Typical Meteorological Year	31
3.3.1	Data Acquisition and Preprocessing	31
3.4	Statistical Modelling of Indirect Emissions for Renewable Technologies	34
3.4.1	Data Collection and Literature Review	34
3.5	Renewable Energy Sources Life Cycle Inventory Analysis	37
3.5.1	Wind Power	37
3.5.2	Solar PV	39
3.5.3	Hydropower	41
3.5.4	Biomass Power	43
3.5.5	Nuclear Power	45
4	Input Data for the 2050 100% RES grid scenario	47
4.1	Electricity Demand	47
4.2	Variable Renewable Energy Sources and Capacity Factors	48
4.3	Central Power Production	50
4.4	Biomass	51
4.5	International Interconnection	52
4.6	Energy Storage Systems (ESS)	52
4.6.1	Pumped Hydro Energy Storage	53
4.6.2	Green Hydrogen Storage	53
4.6.3	Lithium-Ion Battery Storage	54
4.7	Critical Excess of Electricity Production and Curtailment	55
5	Results and Discussion	56
5.1	EnergyPLAN Validation Outputs	56
5.1.1	Validation Metrics and Comparative Analysis	56
5.1.2	Daily and Hourly Validation Challenges	57
5.1.3	EnergyPLAN’s Applicability	58
5.2	TMY Profiles for EnergyPLAN Modelling	58

5.3	Statistical Characterization of Emission Profiles and Monte Carlo Simulation for RES	60
5.3.1	Wind Power: Emission Profile and Monte Carlo Analysis	60
5.3.2	Solar PV: Emission Profile and Monte Carlo Analysis	64
5.3.3	Hydropower: Emission Profile and Monte Carlo Analysis	67
5.3.4	Biomass Power: Emission Profile and Monte Carlo Analysis	71
5.3.5	Nuclear Power: Emission Profile and Monte Carlo Analysis	75
5.4	EnergyPLAN Simulation of the 100% RES Grid	79
5.4.1	Scenario 1: Simulation with TMY-Based Capacity Factors and without ESS	80
5.4.2	Scenario 2: Simulation of Potential Generation Using PNE-Based Capacity Factors	81
5.4.3	Scenario 3: Simulation with Grid Operation Constraints and PHES	82
5.4.4	Scenario 4: Integration and Sensitivity Analysis of Lithium Battery and Green Hydrogen Storage	88
5.4.5	Final Scenario: Full Storage System Integration	95
5.5	Monte Carlo Analysis of Indirect CO ₂ eq Emissions from RES in the Final Scenario	96
6	Conclusions	100
6.1	Limitations and future research	101
	Bibliography	103
A		A2

List of Tables

2.1	Overview of most used energy planning tools [1]	16
4.1	Installed Capacity by Source in 2050	49
4.2	Expected Electricity Generation by Source in 2050	50
5.1	Validation metrics for TMY profiles of each energy source	59
5.2	Goodness-of-fit metrics for wind emission distributions	61
5.3	Descriptive statistics of Monte Carlo simulation	62
5.4	Goodness-of-fit metrics for PV emission distributions	64
5.5	Descriptive statistics of PV Monte Carlo simulation	66
5.6	Goodness-of-fit metrics for hydro emission distributions	68
5.7	Descriptive statistics of Hydropower Monte Carlo simulation	69
5.8	Goodness-of-fit metrics for biomass emission distributions	72
5.9	Descriptive statistics of Biomass Monte Carlo simulation	73
5.10	Goodness-of-fit metrics for nuclear emission distributions	76
5.11	Descriptive statistics of Nuclear Monte Carlo simulation	77
5.12	Scenario 1: Comparison between EnergyPLAN simulation results and EPE's PNE 2050 projections for annual generation without correction factor	80
5.13	Comparison of Capacity Factors between TMY and PNE 2050	82
5.14	Comparison between EnergyPLAN simulation results (adjusted CF) and PNE 2050 projections	82
5.15	Comparison between EnergyPLAN results with grid constraints and PHES, and PNE 2050 projections	83
5.16	Annual electricity imports (TWh) as a function of lithium-ion storage power capacity (GW) and energy capacity (GWh).	89

5.17	Annual electricity imports (TWh) as a function of hydrogen storage system configuration — electrolyzer/fuel cell power capacity (GW) and storage energy capacity (GWh).	93
5.18	Comparison between the final scenario results and PNE 2050 values for electricity generation and system balance.	96
A.1	Life Cycle Assessment Data for Wind Power Technologies	A2
A.2	Life Cycle Assessment Data for Photovoltaic Technologies	A6
A.3	Life Cycle Assessment Data for Hydropower Technologies	A9
A.4	Life Cycle Assessment Data for Wind Power Technologies	A10
A.5	Life Cycle Assessment Data for Nuclear Power Technologies	A12
A.6	EnergyPLAN simulation input data	A15
A.7	Gaussian curvature (K) values computed from the avoided electricity import surface $Z(x, y)$. This curvature indicates the inflection region where diminishing returns begin with increasing storage capacity.	A16
A.8	Hessian determinant (H) values computed from the avoided electricity import surface $Z(x, y)$ for the hydrogen storage system. These values approximate the local curvature and guide the identification of the True Knee Point. Included in Appendix A.8.	A18

List of Figures

3.1	Methodological workflow for scenario-based energy system modelling	29
3.2	United Nations Statistics Division (UNSD) geoscheme regional classification [2]. .	36
3.3	Lifecycle GHG emissions by electricity generation technology and region (2020) [3]	37
5.1	Probability density trace of wind emission values showing a modal concentration between 5-13 gCO ₂ eq/kWh	60
5.2	Quantile plot showing loglogistic distribution fit alongside other candidate distri- butions including Normal distribution	61
5.3	Frequency distribution with fitted loglogistic density curve compared to multiple distributions fit	62
5.4	Empirical distribution of simulated emissions showing loglogistic fit.	63
5.5	Cumulative distribution function for Wind Power.	63
5.6	Probability density trace of solar PV emission values in gCO ₂ eq/kWh	64
5.7	Quantile-quantile plot showing Weibull distribution fit with comparison to alter- native distributions	65
5.8	Frequency distribution with fitted Weibull density curve alongside possible can- didates showing good agreement across all emission ranges	65
5.9	Empirical distribution of simulated PV emissions showing Weibull fit.	66
5.10	Cumulative distribution function for solar PV.	67
5.11	Probability density trace of hydro emission values showing a highly right-skewed distribution with most values below 20 gCO ₂ eq/kWh	68
5.12	Quantile plot showing lognormal distribution fit alongside other candidate distri- butions.	69
5.13	Frequency distribution with fitted lognormal density curve alongside possible can- didates showing good agreement across all emission ranges	69
5.14	Empirical distribution of simulated Hydropower emissions showing Lognormal fit.	70

5.15	Cumulative distribution function for Hydropower emissions.	71
5.16	Probability density trace of biomass emission values showing extreme range (-395.0 to 510.0 gCO ₂ eq/kWh)	71
5.17	Quantile plot showing smallest extreme value distribution fit alongside other candidate distributions.	72
5.18	Frequency distribution with fitted smallest extreme value density curve showing agreement across the extreme emission ranges	73
5.19	Empirical distribution of simulated Biomass emissions showing Smallest Extreme Value fit.	74
5.20	Cumulative distribution function for Biomass emissions.	75
5.21	Probability density trace of nuclear emission values showing concentration between 5-20 gCO ₂ eq/kWh	75
5.22	Quantile plot showing Gamma distribution fit alongside other candidate distributions.	76
5.23	Frequency distribution with fitted Gamma density curve showing good agreement across all emission ranges	77
5.24	Empirical distribution of simulated Nuclear emissions showing Gamma fit.	78
5.25	Cumulative distribution function for Nuclear emissions.	78
5.26	Hourly electricity generation and demand during a typical operational week for each season for Scenario 3.	85
5.27	Average monthly electricity imports throughout the year for Scenario 3.	86
5.28	Monthly capacity factor variation for each renewable energy source, showing seasonal trends and resource complementarity.	87
5.29	Isoline map of avoided electricity imports (TWh) as a function of energy storage capacity (GWh) and installed power capacity (GW) of Lithium-ion batteries, overlaid with technical gradient lines (∇Z). Two reference points are highlighted: the Early Threshold Point (100 GWh, 15 GW), located exactly on the $\nabla Z = 1.0$ gradient line, and the True Knee Point (60 GWh, 15 GW), identified by the Hessian determinant as the point of maximum curvature where the system begins to exhibit strong diminishing returns.	92

5.30	Three-dimensional surface of avoided electricity imports (TWh/year) as a function of energy storage capacity (GWh) and installed power capacity (GW) of Lithium-ion batteries. The surface illustrates the simulated system’s response to different infrastructure configurations. Two reference points are highlighted: the Early Threshold Point (red circle), where the benefit-to-effort ratio reaches $\nabla Z = 1.0$, and the True Knee Point (blue diamond), mathematically identified through the Hessian determinant as the location of maximum curvature, representing the most critical inflection in the system’s performance surface. . . .	92
5.31	Isoline map of avoided electricity imports (TWh) for the hydrogen storage system as a function of energy storage capacity (GWh) and electrolyser/fuel cell configuration (GW) of green hydrogen storage system. Technical gradient lines (∇Z) are overlaid. The Early Threshold Point (100 GWh, 15/15 GW), where $\nabla Z = 1.0$, and the True Knee Point (200 GWh, 20/40 GW), identified by Gaussian curvature analysis, are highlighted.	94
5.32	Three-dimensional surface of avoided electricity imports (TWh/year) for the hydrogen storage system. Axes represent energy storage capacity (GWh) and electrolyser/fuel cell configuration (GW) of green hydrogen storage system. The Early Threshold Point (red circle) marks the onset of diminishing returns ($\nabla Z = 1.0$), while the True Knee Point (black square) indicates the location of maximum curvature — the most significant inflection point in system performance.	94
5.33	Typical operational week for each season in the final scenario with all storage systems implemented.	97
5.34	Stacked histogram showing the distribution of life cycle specific CO ₂ eq emissions (gCO ₂ eq/kWh) by energy source after Monte Carlo simulation. Each coloured segment corresponds to a technology’s contribution to the total mix.	98
5.35	Probability density of total annual CO ₂ eq emissions (MtCO ₂ eq/year) for the 2050 fully renewable scenario. Results derived from 1,000,000 Monte Carlo simulations.	99
A.1	Monthly capacity factor comparison for Wind Power: TMY vs. Historical min, max, and average	A13
A.2	Monthly capacity factor comparison for Solar PV: TMY vs. Historical min, max, and average.	A13
A.3	Monthly capacity factor comparison for PCH Hydro: TMY vs. Historical min, max, and average.	A14

A.4	Monthly reservoir level comparison: TMY vs. Historical min, max, and average.	A14
A.5	Monthly capacity factor comparison for ROR Hydro: TMY vs. Historical min, max, and average.	A15
A.6	Share of annual electricity generation by source in the simulation with TMY-Based Capacity Factors and without ESS. All values are expressed in TWh/year.	A16
A.7	Hourly electricity generation and demand during a typical operational week for each season in the simulation with TMY-Based Capacity Factors and without ESS.	A17

List of Acronyms

CCS Carbon Capture and Storage. 45

DG Distributed Generation. 48

EPE Empresa de Pesquisa Energética. 2, 9, 47

GESEL Grupo de Estudos do Setor Elétrico. 53

GHG Greenhouse Gas. 24, 34, 42, 45

GWP Global Warming Potential. 42

GWP-100 100-year global warming potentials. 35

IEA International Energy Agency. 23

LCA Life Cycle Assessment. 4, 23–25, 34, 35, 38, 40, 42

LCI Life Cycle Inventory. 24, 34

LEAP Long-range Energy Alternatives Planning. 3

MCDA Multi-Criteria Decision Analysis. 4

MME Ministério de Minas e Energia. 2, 9

NDC Nationally Determined Contributions. 30

NTC Net Transfer Capacity. 22

ONS Operador Nacional do Sistema - National System Operator. 31

PCH Pequena Central Hidrelétrica - Small Hydropower Power Plant. 32

PDE Plano Decenal de Expansão de Energia. 9

PHES Pumped Hydro Energy Storage. 52, 79

PNE Plano Nacional Energético. 2, 6, 9–12, 28, 43, 45, 47

PNMC National Policy on Climate Change. 9

PV Photovoltaic. 4, 12, 13, 31, 34–37, 39

PVGIS Photovoltaic Geographical Information System. 31

PWR Pressurized Water Reactor. 45

RES Renewable Energy Sources. 2, 3, 5, 12, 19, 20, 23, 36, 46, 52, 58, 59

ROR Run-of-river. 42

SOC state-of-charge. 21

TMY Typical Meteorological Year. 32, 59

UNCED United Nations Conference on Environment and Development. 9

UNSD United Nations Statistics Division. xiv, 36

VRES Variable Renewable Energy Sources. 6, 20, 21

Chapter 1

Introduction

In the past few decades, climate change has led to major changes in energy production, the way energy is used, economic policies, and laws. This transformation is supported by international agreements, growing advancements in green technologies and expanding use of electricity in different areas. As nations strive to create zero-carbon methods, energy systems are increasing in complexity and including more intermittent energy sources such as solar and wind. However, indirect emissions from life cycle processes, such as manufacturing and decommissioning, can compromise the carbon neutrality of renewable systems.

Therefore, long-term energy planning plays an essential role in increasing the system's resilience, affordability and sustainability. Such planning must take into account not only the technical constraints but also for uncertainties related to climate variability, demand growth and technological development. This is especially critical and necessary for developing countries, where infrastructure developments happens rapidly, investment decisions have long-term implications and the effects of climate change impacts are often more severe and immediate.

In this context, Brazil emerges as a key actor in South America's energy transition. The influence of these impacts is predicted to be significant, since the country heavily uses renewable sources that can be easily affected by changes in natural resources and the climate. Therefore, it is crucial to consider climate projections and their results when planning the electricity sector for the long term, so that systems can operate even when faced with adversity.

Currently, Brazil emerges as the leading energy producer (59%) in South America [4] [5]. Projections indicate a steady increase in electricity demand across the continent in the coming decades, largely attributable to its comparatively low per capita consumption (1,871 kWh per year) - approximately one third of the average in countries such as Portugal, Spain and Italy, which is around 5,500 kWh per year [6].

Riva et al. [7] state that effective energy planning involves a complex and detailed decision-making process in order to elaborate strategies to better allocate energy resources. The process must review a wide set of variables, such as technical feasibility, economic viability, social impacts, and impacts on the environment. Also, for energy planning to be effective, one must consider and predict upcoming energy needs to ensure resources will not be wasted or overused.

In this regard, energy planning tools play a crucial role in supporting the analysis and decision-making of energy analysts and policymakers in the energy sector. These tools make it possible to evaluate future impacts related to the integration of new energy sources into the power sector and to carry out scenario-based studies, including assessments of greenhouse gas (GHG) emissions and other key issues [8].

There is a wide range of energy planning software solutions on the market, such as TIMES, OSeMOSYS, MESSAGE, MARKAL, and EnergyPLAN. Because of their distinct functionalities, benefits, and limitations, each of these tools allows energy analysts and policy makers to pick one that fits their unique needs and analysis [9] [10] [11] [12].

In Brazil, the Ministry of Mines and Energy (in Portuguese, – Ministério de Minas e Energia (MME) in collaboration with the Energy Research Office (in Portuguese, – Empresa de Pesquisa Energética (EPE)), organized the National Energy Plan (in Portuguese, – Plano Nacional Energético (PNE)) [13] to forecast the possible expansion solutions for the energy expansion projects in the country by the year of 2050. According to the PNE 2050, the demand for energy could grow by as much as 2.2 times the current level, under similar development conditions. The projection shows that there is a pressing need to introduce such policies as sustainability is becoming vital for production and consumption.

The energy sector often faces challenges due to the complex and unpredictable nature of interrelated factors such as political, cultural, ecological, and technological aspects [14]. The fact that these elements are interconnected and difficult to forecast makes it hard to predict their combined effects accurately. This difficulty is further increased by the long time span involved in scenario planning, which adds to the risks and uncertainties in producing reliable future forecasts.

Dranka et al. [15] point out that the intermittent nature of RES such as photovoltaic solar and wind power leads to many operational issues. According to authors, this variation introduces levels of difficulties to keep the electricity system stable. Grids powered by low-inertia energy sources are more likely to face disturbances and instabilities, primarily due to the absence of supplementary control networks capable of enhancing system inertia. Therefore, Renewable

Energy Sources (RES) tend to hinder system inertia and bring down the system's overall stability. Increasing the amount of RES in the system weakens the effectiveness of voltage and frequency control systems. The decrease in quality negatively influences the transient and steady-state behaviour of voltage and frequency in power systems [16].

At the same time, to develop a robust energy scenario, it is required a flexible approach that accounts for a complex interconnection within energy systems. These scenarios must incorporate the potential for unexpected changes and include strategies to effectively respond to challenges and uncertainties that might come in the future.

The study of Andrade Guerra et al., [17], uses Long-range Energy Alternatives Planning (LEAP) to look ahead and research Brazil's energy future, by carrying out simulations for standard and improved nuclear energy use as well as renewable energy. Renewable electricity is mainly generated in Brazil, where hydropower amounted to almost 90% in 2011, but the researchers point out that wind, solar, and biomass energy could greatly enhance its growth. While it is projected that the economy will experience a 67% increase in energy demand by 2050, mitigation strategies are now available that can help to cut down energy consumption by implementing renewable energy, boosting efficiency, and using sugarcane bagasse for power generation. Even so, transportation remains heavily dependent on fossil fuels, so new policies are still needed. Researchers suggest that Brazil can develop solar energy further and decarbonize its industry through international cooperation.

Dranka and Ferreira [18] present an essential model for forecasting the Brazilian electricity sector through their work with the EnergyPLAN simulation tool. The model performance was validated through 2016 operational data while future scenarios for 2050 were explored, particularly a comprehensive 100% renewable energy simulation. Detailed analysis demonstrates Brazilian technical capability to shift their electricity sector to an entirely renewable system, yet the findings reveal the necessity of building substantial extra capacity to handle changes in hydroelectric and wind power generation during different seasons. Furthermore, the analysis explores both the export opportunities of excess renewable energy and how to address technical challenges, environmental risks, and economic considerations of high renewable energy penetration.

In addition, the use of more renewable energy resources in local power systems has become a key interest for recent studies, particularly in South America. Moura et al. [19] present an overview of the integration of power systems in South America and detail the way Brazil helps promote exchanges of electricity across countries. The authors run the OSeMOSYS SAMBA

model to assess three different scenarios. A reference-based plan following national roadmaps, a scenario that unites area-wide hydropower plans, and one that focusses on solar Photovoltaic (PV) and biogas plants. The analysis points out that Brazil could spend less on domestic energy plants by generating power in foreign countries, but big hydro projects in the Amazon carry both environmental and social risks. In addition, the researchers use cooperative game theory and the Shapley value to determine the bargaining power of these countries, indicating that Argentina, Brazil, Paraguay, Peru, and Guyana have important roles as exporters or importers. This study underlines that cooperation among nations and the use of eco-friendly policies are necessary for the economy and the environment.

Complementing these assessments, Santos et al. [20] conducted evaluations of Brazilian power system transitions from 2015 to 2050 by integrating MESSAGE-Brazil energy modelling with Multi-Criteria Decision Analysis (MCDA) and Life Cycle Assessment (LCA) techniques. The researchers used MESSAGE-Brazil as their first step to create five simulation scenarios from baseline operations to low-carbon choices, followed by an LCA-Based MCDA framework assessment against 15 technical, economic, and environmental criteria. Historical decision-making focused on scenarios that integrated substantial wind power and biomass utility, as these options delivered effective price-performance ratios and sustainable results according to 33 stakeholder opinions. Importantly, the study used stringent sensitivity modelling to verify stakeholder preferences across numerous viewpoints, and its LCA section exposed essential lifecycle environmental details that are usually neglected in energy development plans. This research thus confirms how extensive assessment tools demonstrate their usefulness in advanced energy transition analyses by showing when renewable energy diversity outperforms dependence on fossil fuels.

Turning to broader international applications, Connolly, Lund, and Mathiesen present a comprehensive 100% renewable energy scenario for the European Union by 2050 using the Smart Energy System approach, modelled in EnergyPLAN. The study transitions from a business-as-usual baseline through nine strategic steps—including nuclear phase-out, heat savings, electric vehicle adoption, and sector integration—demonstrating how intermittent renewable penetration can exceed 80% without unsustainable bioenergy reliance. Key findings reveal that a fully renewable EU system would incur 10–15% higher costs than fossil-dependent alternatives but eliminate CO₂ emissions while creating 10 million jobs through localized investments. The analysis emphasizes cross-sectoral flexibility via district heating, thermal storage, and electrofuels for hard-to-decarbonize sectors, arguing that political and institutional barriers—rather than technical or economic feasibility—are the primary obstacles to implementation [21].

In a similar research, Franco and Salza [22] applied the EnergyPLAN tool to study strategies for higher use of renewable resources in Italy's energy sectors. It shows that controlling electricity at times of plenty renewable energy, such as from photovoltaics and wind, could be challenging, but also outlines the need for coordinated work among power, heat, and transport sectors. A number of scenario reviews reveal that renewable energy systems encounter technological difficulties, which can be resolved if three sectors put their efforts together through mutual opportunities. Integrated systems with heat and power, as well as electric vehicles, demonstrate increased power stability and lower use of primary energy. However, Italy must first upgrade its separate energy systems before using the coupled system. It shows that reaching high RES targets sustainably would depend on effective uses of hydro storage and demand-side management.

Building on this, using Denmark as a critical case, Lund evaluates the path toward renewable energy systems that generate 100% of electricity from wind power and energy efficiency methods combined with sector-linked operations. The examination outlines three vital elements for sustainable energy strategies, which combine production efficiency enhancements along with renewable fuel deployment instead of fossils and reductions in energy consumption on the demand side. Computer modelling with EnergyPLAN shows how Denmark can reach carbon neutrality through resolving major obstacles that centre on transport sector electrification with biofuels and wind power management by flexible CHP units. Moreover, the study demonstrates that the power system requires better flexibility capabilities and smart grid implementations alongside sectoral coordination systems to handle renewable power variation. Although technological and infrastructure hurdles exist, a supported strategy of policy action alongside technological progress demonstrates that fully renewable energy systems become achievable [23].

Fernandes and Ferreira [24] uses EnergyPLAN to model how Portugal can transition to a system without fossil fuels and lessen its dependency on foreign energy in Portugal. Four separate simulation models are built, one is the 2010 reference case, one follows the 2020 PNAER plan, one reflects the 2022 grid development strategy, and one assumes that all fossil fuels are replaced with 100% renewable generation. The research shows that it is technologically achievable for renewables to provide all the electricity, with wind and hydropower systems taking the lead in electricity production, whereas the grid needs to be developed much further to cope with sudden changes in demand. These systems might cost a lot in the beginning, but their longevity results in cheap running costs. Essentially, managing the stability of the power grid and recycling/using unused energy is now a main concern, which points to the importance of integrated storage

systems and mutual exchange of power from other countries.

In their research, Krajačić et al. [25], have proposed a strategy to produce an independent energy system in Croatia by adding smart energy storage and renewable sources, which can lower carbon dioxide emissions. H₂RES and EnergyPLAN are used by the research to analyze the movements of energy at the hourly level in various scenarios, especially looking at cooperation between pumped hydro storage, thermal storage, and electric vehicles when there is intermittent renewable energy. Based on the results, Croatia could use renewables in 78.4% of its energy, which would result in lowering emissions by 20 Mt of CO₂. Nevertheless, it is still difficult to reach full independence due to the way different sectors are currently using energy. The research makes it clear that because storage systems support grid stability and play a key role in integrating renewable energies, their high expenses should be dealt with. All these strategies highlight how strongly it is necessary to manage the flexibility of power plants, plan consumer use, and cooperate on grid development to optimize the smart grid usage of energy storage.

Despite Brazil having one of the world's most RES energy matrix, long-term plans often fails to adequately predict two critical challenges: (1) the operational complexities of integrating Variable Renewable Energy Sources (VRES) into a hydro-dominated system, and (2) the environmental impacts of renewable technologies, which are almost always considered zero because they do not produce CO₂ emissions during generation, but they do have a carbon footprint during their life cycle. Traditional deterministic models, such as those employed in the PNE 2050, struggle to quantify uncertainties tied to climate variability, technological evolution, and policy shifts, potentially leading to overoptimistic projections. In addition, because tools like TIMES and LEAP are excellent at reducing costs, their broad modelling period makes it harder for them to demonstrate hourly grid stability when high levels of VRES are present, which is a major issue in Brazil due to the seasonal variations of hydropower and the intermittency of renewables such as solar and wind.

Over the last few decades, the increasing concern of climate change and the global effort to achieve sustainable development has made it imperative to shift from fossil fuels to renewable energy systems. While Brazil has made great progress, planning for a fully renewable electricity future is not only a technical and economic challenge, it is also one of environmental responsibility. Indirect GHG emissions associated with renewable technologies across their life cycles are often significantly underestimated or even completely overlooked in traditional energy planning tools and long-term national strategies. Emissions from construction, manufacturing, maintenance, and decommissioning processes can substantially affect the environmental profile

of future scenarios. This growing need leads to the necessity of integrated modelling approaches that can combine high-resolution system simulations with probabilistic life cycle assessments to assure that the path to decarbonization is both technically feasible and environmentally robust.

The main objective of this dissertation is to investigate whether it is feasible for Brazil to create a 100% renewable electricity system by 2050 with high-resolution computer simulations and a probabilistic approach. For these purposes, the EnergyPLAN model is used to calculate the interaction of energy flows from RES, energy storage systems and cross-border electricity exchange all at the national level. To enhance the model's accuracy, historical data is used and a Typical Meteorological Year (TMY) is assembled for a better reflection of the expected behaviour of the system in a typical operational year. Also, statistical modelling and Monte Carlo simulations were included in this study to help estimate how much GHGs are indirectly linked to the five key electric generation technologies used in this 100% RES Grid scenario, which includes wind, solar PV, hydropower, biomass and nuclear power. Furthermore, this dissertation aims to suggest enhancements to Brazil's National Energy Plan, especially in energy storage systems since the current plan does not offer much detail or explicit guidance on the role, scale and types of storage that could be used.

Chapter 2

Theoretical Background

2.1 The Brazilian Electricity System and Long-Term Planning

2.1.1 Historical Evolution and Renewable Energy Sources

In Brazil, most of the energy is produced through hydroelectric power plants, which predominantly take advantage of river waterfalls on plateau terrains. In 2019, this type of plant accounted for 68% of the installed capacity of the Brazilian electricity matrix, whereas around 30 years ago, it represented more than 95% of the electricity supply. Wind energy accounted for 9%, followed by natural gas and biomass, both with an 8% share [26].

Despite the still significant presence of hydroelectric plants in the Brazilian electricity matrix, this source has been gradually losing its share in the national generation park. Data from the 2009 and 2019 editions of the Energy Balance show that in ten years, the share of installed hydroelectric capacity in the national electricity matrix dropped from 81.9% in 2008 to 66.6% in 2018 [27] [28].

During the same period, wind energy grew from negligible levels to 7.6% in 2018. Additionally, the share of thermoelectric power, considering the set of plants powered by oil derivatives, natural gas, biomass, and nuclear, increased from 18.2% to approximately 25.2% of total supply [27] [28].

2.1.2 Energy Planning Instruments (PNE 2050 & PDE)

This study adopts its methodological approach based on the analytical structure described in Brazil's National Energy Plan for 2050 (*in Portuguese, Plano Nacional de Energia 2050*) [13] which serves as Brazil's primary tool for energy planning. The PNE 2050 emerged from

systematic evidence-based development to become Brazil's fundamental concept for analysing future energy routes while addressing future uncertainties.

After being developed through a rigorous multi-year process involving the MME and the EPE, and following several technical analyses and meetings with stakeholders and experts, the document was officially published in 2020. The PNE 2050 utilizes a multiple scenario planning as its basis because of the acknowledged uncertainties involved in a long-term energy forecasting. The plan recognizes that Brazil's future energy landscape will be shaped by the convergence of multiple dynamic factors, including pathways of economic development, trajectories of technological innovation, and evolving climate policy frameworks [29].

Regarding the electricity sector there are two main plans developed: one with a ten-year horizon Plano Decenal de Expansão de Energia (PDE) and another with a horizon of around 30 years, the National Energy Plan – PNE. While the PNE assesses trends in production and consumption, exploring strategies for expanding supply, the PDE primarily aims to indicate projects that will ensure short-term demand coverage [13].

In both the PDE and PNE studies, reference configurations ("base scenarios") and alternative scenarios are considered based on variations in demand or supply. Each configuration includes specific details [30] [31]. In the case of the PNE, each scenario is built upon distinct hypotheses about the future of the economy, society, public policies, technology, and consumer behaviour [13].

2.1.3 Demand Projections and Strategic Scenarios

In 1992, the United Nations Conference on Environment and Development (UNCED) was held in Rio de Janeiro with many countries, including the European Union. In that meeting, it was decided to keep holding conventions to discuss issues concerning the climate and human action to address them [32]. As a result of the conference, Brazil introduced Law No. 12.187, also known as the National Policy on Climate Change (PNMC), on December 29, 2009. The goal of the policy involves making sure there is low emissions of greenhouse gases when considering economic and social development. The National Energy Plan 2050 was conducted by the Brazilian government to explore how energy supply and demand would develop up to the year 2050 and was approved in December 2020.

The PNE 2050 consists of a set of recommendations and guidelines to be implemented throughout the time horizon up to 2050, using the decades from 2020 to 2050 as the temporal framework [13].

In operational terms, the projection model was based on the sectoral structure of the economy defined in each of the considered macroeconomic scenarios, with the first output being the value added by each sector in the economy. Thus, based on the annual GDP growth rate and the value added by industry, services, and agriculture, the share of each of these three major sectors was determined, along with their respective value added. The value added by each segment is an input variable for estimating sectoral energy consumption, which in turn is established in terms of useful energy demanded by use and by source [13].

In this process, the following were generally considered as independent variables:

- Physical production indicators, based on useful energy by end use and physical production of the segment;
- Share of a given energy source in a specific end use;
- Conversion efficiencies of useful energy into final energy or specific consumption of equipment and processes;
- Share of each technology in the production of a given product.

The PNE studies cover the broad range of uncertainties related to technologies, habits, behaviours, business models, regulation, and other factors through 2050 by means of two boundary scenarios, summarized by two trajectories of potential energy consumption evolution: the upper boundary scenario ("Expansion Challenge") and the "Stagnation" scenario [13].

Base Scenario

This is the main scenario, considered the most likely, with balanced and conservative assumptions, serving as a baseline for comparison with other scenarios. It incorporates:

- Moderate and stable economic growth.
- Public policies already implemented or highly probable.
- Technological evolution consistent with historical trends.
- Gradual increase in energy efficiency.
- Compliance with already assumed climate commitments.

Alternative Scenarios

These scenarios are used to test different combinations of variables and assess their impacts on the future energy system. They include:

- **High Economic Growth Scenario:** Faster GDP growth, higher energy demand, stronger investment.
- **Low Economic Growth Scenario:** Limited GDP growth, constrained demand and investments.
- **Accelerated Energy Transition Scenario:** Rapid renewables deployment, strong climate policies.
- **Inertial Scenario:** Business-as-usual, slow transition, weak climate policies.
- **Technological-Innovative Scenario:** Advances in efficiency, digitalization, EVs, smart grids.

2.2 PNE 2050: Assumptions, Strategies, and the 100% Renewable Scenario

2.2.1 Strategic Methodology and Governance Principles

The first sections of the PNE 2050 discuss key principles that direct the development of Brazil's energy strategy. The principles in place carefully align the development of the economy with technological means to address climate problems as guided by adaptive leadership. According to the approach, energy planning remains adaptable, while the Prologue underlines the need to respond to fluctuations such as trouble with politics, innovative advancements, and unpredictable situations such as the caused by COVID-19.

The starting point for scenario-based methodology is to develop two main scenarios, known as the Expansion Scenario and the stagnation scenario, that we discussed earlier. The Prologue points out that such scenarios do not predict the future, but instead help analyze decision-making in different scenarios, especially when dealing with unexpected events like pandemics or global crisis of energy sources.

The Introduction explains that the strategy consists of three steps: developing, implementing, and monitoring. The five-year periodic reviews of the plan required under Portaria n.

6/2020 [33] aim to catch up on new changes and updated data due to new social and political circumstances and advancing technology. The main expectation of the plan is based on Brazil having so much RES such as wind power, solar, hydropower and biomass that it can provide more power than is projected to be required because of the rapid growth predicted in the section. It further underlines that Brazil's policy on energy is aligned with global climate objectives, mainly through the Nationally Determined Contribution (Brazil NDC 2024) [34].

In the Introduction, the document lays out ten governance principles such as technological neutrality, precaution, and sustainability to ensure things are carried out effectively. These ten principles support promoting markets, authority decentralization, horizontal sharing of benefits, and making sure not to favor one technology over another. To illustrate, the principle of precaution forbids supporting only particular technologies, as it suggests picking strategies by the results achieved, rather than the technology, which supports the feasibility of the 100% Renewable Grid sub-scenario examined in this thesis.

2.2.2 Energy System Structure and Key Assumptions

Under the Expansion Challenge Scenario mentioned earlier, the PNE 2050 predicts that electricity use will reach 2,100 TWh each year by 2050. Economic and urban progress, along with building more electric grids, are expected to increase demand by 3.5% per year. Therefore, more than 80% of centralized power will come from renewable energies (RES), with main sources including hydropower, wind energy, and solar. Hydropower currently supplies 70% of energy, but extra development is blocked due to both environmental and social constraints. There are 12 GW of hydropower with new facilities outside protected regions, and the maximum can rise to 52 GW by developing hydropower in both protected and unprotected lands such as indigenous and quilombola territories and conservation units. The study will concentrate on the 12 GW scenario that excludes protected areas as it is seen as the best approach for sustainable growth.

The framework regards wind power and solar power as workable at all scales, but solar PV and onshore wind are given a low level of difficulty. Nevertheless, since solar and wind power both intermittent and dependent on the weather, there is an ongoing need for investments in grid flexibility equipment, such as storage systems and technology for improved grid management. The plan still relies on the hydropower as the primary source of electricity production, highlighting a strategic dependence on its legacy infrastructure, while variable renewables remain secondary in grid stability control.

The research premises point out major problems in the PNE 2050 electricity sector plan,

which illustrates the need for on-going policy adjustments. Brazil's ability to use its strong renewable energy sources reliably depends on the continued shift in grid infrastructure and how it operates. The assumptions act both as the base for developing grid flexibility models and informing policy evaluations when analysing the 100% Renewable Grid sub-scenario.

Hydroelectric systems are a key power source for Brazil, but the country is also interested in developing other renewable sources of energy. Although it is possible to produce solar and wind power on a big scale in the country, the existing power grid is mainly set up for hydropower and could cause operational difficulties in the future.

Grid stability and control of frequency drifts in Brazil depend on the high rotational inertia given by its hydropower and thermal power plants. More renewables being linked to grids via inverters causes the natural system inertia to fall, which creates new problems for grid operators.

Because of their rotating masses, traditional synchronous generators can quickly adjust and control the frequency in the power system during disturbances. However, solar PV and wind turbines that use power electronics to connect with grids do not automatically give the grid inertia. Studies have shown that the wind-dominated facilities in the Northeast region of Brazil create inertia reductions, so dedicated control measures are needed [35].

Strict regulations also form significant barriers in the market. As things stand today, it is difficult for decentralized power sources to get fair recognition and contribute to better grid flexibility. Because of the clear regulations in the power sector, investors tend to avoid backing storage projects for electricity grids. The strategy for separating distribution and commercialization in the plan is strong in theory but requires careful planning and a smooth transition.

Technological dependencies create another vulnerability. The renewable energy transition of Brazil depends on foreign imports and technical expertise to operate advanced storage solutions and smart grid technologies. In order to make this transition the energy sector is dependent heavily on foreign rare earth minerals, which in turn leads to issues with supply chains and rising costs, and complicates the timeline and possibility of completing the shift [36].

2.2.3 Renewable Technology Pathways and Systemic Challenges

The Brazilian energy transition will heavily rely on its hydropower resources. The PNE highlights to possible paths to explore: the first one, exploring the countries' restricted 12 GW estimated potential or extend to 52 GW with projects in areas that are currently considered environmentally vulnerable by the Brazilian legislation, such as indigenous and quilombola lands or environmental reserves. Under the first scenario, the system costs are elevated in approximately

3.5%, because the system will require extra backup power for generation. Alternatively, the second option will require a change in current legislation before hydropower resources can be explored. In cases of extremely dry periods such as the one experienced in Brazil in 2021 might decrease the supply reliability, which calls for additional solutions.

According to the plan, wind power stands as the most promising technology to be explored in future years, specially in the Northeast region, that is expected to generate about 20% of the entire system electricity by 2050. Analysis demonstrate that the wind power can hold up to a remarkable 20% of grid stability share through its foreseeable electricity output patterns. However, the inverter-based nature of modern wind turbines suffer from a critical drawback since they lack rotational inertia which makes frequency regulation more difficult. Although the PNE recognizes this matter, it fails to establish specific solution to address this issue such as investing in synthetic inertia and battery-based frequency control systems. Similarly, solar PV is recognized as another source of attention, with projections of 85 GW of installed capacity, with a complemented by a 30 GW provided by distributed generation (DG), but it is still viewed as a limited resource to expand due to the limited contribution during evening peak demand, restricting its share of generation to 12%.

The plan's approach to dealing with system flexibility are however reveals assumptions that must be criticality investigated. In the 100% RES Grid scenario, Biodiesel-fired generation occupies a central role as a complementary source to the system, with a projected 85 GW of installed capacity by 2050. The reliance on biodiesel generation appears to be unrealistic and unjustifiable, given that Brazil has little biodiesel energy and no country has adopted systems at this scale, making it a theoretical solution convenience than a practical pathway for grid balancing [37].

While the plan suggests that other options can replace the biodiesel generators, there is not enough exploration of actual substitutes present in the analysis. It is a weakness in the planning process that making doubtful selections for renewable power and sustainable solutions does not match with Brazil's current abilities or energy needs. The plan omits looking closely at performance metrics of battery storage, pumped hydro, and hydrogen-based systems that are emphasized as possible plans to replace biodiesel. Unspecified alternatives for flexibility in energy resources leaves a major hole in planning, as it makes it difficult for policymakers and others to get solid information for comparing performance.

2.3 Energy System Modelling Approaches and Tools

The computational simulation of energy systems is used as a standard way to look at long-term energy projections. Energy system analysis has two main ways to model things: top-down and bottom-up, and these each have their own benefits and problems [38] [39].

Top-down models look at energy systems by incorporating parts of the bigger economy, like GDP growth, industry productivity, and price responsiveness, to help predict how much energy will be needed in the markets [40] [39]. The models use things like how much the country's GDP grows, how productive each sector is, and how sensitive prices are to production levels to figure out how much energy will be used in the market. The approach uses rules in economics to look at how energy markets change when the economy changes and uses math based on past data to connect energy and market trends [40]. The main advantage of this method is that it looks at how broader economic changes can affect the way markets work after prices change, even when other ways to model the energy market don't focus on this sort of thing. These models show how changes in energy prices affect different groups in society and how resources move around after something happens in the market by looking at how the economy works overall.

The bottom-up approach relies on a technology-specific framework which builds energy system representations by considering their physical engineering specifications. Detailed technical specifications regarding power plant performance curves together with fuel characteristic data and grid transmission losses and end-use device penetration levels feature in these models. Da Silva et al. [41] explain how bottom-up models deliver better analysis resolution because they properly depict energy system elements and how they relate to one another. Increased data requirements and higher complexity during computations become major challenges when modelling extensive systems which contain many interconnected components.

Energy system models follow basic operational approaches for their classification which exists within these major categories, i.e., simulation and optimization-based approaches. Simulation-based tools employ operational analysis through models built with precise energy system time intervals which approach both hourly and shorter periods [42]. These mathematical models deliver exceptional value when evaluating technical renewable energy possibilities because they understand the operational characteristics between supply-demand balance and switching conditions in combination with power grid operational restrictions [43]. Simulation methods deliver their essential strength by mimicking real system functioning without needing any specified

notions about optimum performance output [44]. However, this comes at the cost of not automatically identifying least-cost solutions or efficient policy pathways.

On the other side, optimization models employ mathematical programming techniques to identify optimal system configurations according to specified objective functions and constraints. Most optimization models reduce total system expenses while satisfying predetermined energy requirements together with specific policy standards [45]. The optimization models identify effective long-term energy pathways yet deliver solutions which might encounter obstacles from political structures along with social institutions and institutional frameworks during practical implementation [46].

The choice between these methodological approaches depends critically on the research questions being addressed. Top-down models are particularly well-suited for analysing the macroeconomic impacts of broad energy policies, such as carbon pricing mechanisms or energy subsidy reforms [44]. Their economy-wide perspective enables assessment of how energy system changes might ripple through market options, trade patterns, and income distribution. Bottom-up models, by contrast, are indispensable for analysing the technical and engineering aspects of energy system transitions, including the infrastructure requirements for renewable energy integration, the operational challenges of balancing variable generation, and the technology-specific impacts of energy efficiency measures [43].

Various computational tools exist in the field of energy system modelling because they aim to solve distinct analytical problems for overall energy planning and policy research. The multiple computational tools designed for energy system modelling differ based on their fundamental approach and their operational features as well as their real-world uses which reflect complex energy system issues.

Seven widely used tools are compared in Table 2.1 using categories that include developer, model type, and analytical approach. These analyses reveal basic conflicts between optimization-focused tools and simulation-based systems as well as possible combinations between these approaches.

Table 2.1: Overview of most used energy planning tools [1]

Tool	Developer	Model Type	Category	Period	Scale
MARKAL	IEA-ETSAP	Bottom-up	Optimization	20-50 yr	Global
EnergyPLAN	Aalborg Univ.	Bottom-up	Simulation	1 yr	National
LEAP	SEI	Top-down	Simulation	20-50 yr	Global
HOMER	NREL	Bottom-up	Optimization	1 yr	Community
MESSAGE	IIASA	Bottom-up	Optimization	Up to 100 yr	Global
OSeMOSYS	KTH/IIASA	Hybrid	Optimization	10-100 yr	National

MARKAL (Market Allocation) [10] functions as one of the original optimization tools that gained substantial acceptance for energy system analysis. The Energy Technology Systems Analysis Program under International Energy Agency developed MARKAL via bottom-up optimization techniques using linear programming methods to find cost-effective technology pathways subject to certain restrictions. The model achieves its strength through its precise modelling of conversion technologies while it evaluates extended energy paths covering multiple sectors [47]. The coarse time resolution along with restricted system operation modelling in MARKAL has motivated the creation of more sophisticated successors including the TIMES model.

EnergyPLAN provides users with a simulation-based alternative through its development at Aalborg University [48]. The bottom-up tool performs simulation of integrated energy systems at an hourly resolution for systems with substantial variable renewable energy components [49]. A detailed operational model structure permits users to measure essential problems regarding renewable energy resource restraint while evaluating storage needs and inter-sectoritious integration capabilities. The open nature of this system along with its transparent approach drives academic and policy institutions to frequently use it across national energy system examinations.

The Long-range Energy Alternatives Planning (LEAP) system under the Stockholm Environment Institute operation provides an adaptable framework capable of conducting both top-down and bottom-up analyses [50]. LEAP excels because its scenario analysis functions combine with a simple interface thus enabling users like developing country policymakers to easily access its analysis features. Substantial energy-environment-emissions analysis capabilities exist within the tool because of its integrated accounting structure even though it provides less technical sophistication than dedicated analytical programs [51].

The HOMER (Hybrid Optimization Model for Multiple Energy Resources) software created by NREL examines micro-grid and distributed energy system analysis [52]. HOMER represents an effective bottom-up optimization software designed to analyse hybrid renewable energy systems through technical and economic feasibility assessment especially for off-grid and weak grid situations. The technology evaluation process enabled by HOMER helps optimize energy system combinations which makes it useful for planning rural electrification projects and island energy systems [53].

MESSAGE (Model for Energy Supply Strategy Alternatives and their General Environmental Impact) developed by International Institute for Applied Systems Analysis stands as a key bottom-up optimization tool which uses the Model for Energy Supply Strategy Alternatives and their General Environmental Impact [54]. The main strength of MESSAGE comes from

its ability to analyse energy-economy-environment relationships at various spatial and temporal levels [55]. MESSAGE serves as a leading tool which scientists apply to create energy scenarios globally as well as locally for international climate policy development.

OSeMOSYS (Open Source Energy Modelling System) functions today as a fundamental open-source replacement choice for proprietary energy optimization systems [56]. The hybrid model came into being through joint collaboration between IIASA and its partner institutions and synchronizes detailed bottom-up technologies with simplified macroeconomic elements. The structure of modular units and transparent coding in OSeMOSYS attracts developing countries for academic research because of its capacity-building potential [11].

TIMES (The Integrated MARKAL-EFOM System) represents the current state-of-the-art in energy system optimization modelling [57]. As the successor to MARKAL, TIMES incorporates enhanced technological detail, improved temporal resolution, and more sophisticated treatment of energy demand [9]. The model's ability to generate cost-optimal decarbonization pathways while accounting for technology learning curves and resource constraints has made it a standard tool for national energy planning in many countries.

The selection process among these tools primarily relies on fulfilling different analytical needs of research queries. Optimization models such as TIMES and MESSAGE perform best for finding minimal cost transition routes, but often lack operational resolution, while EnergyPLAN excels at modelling systems that utilizes high levels of renewable energy for operational analysis [58]. The scale of analysis also influences tool selection, with HOMER being more suited to local-scale systems and MESSAGE to global assessments. Recent trends in energy system modelling emphasize the importance of open-source platforms, improved temporal resolution, and better integration of renewable energy variability - developments that are reshaping the field and informing ongoing model development efforts [59].

2.4 The EnergyPLAN Model

The selected analytical tool EnergyPLAN serves this study because it enables targeted analysis for the specific technical requirements of Brazil's power system which includes hydroelectric dominance and rising renewable power integration. EnergyPLAN stands above generalized energy system models which optimize broad economic analysis by delivering operational details to assess physical system realities when renewable energy reaches high penetration levels [60]. Brazil faces critical operational challenges because its intricate hydropower management meets

intermittent renewable power generation requirements in ways that typical modelling techniques are unable to reproduce effectively [18].

EnergyPLAN serves as a fixed-simulation program which analyses complete energy system networks at country or regional levels to study renewable power integration. Refined analysis of electrical power generation and consumer demand and grid stability is manageable through the hourly simulation periods used by EnergyPLAN's mathematical system. The following segment provides insights into the processing mechanism of the software through detailed examination of electricity sector needs relevant to this analysis. This analysis evaluates the input data parameters together with mathematical algorithms and dispatch methodologies of EnergyPLAN along with the validation procedures it employs. The research draws information from the EnergyPLAN official documentation [48] together with Lund et al.'s EnergyPLAN – Advanced analysis of smart energy systems [12] and Østergaard et al.'s Review and validation of EnergyPLAN [61]. The three primary sources have established the technical basis for understanding EnergyPLAN's structure and modelling capabilities for smart energy systems.

2.4.1 Data Input Structure

The simulation of electricity systems by EnergyPLAN depends on precise establishment of necessary input elements. The model takes in three different types of data identified as static parameters together with time-dependent distributions as well as operational constraints. The model requires static input data which includes the capacity of all existing power plants along with annual electricity demand in TWh/year and connecting power line capacity for energy import and export.

The dynamic system behaviour becomes fully tangible through time-dependent distributions. Electricity demand follows hourly load profiles while renewable resources such as wind speed and solar irradiation together with river flow (for run-of-river hydroelectric plants) exist as hourly distributions.

Operational constraints help to specify how the model operates. The model incorporates three operational guidelines through priority rules to manage dispatch among sources and determine storage capacity usage and protocols for curtailing surplus RES. EnergyPLAN develops an extensive depiction of the electricity system when all available inputs are integrated to support scenario analysis and long-term planning. Through its modelling process EnergyPLAN allocates sufficient energy supplies for each hour during the annual period while making sure to prioritize RES in preferred operational conditions.

2.4.2 Dispatch Priorities and Internal Logic

EnergyPLAN implements a clear dispatch mechanism for its energy supply sources which enhances grid stability by using fewer fossil fuels. The procedure defined in the official EnergyPLAN manual guides the dispatch operations through the following order:

1. **Must-Run Sources:** Nuclear and run-of-river hydroelectric plants deliver their complete operational capacity because their power output either requires fixed operations or depends on natural upstream conditions.
2. **VRES:** The output from wind and solar generators gets priority according to current resource conditions such as wind velocity and solar radiation levels.
3. **Storage Discharge:** The deployment of energy storage systems such as hydrogen technology and pumped hydro solutions serves to support times when renewable power generation fails to satisfy total energy requirements.
4. **Dispatchable Sources:** Thermal power generation begins its operations when RES with storage reach their complete capacity depletion point to balance supply versus demand.
5. **Import/Export:** The remaining power imbalances are resolved either through power import or export operations which depend on transmission line capacity limits.

2.5 EnergyPLAN Electricity Dispatch Model

EnergyPLAN executes dispatch simulations through a step-by-step operational sequence that operates on an hourly basis. This mathematical system incorporates physical boundaries together with operational requirements and efficiency factors into its framework. The following section describes the governing equations along with variable definitions alongside their physical interpretations in detail.

2.5.1 Must-Run Generation Sources

The inflexible nature of nuclear and run-of-river hydroelectric power plants requires them to maintain their maximal technical production levels despite varying demand. Hourly generation output calculations for these sources are as follows:

$$E_{\text{nuclear}}(h) = C_{\text{nuclear}} \cdot \delta_{\text{nuclear}}(h) \quad (2.1)$$

$$E_{\text{hydro_run}}(h) = C_{\text{hydro_run}} \cdot \delta_{\text{hydro_run}}(h) \quad (2.2)$$

The nuclear power technology accounts for both installed nuclear capacity C_{nuclear} in megawatts (MW) and hourly capacity factor $\delta_{\text{nuclear}}(h)$ that faces restrictions from maintenance schedules and refuelling cycles. The hourly capacity of nuclear facilities before scheduled outages typically operates at levels between 0.90 to 0.95. The rated maximum capacity of run-of-river hydro plants is identified by $C_{\text{hydro_run}}$ while $\delta_{\text{hydro_run}}(h)$ represents historical river discharge information normalized to the [0,1] interval. The plants experience limitations in rapid generation adjustments because environmental flow regulations make them behave like mandatory continuous operation assets.

2.5.2 Variable Renewable Energy Sources Generation

Variable Renewable Energy Sources are dispatched after must-run plants, with possible curtailment during overproduction:

$$E_{\text{VRES}}(h) = \sum_{i=1}^N (C_{\text{VRES}_i} \cdot \delta_{\text{VRES}_i}(h) \cdot \text{FAC}_{\text{curtail}}(h)) \quad (2.3)$$

Installed capacity values C_{VRES_i} define the operational capacity of technology i . At the same time $\delta_{\text{VRES}_i}(h)$ represents normalized resource availability over one hour. The calculation of wind turbine availability $\delta_{\text{wind}}(h)$ depends on the cube of wind speed $v^3(h)$ at hub level while considering cut-in ($v_{\text{cut-in}} \approx 3$ m/s) and cut-out ($v_{\text{cut-out}} \approx 25$ m/s) speed constraints.

Solar PV availability $\delta_{\text{PV}}(h)$ uses manufacturer temperature coefficients to calculate the plane-of-array irradiance levels. Grid stability depends on the curtailment factor $\text{FAC}_{\text{curtail}}(h)$ activating during overgeneration conditions ($E_{\text{total}}(h) > D_{\text{total}}(h) + C_{\text{transmission}}$) to manage VRES output linearly from 1 to 0.

2.5.3 Energy Storage Dynamics

Storage systems discharge to meet residual demand, with state-of-charge (SOC) dynamics governed by:

$$E_{\text{discharge}}(h) = \min \left(\frac{\text{SOC}(h-1)}{\Delta t}, C_{\text{discharge}}, D_{\text{residual}}(h) \right) \quad (2.4)$$

$$\text{SOC}(h) = \text{SOC}(h-1) - \frac{E_{\text{discharge}}(h)}{\eta_{\text{discharge}}} \cdot \Delta t + E_{\text{charge}}(h) \cdot \eta_{\text{charge}} \cdot \Delta t \quad (2.5)$$

The state-of-charge, $\text{SOC}(h)$ (in MWh), evolves hourly based on three physical limits: (1)

energy availability from the previous hour ($\text{SOC}(h-1)$); (2) maximum discharge rate $C_{\text{discharge}}$ (MW), dictated by power electronics and conversion systems; and (3) residual demand $D_{\text{residual}}(h) = D_{\text{total}}(h) - \sum E_{\text{generation}}(h)$ after prior dispatch steps. The process of charging occurs in surplus conditions when $E_{\text{total}}(h) > D_{\text{total}}(h)$ using electrolysis with a charging efficiency $\eta_{\text{charge}} \approx 0.70$ and discharging loses power due to fuel cell conversion at $\eta_{\text{discharge}} \approx 0.55$. The discrete 1-hour time-step ($\Delta t = 1$) maintains uniformity between units of energy measured in MWh and power expressed in MW.

2.5.4 Thermal Power Plant Activation

Conventional thermal plants activate only when renewable and storage resources are insufficient:

$$E_{\text{thermal}}(h) = \min(C_{\text{thermal}}, D_{\text{residual}}(h)) \quad (2.6)$$

The maximum available thermal generation capacity C_{thermal} measures MW power in size but can be limited by operational restrictions and maintenance schedules. The $D_{\text{residual}}(h)$ term shows the unmet electricity requirement for hour h after considering all demand provided by sources other than thermal generation.

The optimization finds the minimum required thermal generation $E_{\text{thermal}}(h)$ that satisfies both the physical unit limits and all remaining unmet electrical demand. Thermal generation acts as a supplement to fulfil unmet electricity needs but operates within its rated capability.

2.5.5 Cross-Border Electricity Exchange

Final system balancing occurs through interconnection lines:

$$E_{\text{import}}(h) = \min(\max(D_{\text{total}}(h) - E_{\text{total}}(h), 0), C_{\text{transmission}}) \quad (2.7)$$

$$E_{\text{export}}(h) = \min(\max(E_{\text{total}}(h) - D_{\text{total}}(h), 0), C_{\text{transmission}}) \quad (2.8)$$

The total power generation $E_{\text{total}}(h) = E_{\text{nuclear}} + E_{\text{hydro_run}} + E_{\text{VRES}} + E_{\text{discharge}} + E_{\text{thermal}}$ sums all supply sources alongside $C_{\text{transmission}}$ which includes Net Transfer Capacity (NTC) values adjusted for loop flows and contingency reserves. Power import and export decisions evaluate neighboring system marginal costs to derive prices which equal the variable costs of their last-dispatched thermal generation unit. Cross-border losses exist only through reductions applied to NTC values instead of using explicit loss factors.

2.6 Life Cycle Assessment and Carbon Footprint

According to ISO 14040/44 standards Life Cycle Assessment serves as the systematic “compilation and evaluation of the inputs, outputs, and potential environmental impacts of a product system throughout its life cycle” for measuring total emissions throughout each stage of technology development from raw material collection through disposal [62]. The LCA framework consists of four successive phases: (1) goal and scope definition, (2) inventory analysis, (3) impact assessment, (4) data interpretation. That enforce strict data quality criteria as well as system boundary rules and transparency standards for creating studies that stand as credible assessments among global researchers [63]. According to Kabayo et al. [64], renewable energy technologies display varying carbon footprint values, influenced by factors such as the geographic location of production, material composition, and specific technical characteristics.

National electricity-sector emissions inventories typically exclude indirect emissions that occur during the manufacturing and transportation processes of RES infrastructure construction along with the end-of-life disposal phase which leads to misclassification of renewable energy as zero-emission . The failure to incorporate complete environmental impacts through this oversight generates inaccurate policy decisions that fail to represent actual RES consequences. According to the International Energy Agency (IEA) Brazil’s electricity system demonstrates the importance of full life-cycle accounting because its operational cleanliness measures 97.2 gCO₂eq/kWh which is significantly lower than the global average of 480 gCO₂eq/kWh (2023 data) [65].

2.7 Deterministic versus Probabilistic analysis

Probabilistic LCA has gained increasing application in future electricity system assessment due to its ability to examine environmental uncertainties precisely. Research by Dale et al. [66] developed a Brazil electricity sector life-cycle model that combines the MESSAGE scenario data with Monte Carlo analysis technique to predict greenhouse gas emissions and environmental impacts across 2040. Brazil faces major environmental difficulties as it moves toward power diversification by identifying growing conflicts between renewable energy expansion and affected ecosystems according to their research results. The present research shares identical goals with this study since it wants to apply probabilistic assessment techniques for analysing high renewable penetration scenarios. This research develops more reliable impact assessments for upcoming power systems by using scenario-based modelling alongside Monte Carlo simulations

which enhances current frameworks for better energy transition resilience planning.

Chambile [67] uses Monte Carlo simulations to expand LCA applications for assessing carbon emission levels throughout national grid systems. Life-cycle emissions from generation and transmission systems are analysed in Kenya, Rwanda and Tanzania as his research examines different energy transition scenarios. The research uses stochastic methods in grid-level assessments to demonstrate how uncertainties around emission factors with technology mixes affect long-term decarbonization goals. The research used a Monte Carlo probabilistic modelling to track environmental impacts caused by big renewable energy additions.

Herbert et al. [68] develop a typology for world electricity production mixes to provide support in the creation of long-term Consequential Life Cycle Inventories (CLCI). The data analysis of 91 national electricity grid compositions combined with their lifetime Greenhouse Gas (GHG) emissions establishes categories of electricity systems based on intensity levels using percentile-based techniques for uncertainty reduction. The researchers analyse mix structure for their method instead of protocol models yet their work demonstrates why grid structure and emission impacts need evaluation in future electricity system LCA assessments. This typology develops a scalable macro-level framework which policy evaluators can use together with the assessment methods from the previous section to strengthen analysis in dynamic environmental studies of grid systems that adopt renewable energy.

Despite these important advances, the integration of complete life cycle assessments of renewable energy technologies into national grid emission forecasting remains limited in the current literature. Scenario modelling for future predictions includes minimal consideration of complete related impacts between renewable sources during the assessment of decarbonization routes. A new methodology will be presented in this thesis which systematizes the assessment of all emissions across renewable energy technology life cycles during scenario modelling of national grids. By explicitly accounting indirect environmental impacts, this method aims to improve the precision of future grid emission forecasts and to support more robust, sustainable energy transition planning.

The standard methodology of LCA generates one estimate of impact through a deterministic approach following material consumption-related and emission-related assignments [69]. Through this method input and output relationships stay constant because the process ignores all data uncertainties. Specialized Life Cycle Inventory (LCI) databases e.g. Ecoinvent [70] supply the required data through detailed records of resource use and emission release rates connected to the product system components and materials and manufacturing processes. The

standard procedure to handle uncertainty involves sensitivity analyses where practitioners modify single variables within realistic limits to track their effects on impact assessments [71]. Despite showing individual parameter importance the method cannot represent joint parameter uncertainties or their mutual interactions while also producing underestimate projections of future scenarios.

The steady approach adopted by Deterministic LCA encounters specific difficulties during examinations of upcoming renewable energy technology systems because it depends on unchangeable parameters. Emissions' important factors can evolve unpredictably when materials technologies, manufacturing, energetic, policy and components innovations [72]. The generated forecasts using deterministic methods fail to represent the true central value and potential outcomes correctly which misleads decision makers about their precision level. The resolution of this challenge will be achieved by implementing probabilistic models.

Probabilistic LCA represents uncertain input values by using probability distributions from empirical data and expert estimates which may be normal, lognormal, triangular, weibull or other types [73]. The most common method for conducting probabilistic LCA analyses utilizes Monte Carlo simulation which randomly selects thousands of model inputs from distribution sets to create statistical distributions of output results [74]. Probabilistic LCA measures both impact expectations as well as distribution certainty ranges and threshold-crossing probabilities with respect to policy targets. The method delivers refined views of uncertainty and risk levels beyond the capabilities of single-deterministic sensitivity evaluations [75].

This thesis employs probabilistic LCA techniques to estimate future emission profiles of various renewable electricity technologies. These profiles are then integrated into simulations of the Brazilian power sector. By applying Monte Carlo simulations, it is possible to generate distributions of life cycle carbon intensities ($\text{gCO}_2\text{eq/kWh}$) for the selected technologies, namely wind power, solar photovoltaic (PV), and hydroelectric energy, under multiple plausible policy and technological scenarios.

2.8 Monte Carlo Method

The Monte Carlo method represents a common computing tool for uncertain problem solutions particularly in applications where researchers cannot find mathematical solutions. Monte Carlo simulation uses random sampling to calculate system behaviour through repeated outcome evaluations from probabilistic variable inputs [76]. Through emissions modelling the method serves

to study multiple potential emission scenarios based on natural data variability found in the input lifecycles of various energy technologies. The technique is crucial in domains with indeterminable uncertainties because it establishes probabilistic outcome ranges which better mirror natural variability patterns [77].

The simulation method of Monte Carlo requires producers to generate numerous random samples from the distribution models for all input variables. During each iteration the selection of random values at specific points from distribution types indicates possible emission results for individual technologies. A model that represents total emissions combines the selected values for a particular energy mix calculation. Thousands of repetitions using this method create a distribution that shows possible total emission results [78].

The success of Monte Carlo simulations depends heavily on using appropriate probability distributions which properly represent input parameter uncertainties. The assignment of likelihood values across different random variable values by probability distribution models indicates which values the variable is expected to take. Distribution application in Monte Carlo modelling serves as a fundamental requirement that controls simulation behaviour because distribution selection determines how each input parameter plays out through generation range and frequency and outcome dispersion [79].

2.8.1 Monte Carlo Simulation for Emissions Modelling

Monte Carlo simulation is a versatile, probabilistic technique for propagating input uncertainties through complex environmental models. In LCA of energy systems, it enables the exploration of how variability in emissions factors—arising from differences in technology design, regional resource quality, supply-chain logistics, and methodological assumptions—affects aggregate GHG outcomes.

Let X_1, X_2, \dots, X_n denote the uncertain parameters of interest (e.g., life cycle emission factors in gCO₂eq/kWh) for n distinct energy technologies. Each X_j is characterized by a probability distribution P_j , which may be chosen according to data availability and expert judgment:

- **Parametric distributions** (e.g., Normal, Lognormal, Uniform, Triangular, Beta) when statistical moments or bounds are known;
- **Empirical distributions** derived directly from observed or meta-analytical datasets.

Certain heavy-tailed laws (e.g., Cauchy) lack finite moments, but remain tractable in a purely

empirical Monte Carlo framework.

The Monte Carlo algorithm proceeds as follows for $i = 1, 2, \dots, N$ iterations:

1. **Sampling:** Independently draw

$$X_j^{(i)} \sim P_j, \quad j = 1, 2, \dots, n. \quad (2.9)$$

2. **Aggregation:** Compute the total emissions output

$$E^{(i)} = f(X_1^{(i)}, X_2^{(i)}, \dots, X_n^{(i)}), \quad (2.10)$$

where f represents the system-level emissions model. In many energy-system applications,

$$E^{(i)} = \sum_{j=1}^n w_j X_j^{(i)}, \quad (2.11)$$

with weights w_j reflecting each technology's fractional contribution to total generation ($\sum_j w_j = 1$).

After N realizations, the collection $\{E^{(1)}, E^{(2)}, \dots, E^{(N)}\}$ constitutes an empirical distribution of possible emissions outcomes. When the input distributions admit finite moments, summary statistics can be estimated by:

$$\hat{\mu}_E = \frac{1}{N} \sum_{i=1}^N E^{(i)}, \quad \hat{\sigma}_E^2 = \frac{1}{N-1} \sum_{i=1}^N (E^{(i)} - \hat{\mu}_E)^2, \quad \hat{\sigma}_E = \sqrt{\hat{\sigma}_E^2}. \quad (2.12)$$

By yielding not only an expected value but also confidence intervals, probability percentiles, and tail-risk measures, this approach allows for robust integration of variability in emissions estimates, offering probabilistic insights into system-level behaviour. This probabilistic insight is essential for decision-makers to evaluate trade-offs, prioritize mitigation strategies, and design resilient, low-carbon energy portfolios [80, 81].

Chapter 3

Methodology

3.1 Research Design and Methodological Framework

Addressing energy system transitions in the 21st century requires a methodological approach capable of evaluating dynamic interactions between technological potential, policy constraints, and socio-economic trends. Scenario-based modelling and simulation frameworks have emerged as essential tools for analysing long-term energy strategies that balance reliability, sustainability, and economic feasibility.

The methodology is divided into four stages as depicted in Figure 3.1: (A) Scenario-based modelling of energy system according to PNE 2050 goals, (B) acquisition and verification of data from historical generation datasets from ONS and PDE 2023, (C) simulation of a 100% renewable grid scenario at hourly resolution using EnergyPLAN and (D) conclusions and recommendations for future scenarios. This systematic workflow ensures consistency with empirical data while addressing technical limitations, including hydropower flexibility and variable renewable integration.

Evaluating Brazil's future power system requires scenario-based and quantitative simulation frameworks. The analysis combines historical data about energy and economics combined with emissions evaluations, renewable resource forecasts, and regulatory constraints. The study aims to identify robust strategies that address national energy needs while aligning with global decarbonization principles.

This research evaluates Brazil's extended power system growth through scenario modelling and quantitative simulation frameworks that analyse shifting socio-economic and environmental boundaries. The research design adopts the analytical framework of PNE 2050 focusing on the

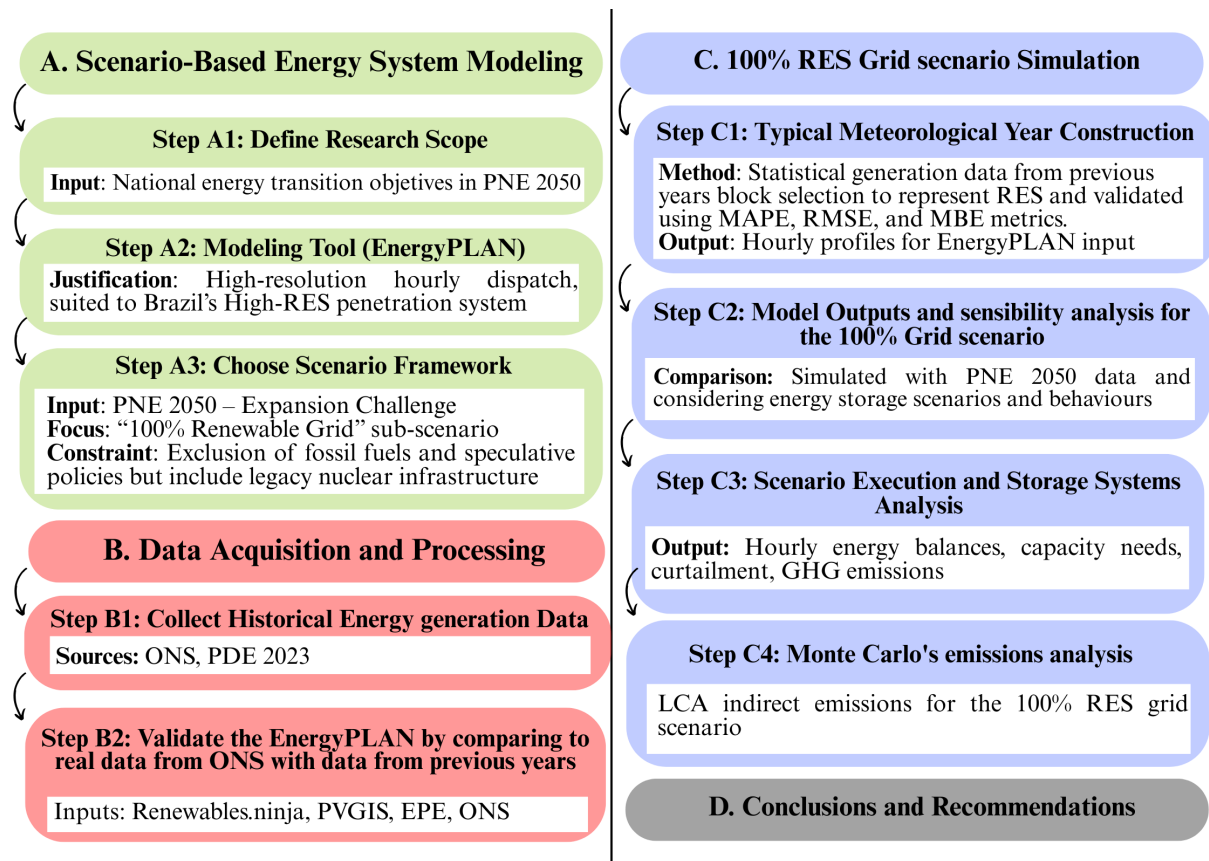


Figure 3.1: Methodological workflow for scenario-based energy system modelling

Expansion Challenge Scenario as the primary reference. A specific emphasis is placed on the sub-scenario "Matriz 100% renovável" (100% Renewable Grid) which investigates the feasibility of a fully renewable power generation system. This scenario is rooted in Brazil's regulatory and environmental context, applying current legislative standards rather than speculative future policies. The analysis deploys a demand-side framework, which merges historical energy consumption per GDP relationships with analysis of industrial as well as transport emissions alongside supply-side specifications regarding renewable resources' potential and limits involving hydroelectric constraints within sensitive regions coupled with wind energy distribution patterns [82].

The wide difference between Brazil's potential for RES and the estimated electricity demand is remarkable, when compared to the energy predicaments of the late 20th century. Historical data indicate that electricity consumption in Brazil has been increasing continuously even if in the short term economy experiences fluctuations [83]. This tendency is even visible in the opposite picture of future scenarios: the "Expansion Challenge" forecasts 2.5% annual growth, resulting in over 2100 TWh to 2050, and even the more cautious 'Stagnation' options still speculates about nearly 870 TWh [13]. These projections show that in Brazil, energy demand

continues to climb—whereas, in the past, the causes of crisis were largely infrastructure and supply constraints rather than slow demand.

However, this study excludes the analysis of the Stagnation Scenario due to its lack of empirical support. Historically, Brazil’s electricity demand has expanded consistently, even during economic downturns, making flat growth assumptions implausible [84]. Energy use data between 1980 and 2017 show that real GDP per capita and energy consumption exhibit a durable and positive relationship that results in a 0.38% increase in GDP for every 1% increase in energy use [13, 85]. A system with feedback characteristics contradicts the potential for economic expansion or growth under limited energy resources. The three arguments establish that the core assumptions of the Stagnation Scenario conflict with both empirical historical patterns and verified statistical correlations between energy consumption and economic output in Brazil.

The scenario’s validity depends on three policy constraints to follow Law 14,299/2022 which sets 85% renewable energy targets [86] together with Brazilian Nationally Determined Contributions (NDC) for a 48% emissions reduction against 2005 levels [87] and the need for environmental licensing. The scenario’s operating boundaries and regulatory importance are safeguarded through policy restrictions followed by the additional requirement in 100% Renewable Grid sub-scenario that entirely bans fossil fuel-based power generation.

A structured process with EnergyPLAN software executes the methodology to simulate Brazil’s hydro-dominant renewable system. EnergyPLAN performs hour-by-hour energy system operation simulations that highlight the relationships between hydro power production with variable renewable integration. The hourly resolution provides extensive assessment of operational problems affecting power stability and RES integration in Brazil’s hydro-based electricity system against its 100% Renewable Grid initiative. The operational model incorporates historical electricity records along with consumption patterns and current power generation resources for calibration purposes and obeys policy requirements.

The EnergyPLAN software is used to simulate Brazil’s hydro-dominant renewable system. This tool performs hour-by-hour operational simulations, making it especially well-suited to Brazil’s system characteristics. It enables evaluation of how VRES like wind and solar interact with flexible hydropower under operational constraints. EnergyPLAN’s selection is methodologically justified by its capacity to simulate high-resolution dispatch scenarios, which are often inadequately addressed in pure optimization models. Overall, this structured methodology ensures that planning assumptions remain grounded in empirical evidence while exploring technically feasible and policy-compliant routes toward Brazil’s long-term energy transition.

3.2 EnergyPLAN’s model validation

3.2.1 Methodology of Model Validation

The model validation process involved a systematic comparison between simulation outputs from EnergyPLAN simulation outputs and operational data Brazil’s National System Operator (ONS) [88]. A three-step research approach based on temporal resolution and technological specificity was adopted to reflect the diversity and operational complexity of the Brazilian power system.

The initial phase required extensive data acquisition from official documentation. Reference year 2022 hourly generation data for hydroelectric, wind, solar PV and thermal units were obtained from the ONS database [88]. These were supplemented by insights from Brazil’s Ten-Year Energy Expansion Plan (PDE 2023), which provided key information on spatial distribution, installed capacity, and capacity factors for different energy technologies [89].

Additional meteorological information supplemented renewable energy modelling to represent effectively the varying behaviour of variable generation. Wind power profiles were sourced from Renewables.ninja [90] platform present calibrated wind speed information specifically for Brazil’s northeastern geographical regions that host most wind farms [91]. Data for solar irradiation came from the European Commission Photovoltaic Geographical Information System (PVGIS) while considering regional specifications for solar power facilities in Bahia and Piauí and Minas Gerais states [92].

The modelling of hydropower systems proved difficult because Brazil operates a complicated network of connected water reservoirs mixed with river-based power plants. Analysis of operational reports and ONS schematic diagrams enabled researchers to divide the power generation facilities into reservoir-based and run-of-river types with a capacity ratio of 40.5% to 59.5%, respectively. River flow data was combined for the main river routes (Paraná-Uruguay and Amazon-Tocantins along with the East Atlantic-So Francisco) based on the main outlet pairs for input compatibility in EnergyPLAN but preserving the natural water stream patterns [88].

3.3 Typical Meteorological Year

3.3.1 Data Acquisition and Preprocessing

This analysis is based on high-resolution hourly electricity generation data and monthly installed capacity values extracted from the *Histórico da Operação* database housed by the Operator

Nacional do Sistema - National System Operator (ONS) in Brazil [88]. The major purpose of choosing this dataset and its associated methodology is to develop a more representative temporal profile of renewable and variable sources of energy that are extremely sensitive to the impact of meteorological and seasonal dynamics. To normalize the generation data, the capacity factor ($CF_{h,m}$) for each hour h in month m is calculated by dividing the hourly generation $G_{h,m}$ by the corresponding monthly installed capacity C_m :

$$CF_{h,m} = \frac{G_{h,m}}{C_m} \quad (3.1)$$

Instead of using a single year of data, which is meteorologically anomalous, or a year from the past that is not representative of a long-term trend, this work uses a construction of a Typical Meteorological Year (TMY) to construct a statistically robust year based on multiple historical years. This is particularly important since the subsequent analysis' simulation model, EnergyPLAN demands the hourly time series inputs for all variable sources. Thus, a TMY approach guarantees that such inputs are representative of normal operation patterns with essential short-term variability maintained in order to sustain better long-term scenario estimations.

The energy sources taken up for this study are run-of-river hydro electric generation, wind power, centralized PV generation, distributed PV generation, Pequena Central Hidrelétrica - Small Hydropower Power Plant (PCH) and reservoir levels for hydropower generation, the latter to serve as a proxy for inflow availability and the reservoir dynamics. In addition, seasonal availability of biomass was also introduced in the TMY construction. Biomass generation in Brazil may show substantial intra-annual variation because of agriculture cycles and regional harvesting patterns, and accordingly also includes a TMY representation. Every one of these sources is an integral part of the Brazilian energy mix and has a variable sensitivity/dependency on the weather and climate conditions affecting the energy sources to some degree justifying an appropriate synthetic year with representative statistical data as opposed to using direct raw historical data.

This resolution finds a compromise between representativeness of numbers from statistics and preservation of pattern dynamics particularly (wind, solar) where number of segments output could vary significantly even within days. As research by Zeng et al. [93] demonstrate, higher-resolution blocks may greatly help to enhance accuracy of typical year representations for system level modelling.

This thesis follows the proposed by [94] methodology for developing the Monthly block

structure of the Typical Meteorological Year (TMY). The study uses a statistical block selection method to construct a typical meteorological year, TMY. Contrary to the Sandia method that utilizes cumulative distribution function and the Finkelstein–Schafer statistic, this method places the emphasis on the minimization of normalized differences in mean and standard deviation over several years. This approach has proved useful in several studies for creating sample meteorological datasets [95,96]. This method is perceived as quite convenient and still effective for application such as those discussed in this thesis, which does not constitute the main focus of the research.

The process entails splitting the multi-year dataset into the fixed-size blocks pertaining to each of the months. The global mean (μ_g) and standard deviation (σ_g) for each block are obtained for all the years. After that, for each year, y , its mean (μ_y) and standard deviation (σ_y) for the same block are calculated. The error made in the estimation for every year is given by the following equation:

$$\text{Error}_y = \left| \frac{\mu_y - \mu_g}{\mu_g} \right| + \left| \frac{\sigma_y - \sigma_g}{\sigma_g} \right| \quad (3.2)$$

The minimum error year for each block, is selected to represent that block in the TMY. These chosen blocks are joined together in such a way that out of them a synthetic year is created which has statistical properties same as the long-term dataset.

After all representative blocks are chosen they are combined in order to generate synthetic year with 8,784 hourly data points. The derived TMY dataset is subsequently validated relative to the multi-year mean by means of the three most widely-used statistical metrics.

Mean Bias Error (MBE)

$$\text{MBE} = \frac{1}{n} \sum_{i=1}^n (\text{TMY}_i - \bar{CF}_i) \quad (3.3)$$

Root Mean Square Error (RMSE)

$$\text{RMSE} = \sqrt{\frac{1}{n} \sum_{i=1}^n (\text{TMY}_i - \bar{CF}_i)^2} \quad (3.4)$$

Mean Absolute Percentage Error (MAPE)

$$\text{MAPE} = \frac{100\%}{n} \sum_{i=1}^n \left| \frac{\text{TMY}_i - \bar{CF}_i}{\bar{CF}_i} \right| \quad (3.5)$$

3.4 Statistical Modelling of Indirect Emissions for Renewable Technologies

In order to accurately evaluate the 100% renewable electricity grid indirect GHG emissions it is needed to acknowledge and incorporate the inherent variability and uncertainty of emission factors reported in the literature. The $\text{gCO}_2\text{eq/kWh}$ emission factors exist as variable outcomes associated with regional manufacturing processes and lifecycle boundary definitions as well as technological implementations and analytical approaches. Statistical models prove effective for executives handling variant emission factors because they reveal all possible values ranges rather than focusing on fixed estimates which proves useful in forecast modelling. This section details the probabilistic approaches used to estimate emission profiles for the fundamental energy sources integrated into the scenario which includes solar PV, onshore and offshore wind, hydroelectricity, biomass and nuclear.

3.4.1 Data Collection and Literature Review

The first crucial aspect of this study focused on organizing documented GHG emission factors across all renewable electricity generation life cycle stages. The assembled dataset acts as a foundation for every model and uncertainty evaluation to follow. A methodologically strict procedure was necessary to build this information because it needed to maintain transparency and scientific validity and enable comparisons. The following section describes the systematic approach to locate GHG emission data in literature and the regional categorization method for analysing geographical variations.

The first data collection step involved conducting an extensive literature review dedicated to locating LCA research which quantifies GHG emissions from every used energy sources throughout their construction phase, operational period and decommissioning stages. The research examination spanned several academic literature and institutional databases made up of Scopus, Web of Science, Google Scholar combined with document collections from the International Energy Agency (IEA), Intergovernmental Panel on Climate Change (IPCC), and the National Renewable Energy Laboratory (NREL). Additionally, the analysis incorporated industrial reports together with technical manufacturing publications as well as Ecoinvent LCI. The wide assortment of sources delivered theoretical information combined with real-world evidence which reinforced the findings from the research.

The review included studies after 2002 but gave priority to research conducted after 2010

due to field advances in LCA methods while data improved procedures became standardized. The review included peer-reviewed academic articles together with trustworthy grey literature reports from government and research institutions that satisfied established methodological requirements.

The evaluation method for candidate studies included the following inclusion criteria for methodological consistency:

1. **Lifecycle Boundary:** At a minimum the study needed to establish a cradle-to-gate system boundary yet cradle-to-grave analyses which included material extraction and all stages up to end-of-life were preferred.
2. **Functional Unit:** The reporting system required the disclosure of emissions information based on units of electrical energy production measured through grams of CO₂-equivalent per kilowatt-hour (gCO₂eq/kWh).
3. **GHG Coverage:** The reported dataset should provide at least CO₂, CH₄, and N₂O emission information combined into CO₂-equivalent values by using standard 100-year global warming potentials (GWP-100).
4. **Transparency and Documentation:** Studies included only when they provided comprehensive information about modelling assumptions encompassing system lifetime, regional context as well as emissions calculation methods.

Research without adherence to these conditions together with exclusive hypothetical or poorly documented cases was excluded from the final dataset during the screening process. The filtering process established reliability which led to valid statistical analysis through suitable methodology.

The structured Microsoft Excel spreadsheet contains processed data collected from chosen sources as base information used for statistical modelling followed by subsequent sections' uncertainty quantification processes. Each study publication produced one dataset entry in this spreadsheet through its unique emission estimate. The system features data filtering capabilities which utilize technology, regional and methodological restrictions. Every data entry required the inclusion of the following fields:

- Technology Type (e.g., Mono-Si solar PV, Onshore Wind, Run-of-River Hydro)
- Emission Factor (gCO₂eq/kWh)

- Reference (Author(s) and publication year)
- Region of Deployment or Study Context
- Type of Research:
 - Scientific Literature and Peer-Reviewed Articles
 - Environmental and Energy Databases
 - International Organizations
 - Government and Industry Reports

To account for geographical variability in emission factors—driven by differences in regional grid mixes during component manufacturing, transportation logistics, construction methodologies, and supply chain practices—each dataset entry was classified into macro-regions following the (UNSD) geoscheme [2], as illustrated in Figure 3.2.



Figure 3.2: UNSD geoscheme regional classification [2].

The inclusion of worldwide lifecycle emissions data in Brazilian renewable energy investigations has methodological support because RES exhibit specific characteristics according to the UNECE Report on Integrated Life-Cycle Assessment of Electricity Sources [3]. According to the report operational parameter normalization reveals that RES emissions vary little between regions because their production procedures use standardized methods together with universal supplier networks which employ standardized technological specifications especially for solar PV and wind power technology no matter their regional location.

The UNECE report provides illustration of worldwide GHG emissions for electricity technology lifecycles in Figure 3.3. Wind and solar photovoltaic (PV) systems under RES demonstrate a minimal spread of emissions throughout every region. Emissions from wind energy (onshore

and offshore combined) fall between 7 and 21 gCO₂eq/kWh throughout all regions and similar results appear in solar PV poly-Si and CdTe ground-mounted system emissions which stay within 23–35 gCO₂eq/kWh. The methodological inclusion of international lifecycle benchmarks for wind and solar resources becomes justified for Brazil when conducting GHG assessment of their electricity generation strategies.

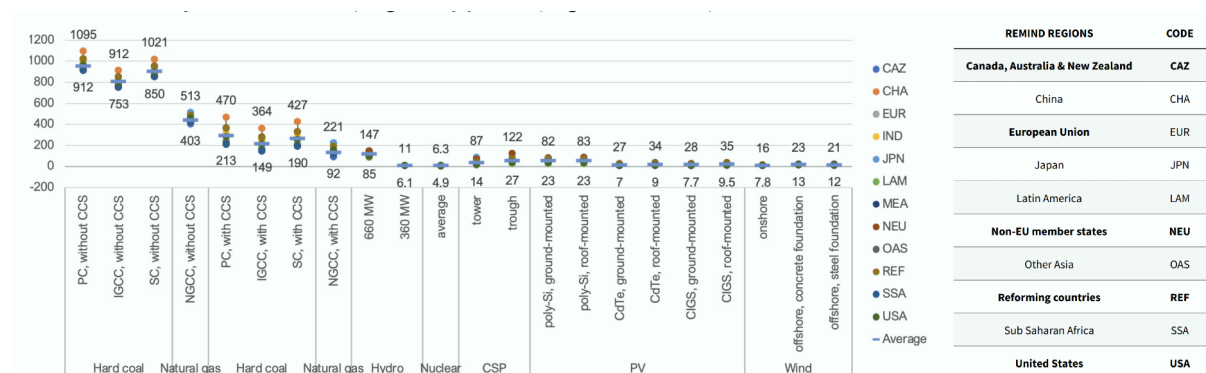


Figure 3.3: Lifecycle GHG emissions by electricity generation technology and region (2020) [3]

3.5 Renewable Energy Sources Life Cycle Inventory Analysis

3.5.1 Wind Power

The gathered LCI information about wind power technologies utilizes 70 data inputs from independent studies which originated from peer-reviewed literature, international organization reports and environmental databases. The dataset contains emission factor results measured in gCO₂eq/kWh that apply to onshore and offshore wind energy systems for standardized comparison. Data collection followed a systematic review methodology:

- **Sources:** 42 data from scientific articles (SLA), 24 from industry/government reports (IOG), and 5 from database (EED) entries
- **Temporal coverage:** 2002–2025 (with 68% of data from 2015–2023)
- **Geographic distribution:**
 - Global studies: 7 entries
 - European data: 38 entries
 - American data: 18 entries (6 from Brazil)

- Asian data: 7 entries
- African data: 4 entries

- **Technology breakdown:**

- Onshore wind: 47 entries (67.1%)
- Offshore wind: 18 entries (25.7%)
- Both technologies: 6 entries (8.6%)

The scarcity of LCA studies specific to Brazil required researchers to use international data to maintain strong statistical validity. Several technical reasons make the adopted approach scientifically valid as mentioned in the previous section. The wind energy market presents itself as an inherently global industry since Brazilian turbine installations operate under supply from worldwide major manufacturers including Vestas, Siemens Gamesa, GE, Acciona and WEG [97].

Transportation, often a concern in LCA studies, plays a negligible role in the overall emissions profile of wind energy systems. Detailed research shows that transportation accounts for less than 6% of total lifecycle emissions [98] where Brazilian manufacturing of towers and foundations necessitates minimal transportation (centralizing 70-80% of structural mass) [99]. For most Brazilian wind farms, only the nacelle and generator components - representing less than 20% of total system mass.

The environmental impact from modern wind turbines spanning 4-15 MW shows smaller than 10 % fluctuation in lifecycle emissions across multiple regions if researchers normalize results based on capacity factors [3]. Wind farms in Brazil's Class III areas persist within a comparable operational environment as global wind markets because they maintain capacity factors between 35 and 45% [100]. The Brazilian wind power industry follows standardized maintenance guidelines which enhance environmental performance metrics comparability along with its 20-25 year operational timeline [101].

The study takes proper precautions to address the potential limitations. The research controls geographical variations through the removal of datasets from sites possessing distinctive geotechnical conditions. The results from the compiled dataset are available in Table A.1, with emission values expressed in gCO₂eq/kWh. The data shows many advancements in wind power technology during two time periods. Early studies (2002-2010) showed emissions between 9.0 and 29.5 gCO₂eq/kWh while modern installations (2020-2025) showed emissions within 3.7–12.9 gCO₂eq/kWh.

3.5.2 Solar PV

The LCI for solar PV systems contains 59 data points from peer-reviewed literature, industry reports, and environmental databases. Emission factors are measured in gCO₂eq/kWh, covering both crystalline silicon (c-Si) and thin-film technologies. The temporal coverage spans from 2002 to 2023, with 84.4% of data concentrated in the 2012-2023 period.

Source Distribution:

- Scientific literature (SLA): 51 entries (79.7%)
- Industry/Government reports (IOG): 6 entries (9.4%)
- Environmental databases (EED): 7 entries (10.9%)

Geographical Coverage:

- Global studies: 14 entries (21.9%)
- Asia: 20 entries (31.3%)
- Europe: 18 entries (28.1%)
- Americas: 12 entries (18.7%) (6 entries from Brazil)

Technology Breakdown:

- Monocrystalline silicon (Mono-Si): 21 entries (32.8%)
- Multiple/Unspecified technologies: 24 entries (37.5%)
- Multicrystalline silicon (Multi-Si): 17 entries (26.6%)
- Thin-film (a-Si): 2 entries (3.1%)

Key Temporal Patterns:

- 2002-2011: 10 entries (15.6%)
- 2012-2016: 26 entries (40.6%)
- 2017-2023: 28 entries (43.8%)

The environmental impact of solar PV systems throughout their lifecycle displays varied quantities across regions because of varying levels of solar radiation. The Brazilian environment benefits from high solar irradiation levels, which results in a lower emission rate compared to European countries from equivalent systems. The studies retained their comparability by adjusting emission factors to operate at a standard solar irradiance rate of 1,700 kWh/m²/year.

Similar to wind power analysis Brazil faces an insufficient number of LCA studies which required international data alongside Brazilian data for solid statistical evaluation. Solar PV technology upholds its scientific validity when using this methodology but demands particular technical adaptations. The solar PV market shows manufacturing location differences between Chinese and European centres [102]. The normalization process plays a fundamental role in solar PV lifecycle analyses since local solar yield may differ by over 50% which impacts the gCO₂/kWh calculation denominator. The standardized irradiance measurement enables comparability and enables actual regional solar input analysis through sensitivity tests when required [103].

Statistics from the dataset confirm that monocrystalline silicon (Mono-Si) technology maintains its leading position because it represents 32.8% of the sample analysis despite its commercial dominance in the market today [104]. Data from thin-film technologies is adequately collected for LCA since their material usage and manufacturing differ substantially from crystalline silicon processes.

This approach combines international references with local Brazilian information for both practical and analytical reasons. The absence of high-volume Brazil-specific LCA research about solar PV systems leads to a combined analytical approach in wind power assessment. The universal manufacturing processes along with global PV supply chain infrastructure serve as methodological evidence to justify the use of mixed data sources [105]. Regulatory and installation practice differences across locations require specific adaptation of general results before they can be effectively used in Brazilian national planning and policy assessments.

The research enforces quality control measures by applying standardized irradiation normalization procedures (1700 Wh/m²/yr) to enable comparison of regional data. Data in Table A.2 shows that PV emission factors span 12.9-92.8 gCO₂eq/kWh showing distinct technological advances between two generations: The 2002–2015 paradigm showed 15.0-87.3 gCO₂eq/kWh while the 2016-2023 evolution displayed 12.9-50.1 gCO₂eq/kWh. These trends indicate better production of crystalline silicon materials and improved balance-of-system elements.

3.5.3 Hydropower

Evaluation of the hydropower lifecycle inventory includes 34 distinct data points collected from peer-reviewed works and international reports and environmental databases. The emission factors in gCO₂eq/kWh cover all three categories of hydro facilities including reservoirs and run-of-river and hybrid operations. Among the published data between 2005 and 2025 the majority (73.5%) stems from research between 2017 and 2025.

- **Source Distribution:**

- Scientific literature (SLA): 27 entries (79.4%)
- Industry/Government reports (IOG): 6 entries (17.6%)
- Environmental databases (EED): 1 entries (2.9%)

- **Geographical Coverage:**

- Global studies: 4 entries (11.8%)
- Asia: 14 entries (41.2%) (11 from China)
- Europe: 5 entries (14.7%)
- Americas: 10 entries (29.4%) (7 entries from Brazil)
- Africa: 1 entire (2.9%)

- **Technology Breakdown:**

- Reservoir: 17 entries (50%) (2 entries with pumped hydro system)
- Run-of-river (ROR): 8 entries (23.6%)
- Hybrid (ROR with Reservoir): 9 entries (26.4%)

- **Key Temporal Patterns:**

- 2005-2011: 2 entries (5.9%)
- 2012-2016: 7 entries (20.6%)
- 2017-2025: 25 entries (73.5%)

Asian hydropower systems dominate the geographical distribution due to Chinese facilities account for greater than 40% of the total entries. Among all nations in the Americas Brazil leads with seven entries that represent the total ten regional submissions, a close number compared to

China. Brazil's dominant position in hydropower production suits the dataset since it accounts for most power generation while national representation surpasses that of Wind and PV power. A high number of Brazilian data entries improves emission analysis interpretations within their national context, yet the database still need additional information from international sources to fully model complete life cycles.

The lifecycle emissions measured in Brazil match the worldwide emission scope. The seven reviewed studies demonstrate that emitted CO₂ levels in kilowatt-hours typically stay under 20 gCO₂eq/kWh yet they depend on power plant types and reservoir dimensions alongside research methodology options. National environmental assessments become more valid when hydroelectricity data from Brazil replaces proxy estimates from other geographic regions.

Hydropower requires special consideration in emission modelling since emissions depend heavily on both natural geological and ecological settings. The application of global LCA results to national policy or planning requires extensive sensitivity analysis especially those focusing on methane release from submerged biomass and altering precipitation patterns. The dataset in Table A.3 includes emission factor values across reservoir, ROR, and hybrid hydropower systems, represented in gCO₂eq/kWh, providing a basis for benchmarking Brazil's existing and planned hydro assets within an internationally consistent framework.

The main GHG emissions during hydropower plant LCA arise from land flooding needed to create reservoirs. Anaerobic decomposition of submerged organic matter releases high amounts of methane (CH₄) emissions which is a GHG with elevated Global Warming Potential (GWP). The high CO₂-equivalent emission levels of reservoir-based hydropower plants surpass those of run-of-river installations because of methane emissions. Research shows that reservoir flooding produces approximately 98% of lifecycle emissions that exceed all other stages of construction operations and maintenance [106]. The site-specific variables including vegetation density and water temperature and reservoir depth levels substantially affect hydropower carbon emissions which requires specific regional analyses to achieve precise emission measurements.

The Brazilian hydropower installations using large reservoirs such as Balbina and Tucuruí produce abnormally great methane emissions from carbon-rich tropical forest soils located in flooded areas. The Belo Monte dam which operates as Run-of-river (ROR) produces 15–55 gCO₂eq/kWh of emissions mainly from flooded geographic areas accounting for more than 90% of its total lifecycle GHG outputs [107]. The tropical reservoirs in Brazil's Amazon region produce high emissions because heat and organic materials enhance the anaerobic breakdown of underwater vegetation. Future Brazilian power infrastructure requires focus on MW/km² power

density metrics together with analysis of methane hotspots across regions because current global average calculations underestimate hydropower emissions in the Amazon area. The PNE states that the nation possesses 176 GW of potential hydroelectric power capacity which includes 68 GW untapped resources that mainly reside in the Amazon and Tocantins-Araguaia river basins. According to the plan the sectoral development depends heavily on these environmental constraints because 63% of Brazil's unexploited hydropower potential exists within only in the Amazon basin where generated energy releases emissions can be equivalent to fossil fuels [13].

3.5.4 Biomass Power

An evaluation of biomass lifecycle inventory data encompasses 43 specific points that come from peer-reviewed scientific literature and international organization reports alongside environmental databases. The emission factors in gCO₂eq/kWh cover different biomass technological processes across biogas, biodiesel, bioethanol, and solid biomass combustion. The research between 2002 and 2023 demonstrates a major academic and policy focus increase since 2015 as demonstrated by studies published during that period reaching 58.1% of total numbers.

Source Distribution:

- Scientific literature (SLA): 39 entries (90.6%)
- Industry/Organization/Government reports (IOG): 2 entries (4.7%)
- Environmental databases (EED): 2 entries (4.7%)

Geographical Coverage:

- Global studies: 7 entries (11.1%)
- Europe: 23 entries (37.8%)
- America: 15 entries (22.2%) (10 from Brazil)

Technology Breakdown:

- Biogas: 22 entries (51.1%)
- Biomass: 14 entries (32.6%)
- Biofuels: 2 entries (4.7%)
- Multiple/Unspecified: 5 entries (11.6%)

Key Temporal Patterns:

- 2002–2005: 6 entries (13.9%)
- 2011–2015: 12 entries (33.3%)
- 2017–2023: 25 entries (62.2%)

The power generation system based on biomass creates an intricate yet encouraging system for Brazil to move toward renewable energy. This study demonstrates that biomass-derived electricity has a diverse global warming potential varies significantly, with results ranging from 109.295 gCO₂eq/kWh in this assessment to extremes reported in literature from -395 gCO₂eq/kWh [108] to 510 gCO₂eq/kWh [109]. LCA research of biomass systems faces extensive methodological hurdles because of the wide-ranging assortment of feedstocks together with different production approaches and boundary conditions. This wide array of emissions extending from carbon-negative to values approaching fossil fuel capacity demonstrates differences in agricultural farming practices and supply chain logistics and combustion efficiency and co-product management such as ash use for cement production and vinasse use for fertilizer.

The edaphoclimatic environment of Brazil enables extensive biomass feedstock opportunities which extend from sugarcane bagasse and rice husks through wood chips and throws away from agro-industrial segments. The annual availability of harvestable agricultural biomass poses major restrictive factors because sugarcane - the biggest share of the country's biomass generation - can only be collected during a 7-month season [13]. The storage of biomass exists rarely because technical obstacles along with economic challenges prevent safe preservation and supply network development for extensive storage facilities [110].

Modern technological improvements in biomethane and biodiesel and ethanol production methods provide encouraging options especially regarding transportation sector, however the pathways have not reached a cost position that matches direct bagasse and wood chip combustion for power generation [111]. Biomethane offers storage capabilities combined with operational versatility although its implementation demands large investment costs in purification systems and grid injection facilities as well as requiring production costs that exceed solid biomass prices [13]. These technologies demonstrate better viability for transport decarbonization compared to large-scale power generation integration during the present time period.

The environmental performance of biomass energy systems hinges critically on sustainable land use and adherence to Brazil's legal frameworks for forest preservation. While agricultural residues (e.g., sugarcane straw, rice husks) avoid direct land-use change emissions, their climate

benefits depend on efficient logistics to minimize transport emissions [112]. Furthermore, the integration of biomass with (Carbon Capture and Storage (CCS)) could amplify its negative emissions potential, though this remains nascent in Brazil [113].

The dataset in Table A.4 compiles life cycle emission factors (in gCO₂eq/kWh) across biogas, solid biomass, biodiesel, and bioethanol technologies, offering a comparative foundation for evaluating Brazil's bioenergy potential against global sustainability benchmarks and informing future policy on low-carbon energy transitions.

3.5.5 Nuclear Power

The proposed 100% RES grid scenario in Brazil treats nuclear energy as a separate component. The technology remains present in Brazil's national energy framework as legacy infrastructure despite lacking conventional classification as renewable power. The scenario maintains different linguistic distinctions between renewable and clean power sources because it supports operating existing nuclear facilities while rejecting new reactor development. This apparent inconsistency in the scenario's terminology—renewable versus clean—derives from the continued operation of existing nuclear facilities rather than plans for expansive deployment of new reactors [114].

Brazil maintains Angra 1 and Angra 2 as active nuclear facilities and Angra 3 constitutes a construction project at present. Energy security through nuclear power plants functions as the main reason for their sustained operation according to the National Energy Plan 2050 (PNE) when operating hydropower reaches low levels [13]. The steady baseload power generation from nuclear facilities has high capacity operation levels that work well in combination with variable energy sources such as wind power and solar energy [115].

Numerous lifecycle assessments prove nuclear energy generates lower than 20 gCO₂eq/kWh direct GHG emissions making it comparable to low-carbon technologies. The main emission sources stem from upstream activities between uranium mining through fuel processing and construction activities and decommissioning operations because operational waste releases minimal emissions [116]. Nuclear LCA research in Brazil is scarce but international Pressurized Water Reactor (PWR) technology standards can be adopted for assessment due to design similarities.

The implementation of nuclear power into renewable energy systems needs substantial attention paid to operational integration as well as comprehensive management plans and safety protocols for spent fuel and social acceptability strategies. The PNE does not present any plans regarding the expansion of nuclear power generation after Angra 3 while confirming Angra 3's status as a legacy power source instead of an expanding sector. The maintenance of current

nuclear facilities supports both lifecycle emissions reduction and operating cost recovery whereas it does not indicate future nuclear expansion.

From within the proposed framework of 100% RES grid the addition of nuclear power technology enhances grid stability together with resilience. The existing policy choice to maintain nuclear power endorses an operational perspective which combines the preservation of current green infrastructure alongside quick development of pure renewable systems. The dataset in Table A.5 compiles life cycle emission factors (in gCO₂eq/kWh) for nuclear power.

Chapter 4

Input Data for the 2050 100% RES grid scenario

This chapter describes the input data and assumptions as detailed in the modelling/simulation of the 100% Renewable Scenario developed in the work and in accordance with the long-term vision of the Brazilian National Energy Plan (PNE). The scenario is designed to investigate the technical viability and consequences of achieving full electricity demand coverage in Brazil by 2050 using only renewable sources.

The details of all data sources, choices of parameters and the underlying selection of the methodology will be explained in detail for transparency and replication purposes and all the collected data inputs have been summarized in the appendix part on Table A.6. The assumptions are based on most recent projections and applicable datasets made available by official institutions, such as the Energy Research Office (EPE), relevant academic and technical literature.

4.1 Electricity Demand

In the 100% Renewable Grid Simulation, the annual electricity demand in the simulation was computed using the projections of the PNE 2050 and the demand to be fulfilled by the centralized generation systems was given special consideration. For the EnergyPLAN model compatibility, which demands total electricity consumption in TWh/year and hourly demand profile, two major assumptions were adopted: (i) The use of centralized demand projections in the Expansion Challenge scenario, and (ii) use of a static hourly load profile 2024.

As informed by PNE 2050, electricity demand to be covered by the centralized generation of

the Expansion Challenge scenario would grow to 172,000 MW average in 2050 [13]. This level of demand translates into a total consumption of about 1,511.65 TWh/year on an annual basis, based on the typical conversion factor:

$$\text{Energy (TWh/year)} = \frac{172,000 \times 8,760}{1,000,000} = 1,511.7 \text{ TWh/year} \quad (4.1)$$

This value represents the net demand to cover with centralized generation from Distributed Generation (DG) contribution, self-generation, and energy efficiency gains.

In terms of hourly distribution of demand, no such long-term hourly load projections were found in either governmental databanks or academic paper. Therefore, for this study, the hourly electricity load profile for the year 2024 was used as an approximate for year 2050.

However, it is realised that this is a significant limitation of the method. The static load profile does not capture future trends such as an increase in the already observed duck curve associated with high solar penetration or the increasing but previously unrecognized presence of flexible load through electric vehicles [117]. Consequently, this is an area of particular improvement in future research. It further reveals a larger gap in the PNE 2050 framework and current academic literature, demonstrating a necessity for the development of more current, dynamic long-term load forecasting tools that can assist energy system planning more effectively.

4.2 Variable Renewable Energy Sources and Capacity Factors

The simulation includes a wide range of VRES, which are central in the transition towards a fully renewable electricity system in Brazil. The VRES analyzed in the current study consist of Onshore Wind, Centralized Solar PV, ROR Hydropower, DG Solar PV, Small hydropower plants – Pequenas Centrais Hidrelétricas (PCHs), DG Wind Power, and DG Hydropower.

All installed capacity values for these sources were taken from the appendix in the Plano Nacional de Energia (PNE) 2050, consistent with values from the national energy planning projections. The associated capacity factors for the respective source are specified in Table 4.1 [118].

The hourly generation profiles of the following technologies: Small Hydropower, Run-of-River Hydropower, Centralized Solar PV, Onshore Wind and DG Wind Power are obtained from Typical Meteorological Year (TMY) data. This data shows long term averaged hourly behavior using historical climatic and operational data and was processed as described in the methodology section.

Table 4.1: Installed Capacity by Source in 2050

Source / Technology	Installed Capacity (MW)
Hydropower (Total)	127,900
Large Hydropower Plants (UHE)	111,718
Small Hydropower Plants (PCH)	16,182
Wind Power	209,431
Solar Power	80,831
Biomass	18,456
Natural Gas	0
Coal	0
Nuclear	3,395
Complementary Power	85,432
Distributed Generation (DG)	49,888
Total	575,332

There is, however, a critical difference that is noted in DG Solar PV. Unlike centrally located solar plants, DG solar installations, which are usually roof-mounted, do not have built-in solar tracking systems or optimising functions such as tilt and azimuth adjustment. Consequently, their performance lags behind, comparatively, with regard to capacity factor. Moreover, because of the lack of data, the hourly curve for DG Solar PV is calculated only on the basis of the 2024 dataset [88].

As shown in Table 4.2, the ONS provides the expected energy provision from each source by the year 2050. Dividing this annual projection of generation by installed capacity gives us an implied or effective capacity factor. Noteworthy, in some of these cases, the implied capacity factors are significantly different than the TMY-based ones. Such differences could be caused by a variety of factors, such as unaccounted technological improvements in historical datasets, overly optimistic PNE forecasts, or future regional developments to higher yield source regions.

To deal with these uncertainties and strengthen simulation simulation inputs both sets of capacity factor assumptions will be tested in the Simulation Results section:

- One case will use the TMY-based capacity factors that retain the historical representativeness and meteorological realism.
- The second scenario will include the application of correction factors in EnergyPLAN model data collecting upon those estimations of expected capacity factors produced from PNE 2050 projected generation information.

Table 4.2: Expected Electricity Generation by Source in 2050

Source / Technology	Generation (MWh Average)
Hydropower (Total)	51,567
Large Hydropower Plants (UHE)	46,875
Small Hydropower Plants (PCH)	4,692
Wind Power	92,687
Solar Power	22,740
Biomass	5,267
Natural Gas	0
Coal	0
Nuclear	2,873
Complementary Power	0
Distributed Generation (DG)	11,464
Total	186,597

4.3 Central Power Production

The Central Power Production part of the EnergyPLAN simulation consists of two technologies. reservoir-based hydropower and nuclear power plants in.

For nuclear power, an installed capacity is the only input that is required. Nuclear energy is independent of intermittent resources and is thus perceived as ever available, all year round. Although this assumption does not entirely capture the true nature of operations – scheduled maintenance or unplanned outage – it is still largely valid because nuclear power plants tend to operate close to full capacity all year round.

Reservoir hydropower, however, relies on three main aspects. 1) the water inflow to the reservoir, 2) storage capacity of the reservoir, and 3) the installed generating capacity.

Water inflow information was obtained from the ONS operational history records [88] which were used to create a Typical Meteorological Year (TMY) set out of historical water flow entries. Reservoir storage capacity was also retrieved from ONS’s “Reservatórios” database, which offers maximum storage capacity by region [119]. These values were then aggregated to estimate the national potential of reservoir storage.

Estimation of installed generation capacity of reservoir based hydropower is more complicated. Reservoir and ROR plants are not clearly separable between themselves on the basis of ONS public databases. Further, some ROR classified plants such as Itaipu have large reservoir capacity. For that purpose, classifications made reference to the “Schematic Diagram of Hydroelectric Plants of National Interlinked System (SIN)” where plants have been divided as ROR or reservoir based plants. According to this source, ROR is responsible for about 59% of the

installed hydropower capacity, and the reservoir-based hydropower accounts for about 41%.

However, by the year 2050, this proportion will change. The rest of Brazil's potential for the development of hydropower facilities is located in the Amazon region and, due to the geographic and environmental factors, most of it is infeasible to develop it through the construction of large reservoirs. On the assumption that the expected 12 GW of hydropower expansion is all ROR, the revised estimate would be 62% ROR and 38% reservoir-based hydropower. This corrected share was applied in EnergyPLAN simulation as a more realistic embodiment of what Brazil's hydropower system might look like in the future.

4.4 Biomass

In the EnergyPLAN simulation, the biomass is addressed as one of the available technologies in the Centralized Power Production tab of the EnergyPLAN simulation. Nevertheless, the default functionality of this module does not provide a good picture of operation features of biomass production in Brazil. In EnergyPLAN the biomass power plant incorporates a model of an electricity producer who will produce when the demand calls for it and will import biomass freely whenever domestic resources run out. Such logic does not resonate well with the observed behavior in the real world of biomass availability in Brazil.

In the Brazil context, availability of biomass is strongly seasonal and agricultural cycle oriented, especially sugarcane harvest. Sugarcane bagasse is the major source of biomass for generation of power in the country; a by product of sugar and ethanol production. As bagasse is not usually stored for long periods and is utilized soon after being harvested, the availability for bagasse is focused within a particular period of the year, which is similar to the sugarcane crop season [110].

Considering this seasonal behaviour, this study did not use EnergyPLAN's model for a centralized biomass power plant. Instead, the simulation models biomass in the "Waste" in EnergyPLAN, which permits the usage of a user-specified resource availability curve. This curve was plotted based on a TMY dataset obtained from historical data of biomass production and availability, from ONS [88]. This scenario is a better picture of the actual situation of biomass-based electricity generation in Brazil in terms of its temporal narrowness and agricultural dependence.

4.5 International Interconnection

The international interconnection capacity is an important criterion of the simulation of a 100% renewable energy grid for Brazil by 2050. Based on data in Dranka et al. [18] in addition to the CIER (Comissão de Integração Energética Regional) report [120]. This is an important input for the assessment of Brazilian electricity's potential export capacity especially taking into account the increased generation of energy from RES. With Brazil increasing its sources of renewable energy, surplus energy generation gets magnified; this will necessitate considering international transmission as a necessary ingredient for effective management of production of energy.

However, it should be noted that the EnergyPLAN model, assumes that all the Exportable Excess of Electricity Production (EEEP) has buyers as long as the transmission infrastructure exists. That is leaving out the question of whether the neighbouring countries will have the demand to buy this excess energy. In fact, the demand on the market in the neighbouring countries may vary, and the opportunities for export may be restricted due to such factors as economic state, energy policies, and technical progress in these countries.

For any energy that cannot be exported; the EnergyPLAN system lists it as Critical Excess Energy Production (CEEP). The system will try to store this excess energy if storage facilities of energy are available. If no storage solutions exist, the system will institute curtails to cut on production, to avoid overloads and inefficiencies in the grid.

4.6 Energy Storage Systems (ESS)

The PNE 2050 recognizes the need for complementary sources of power to cater for the intermittency of renewable energy. Its suggested solution though, 85 GW biodiesel based generation capacity in 2050 as described in Table 4.1 or around 15% of the total installed capacity, instigates considerable concerns. Interestingly, the PNE Table 4.2 shows zero expected electricity generation from this source, which shows that this source is aimed at stabilizing the grid as opposed to constant energy provision. This is not a desirable approach because Brazil has insignificant biodiesel power capacity and no country has deployed the same systems in such a large scale, but it remains a theoretical rather than a functional problem-solver. In contrast, this study explores three more feasible and proven energy storage technologies: Pumped Hydro Energy Storage (PHES) and green hydrogen storage, and Lithium-Ion Batteries.

4.6.1 Pumped Hydro Energy Storage

PHES is currently the most advanced worldwide large-scale energy storage technology; the total installed power capacity and volume of PHES facilities now represent 96% and 99% of the planet's PHES capacity, respectively. It operates by transporting water from one reservoir to another at different elevations: electricity is utilized to pump waters during low demand periods or during times of energy surplus, while in times of peak demand, the stored water is released through turbines to produce electric-power. Its round-trip efficiency usually lies between 70 and 80 percent [121].

In the Brazilian context, it was a thorough study by Grupo de Estudos do Setor Elétrico (GESEL) [122] who uncovered a theoretical maximum ceiling for PHES installations in the country of 11 GW. The distribution of this capacity is as follow: 6 GW in the Southeast, mostly capitalizing on existing reservoirs of the Furnas system; 3 GW in the South, considering its favourable topography facilitating high-head systems; and 2 GW in the Northeast, which is well-suited for associations with clusters of wind generation. The prospects of achieving this full potential, according to the study, would necessitate the use of combination of brownfield projects – which involves the use of existing hydropower infrastructure, to a small number of new greenfield sites that would satisfy stringent environmental and topographic requirements. The average round-trip efficiency calculated for these potential Brazilian PHES systems is 78%, making it a very reliable and technically effective substitute to biodiesel-based options when it comes to grid flexibility. These regional estimation of the capacity, amounting to 11 GW, will be respectively taken as the installed pumped hydro storage capacity in the simulation that will be presented in this study.

4.6.2 Green Hydrogen Storage

Green hydrogen is a promising solution for long and seasonal energy storage. It is synthesized via electrolysis at a surplus of renewable energy streams and can be stored for the future reconversion into electricity or for direct combustion as a fuel. In contrast with the case of biodiesel, green hydrogen storage has already become part of practical initiatives.

The efficiency of green hydrogen production and reconversion technologies is essential in the viability of such technologies as energy storage. Electrolysis, major process for green hydrogen production, has advanced a lot. However, the round-trip efficiency, that is to convert electricity into hydrogen and back to electricity, is currently poor at around 38% of using hydrogen in the combined cycle power plants [123].

Since green hydrogen is an emerging storage technology, this research will carry out sensitivity analysis by comparing the system's response when subjected to various installed green hydrogen capacity. The idea is to comprehend how different capacities can impact the reliability and flexibility of the grid especially in the balancing of renewables intermittency. This analysis will also be useful to determine the potential of green hydrogen being a complimentary storage option for Brazil's renewable energy transition. The simulated conditions for the green hydrogen storage capacity will be varied in order to attempt to gain insight regarding thresholds at which this technology could contribute to grid stability and energy security in the long term.

4.6.3 Lithium-Ion Battery Storage

Lithium-ion batteries (Li-ion) are currently the most widely used ESS for distributed systems in the world, due to its high energy density, good round-trip efficiency fast response times and favourable economical factors [124]. These factors include the declining costs in production and the growing use of second-life applications such as the repurposing degraded electrical vehicles (EV's) batteries for use in less demanding stationary storage systems with a round-trip efficiency above 90% [125].

Global installations of lithium-ion batteries for storing energy are forecast to reach 778 GW within the next five years due to their rising popularity in the energy sector [126]. Based on research, lithium-ion batteries are expected to become cheaper by 43.5% to 52.5% by the end of the present decade compared to 2020's prices [127]. In Brazil's energy model, lithium-ion batteries can help balance fluctuations from solar PV and wind power during the day, trim the rise in evening power use and effectively diminish the curtailment of RES.

However, this technology presents a critical supply dependency on specific minerals such as cobalt and lithium, which are considered strategic or rare-earth materials due to their geographically concentrated reserves. For instance, the Democratic Republic of Congo is responsible for over 73% of global cobalt extraction, while China dominates the refining stage, processing approximately 65% of the world's lithium and 80% of its cobalt [128]. Additionally, Chile, a member of MERCOSUL holds the world's largest lithium reserves, estimated at 9.3 million metric tons, accounting for about 36% of global reserves [129]. This proximity and trade alliance could potentially facilitate more secure and regionally integrated supply chains for lithium acquisition.

4.7 Critical Excess of Electricity Production and Curtailment

Because of the high share of Variable Renewable Energy Sources (VRES) in the simulated 100% RES grid, the model often finds itself in positions of the excessive generation of electricity – the situations where electricity generation outweighs its instantaneous demand. This phenomenon known as Critical Excess of Electricity Production (CEEP) is an important operation challenge which has to be actively managed in order to ensure grid stability and avoid inefficiencies.

The model of EnergyPLAN offers several options for avoiding overproduction, and it also determines the order of priority in these measures. In this work, the following strategies were applied in the order that the Brazilian system and the operational logic of EnergyPLAN dictate them:

- Reduction of Reservoir Hydropower Production: These plants are dispatchable hence easily adjustable, suitable for supplying ancillary services such as frequency control and balancing. This is similar to the existing practice in Brazil where reservoir hydropower is key in balancing the grid because of its flexibility and ability to store [130].
- Curtailment of VRES Production: In the case when the curtailment of hydropower output is not enough to balance out the surplus, the next step is the curtailment of VRES production. Curtailment refers to planned reductions in electricity generation from renewable sources when the resources (wind or sunlight) is present, but due limits of the systems (absence of demand, inadequate storage, or transmission capacities) [131]. This leads to lost renewable energy that was not able to be used or stored properly. Curtailment is in general undesirable, but becomes a necessity once the flexibility of system is worn out.

Chapter 5

Results and Discussion

5.1 EnergyPLAN Validation Outputs

5.1.1 Validation Metrics and Comparative Analysis

To assess the model's reliability, various quantitative metrics were applied across multiple time-frames and technologies. For a complete presentation of the results, including detailed methodology, additional performance metrics, and extended discussions on model limitations, readers are referred to reference [132], which provides an in-depth exploration of the validation framework and its findings. The core error assessment involved calculating the percentage deviation between the simulated and observed power outputs, serving as a measure of model accuracy.

The base-load technology predictions at annual time frames delivered exceptionally accurate results. Hydroelectric generation represents the leading electricity source in Brazil and produced only a minor difference between predicted and actual results at 0.56%. The performance exhibits EnergyPLAN's superior capacity to simulate Brazil's detailed hydropower infrastructure which handles normal seasonal water operations. The observed data harmonized well with solar PV generation through simulations which produced errors of less than 1.2% annually since the solar irradiation data and conversion parameters properly represented Brazil's photovoltaic fleet.

The validation results regarding wind power generation showed extensive variability through errors ranging from 8% to 12% for each month. The wind resource modelling of Brazilian territories identified elevated uncertainty factors because of natural conditions found in that region. The extensive wind farm distribution in Northeast territories naturally generates simple wind conditions for those locations. Due to a lack of specific performance data for turbines, the model had to use standard power curve specifications. The irregular flow of wind power output

makes it hard to achieve accurate observations for power output levels between predicted and actual values across monthly and short time frames.

The discrepancies in thermal power plants followed distinct patterns from other electricity generating facilities. The annual error levels were kept under 2% yet monthly evaluation showed critical details about EnergyPLAN's dispatch scheduling functions. During peak demand periods the model generated less thermal energy than actual but produced more energy during periods of low demand. Annual energy dispatch from thermal facilities shows good agreement although the timing of dispatch decisions within the model does not represent operational conditions and economic variables present in actual plant operations.

5.1.2 Daily and Hourly Validation Challenges

The model's accuracy was most thoroughly evaluated when applied to both daily and hourly time frames since these periods reveal renewable generation uncertainty and detailed dispatch management requirements. The models produced larger performance deviations during daily validation periods especially for resources with intermittent generation profiles. The model achieved accuracy ranging between 15-18% error during summertime for wind power generation before producing 10-12% error during wintertime. Despite the use of accurate input data the study highlights strong fundamental difficulties in high-resolution forecasting of variable renewable power generation.

Multiple standardized trends emerged from the daily discrepancy measurements. Extreme variations in weather conditions led to most significant errors in wind power generation estimates. The analytical representation of wind speed changes combined with turbine operation responses failed to accurately simulate quick transitions in both processes. The model demonstrated higher deviations when analysing solar power production during days with partial cloudiness compared to clear-sky days which indicates needing better control of diffuse irradiation and cloud impacts.

The validation process revealed a fundamental characteristic of how EnergyPLAN executes its dispatch operations. An overproduction of renewable power levels by the model led to matching underproduction of thermal power levels while the opposite was also true. The analysis reveals that EnergyPLAN properly places renewable power sources first in dispatch priority.

5.1.3 EnergyPLAN's Applicability

The validation procedure shows that EnergyPLAN fulfils Brazil's requirements for modelling its hydro-focused energy system while focusing on high-renewable penetration analysis. The preceding error analysis section established that the model properly models the operational operations of Brazil's multifaceted generation facilities. The primary advantage of EnergyPLAN emerges through its effective merging capability for Brazilian energy characteristics especially regarding the multifaceted interconnection of hydroelectric power alongside variable energy resources. Through its scheduled dispatch operations the model performs precise seasonal modelling of hydroelectric power generation without compromising power grid stability.

Research performed by Dranka and Ferreira [18] demonstrates that EnergyPLAN suits Brazilian energy requirements specifically for dealing with their large-scale energy issues. The model proved its capacity to accomplish these three main functions in their research:

- Simulate the temporal complementarity between hydro, wind, and solar resources
- Evaluate system flexibility requirements under high renewable penetration
- Assess the economic and technical feasibility of long-term decarbonization pathways

The model's ability to resolve data at a one-hour scale helps Brazil's energy sector to effectively understand demand patterns together with RES fluctuations. The model's detailed time allocation system creates precise models of operational problems in which hydro-power runs out during dry seasons and sudden fluctuations in renewable power occur. The evaluation of EnergyPLAN for Brazil shows that the software has sufficient strength to model complex power systems with accuracy.

5.2 TMY Profiles for EnergyPLAN Modelling

For the simulation of realistic renewable energy outputs in future energy scenarios, it is necessary to utilize representative meteorological data with long-term climate trend coverage but with a high computational efficiency. In the current research, TMY profiles are computed and used as input data for the EnergyPLAN model. These synthetic meteorological years are configured to capture the statistical behaviour of multi-year historical weather observations, which allows robust simulation of renewable energy supply under normal conditions.

The performance and representativeness of each TMY profile are illustrated through both quantitative and visual analyses. Table 5.1 presents the validation results for each RES, summarizing the statistical deviation of the TMY from the historical mean. These metrics help assess how closely the synthetic year reproduces the central tendencies and variability of the underlying dataset.

In addition to numerical indicators, visual comparisons further support the TMY’s reliability. The figures referenced in Table 5.1 available in Appendix —show the monthly average capacity factors of each RES in the TMY overlaid with historical data. In these graphs, the blue line represents the TMY profile, the red line with square markers denotes the historical average, while the dashed purple and yellow lines indicate the historical maximum and minimum monthly values, respectively. These graphical representations confirm that the TMY series lies within the expected seasonal range and accurately reflects long-term operational trends.

Table 5.1: Validation metrics for TMY profiles of each energy source

Technology	MBE	RMSE	MAPE (%)	Appendix Image
Wind	0.0013	0.0814	16.71	A.1
Centralized PV	-0.0005	0.0515	11.94	A.2
Small Hydro (PCH)	0.0271	0.0503	7.85	A.3
Reservoir Levels	-0.0179	0.0537	5.17	A.4
Run-of-River Hydro	0.0067	0.0507	9.54	A.5

The validation results presented in Table 5.1 confirm that the constructed TMY profiles are solid and representative for simulating renewable generation under typical operating conditions. All renewable sources showed low MBE values, meaning that the differences between the TMY and historical averages are small. RMSE stayed below 0.09 across all technologies, while MAPE ranged from 5.17% for reservoir levels to 16.71% for wind power. These values show that, although wind has higher variability and is harder to predict with precision, the overall results are accurate enough for long-term scenario analysis.

This is also supported by the figures in Appendix A, where TMY profiles stay within the seasonal range defined by historical minimum and maximum values. In most cases, the curves follow the historical average closely, especially in more stable periods. This behavior comes from how the TMY was built — by choosing months that minimise deviation in both the mean and standard deviation from multi-year data. This way, the process filters out extreme values and keeps patterns that are more representative. Overall, both the quantitative and visual results confirm that the TMY datasets are suitable for EnergyPLAN simulations and help improve the

credibility of the scenario results.

5.3 Statistical Characterization of Emission Profiles and Monte Carlo Simulation for RES

5.3.1 Wind Power: Emission Profile and Monte Carlo Analysis

The statistical modelling of wind power lifecycle emissions required rigorous evaluation of parametric distributions to accurately represent the dataset's underlying probability structure. Figure 5.1 depicts the density trace for the wind distribution.

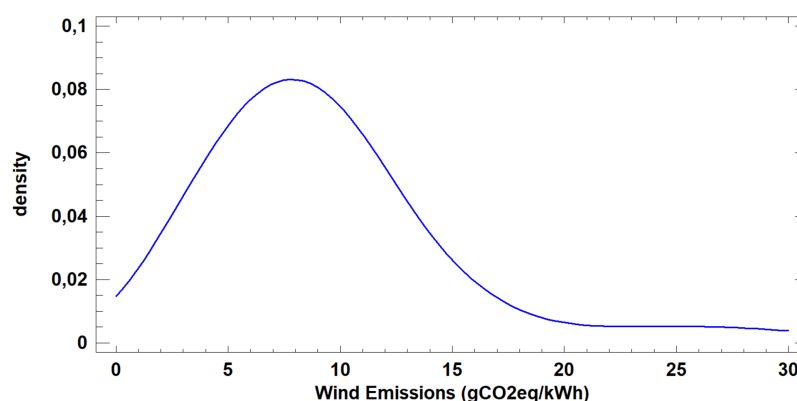


Figure 5.1: Probability density trace of wind emission values showing a modal concentration between 5-13 gCO₂eq/kWh

The evaluation method consisted of Kolmogorov-Smirnov (KS) goodness-of-fit testing in combination with log-likelihood comparisons which evaluated twelve candidate distributions. The KS test used maximum separation (D_n) to measure differences between empirical and theoretical distribution cumulative curves and log-likelihood revealed distribution quality comparison. The analysis first removed distributions which showed p-values under 0.05 coupled with physically unacceptable alignments to emission constraints.

The top candidate distributions are summarized by the metrics presented in Table 5.2.

Results showed the loglogistic distribution was the best fitting model through its demonstration of:

- The KS test yielded a non-significant result with $p = 0.9007$ well above 0.05
- Optimal log-likelihood (-191.757) among all candidates

Table 5.2: Goodness-of-fit metrics for wind emission distributions

Distribution	KS Stat.	p-value	Log-Likelihood	Parameters
Loglogistic	0.0682	0.9007	-191.8	$\alpha = 2.093, \beta = 0.295$
Lognormal	0.0874	0.6489	-192.5	$\mu = 2.129, \sigma = 0.453$
Inverse Gaussian	0.0928	0.3737	-192.4	$\mu = 9.409, \lambda = 4.426$
Weibull	0.1352	0.1547	-205.2	$\lambda = 10.655, k = 1.934$
Normal	0.1749	0.0276	-215.4	$\mu = 9.385, \sigma = 5.289$

- The distribution displays an excellent visual match according to Quantile plot in Figure 5.2
- Positive skewed data placed within a physically reasonable framework with median at 8.107 gCO₂eq/kWh

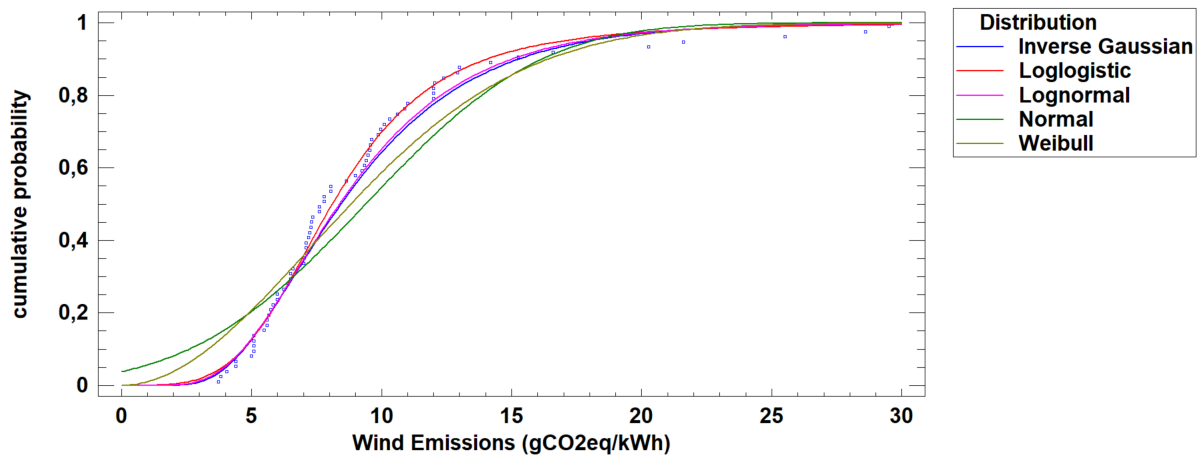


Figure 5.2: Quantile plot showing loglogistic distribution fit alongside other candidate distributions including Normal distribution

The histogram in Figure 5.3 demonstrates how the loglogistic parameters capture both the frequent lower emissions (median at 8.107 gCO₂eq/kWh) and rare higher values (up to 29.5 gCO₂eq/kWh), while the Normal distribution fails to adequately model the right-skewed nature of the data.

Building upon the loglogistic distribution parameters identified in the previous analysis ($\alpha = 2.093, \beta = 0.295$), we conducted a Monte Carlo simulation to model the probabilistic behaviour of wind power lifecycle emissions. This approach enables comprehensive risk assessment by generating synthetic datasets that capture the inherent variability observed in empirical measurements.

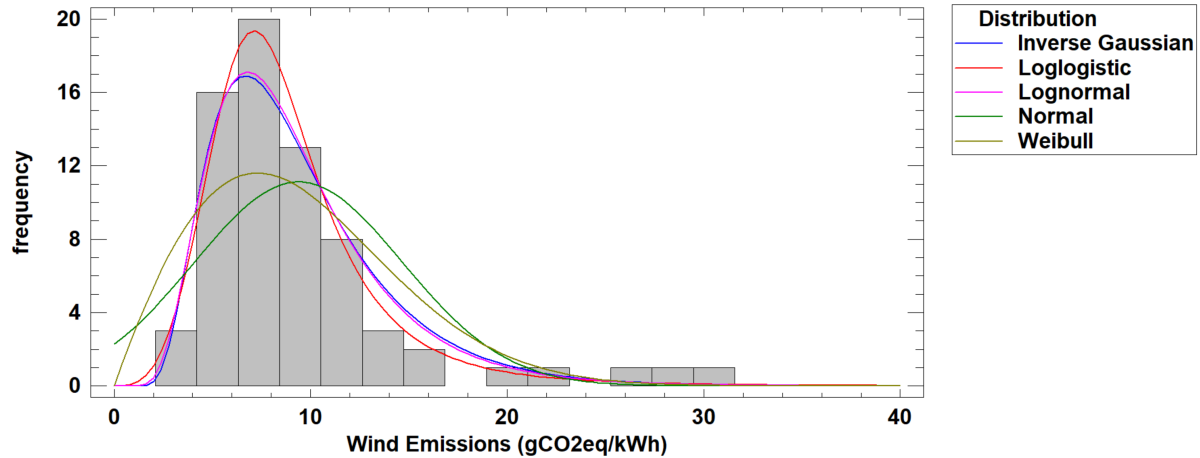


Figure 5.3: Frequency distribution with fitted loglogistic density curve compared to multiple distributions fit

The Monte Carlo simulation (100,000 iterations) produced the statistical characteristics presented in Table 5.3.

Table 5.3: Descriptive statistics of Monte Carlo simulation

Statistic	Value (gCO ₂ eq/kWh)
Mean	8.12
Median	7.56
Standard Deviation	3.41
10th Percentile	4.65
25th Percentile (Q1)	5.93
75th Percentile (Q3)	9.55
90th Percentile	12.12
Interquartile Range	3.62
Minimum	1.24
Maximum	28.97

The simulation results demonstrate:

- **Central Tendency:** Median emissions of 7.56 gCO₂eq/kWh with mean slightly higher at 8.12, indicating moderate right-skewness
- **Variability:** Standard deviation of 3.41 reveals substantial dispersion around the mean
- **Range:** 90% of simulated values fall between 4.65-12.12 gCO₂eq/kWh
- **Extremes:** Maximum observed value of 28.97 confirms the long upper tail characteristic

The cumulative distribution plot (Figure 5.5) confirms these findings, showing excellent agreement between theoretical and simulated distributions across all percentiles.

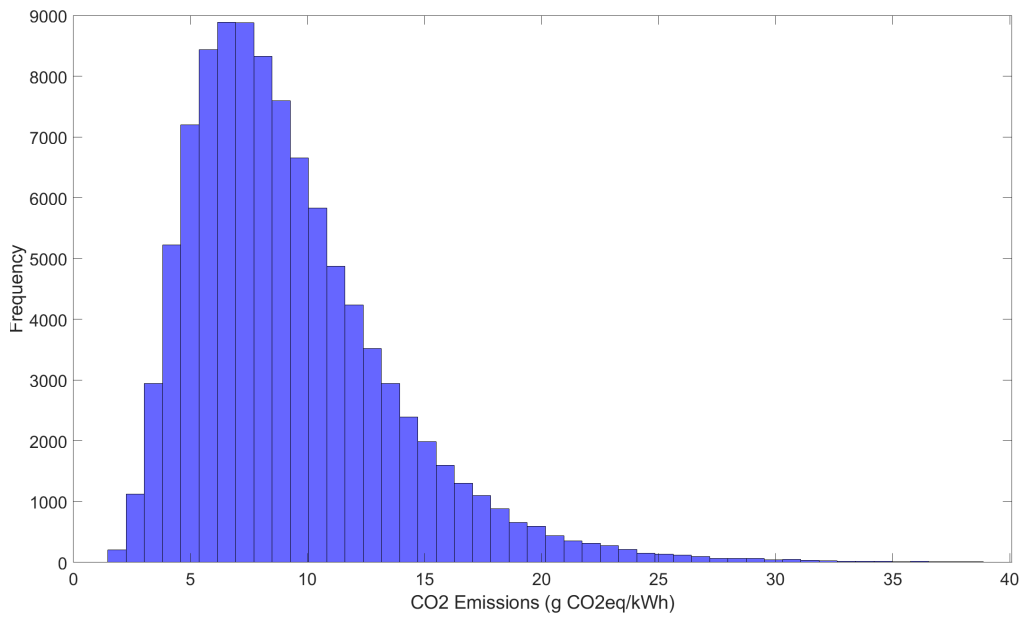


Figure 5.4: Empirical distribution of simulated emissions showing loglogistic fit.

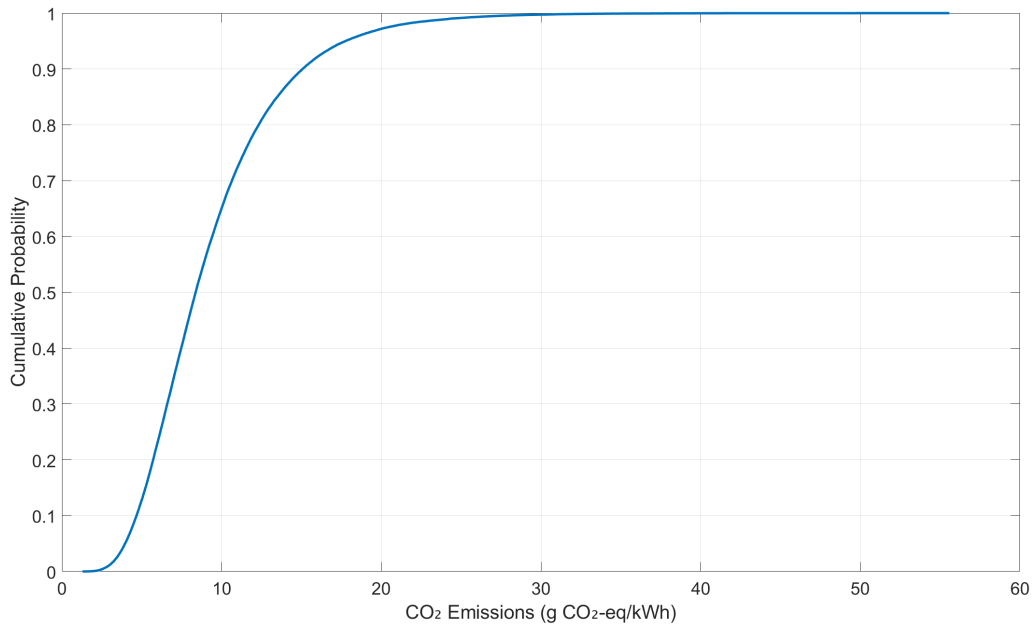


Figure 5.5: Cumulative distribution function for Wind Power.

These results enable more nuanced lifecycle assessments by:

- Quantifying emission variability across installations
- Establishing probabilistic thresholds for policy benchmarks
- Identifying outlier risks in environmental impact studies
- Supporting robust comparative analyses with other energy sources

5.3.2 Solar PV: Emission Profile and Monte Carlo Analysis

The analysis of photovoltaic (PV) lifecycle emissions (12.92-92.79 gCO₂eq/kWh) depended on thorough distribution analysis to properly model the dataset's statistical structure. The data density trace for PV emissions distribution appears in Figure 5.6.

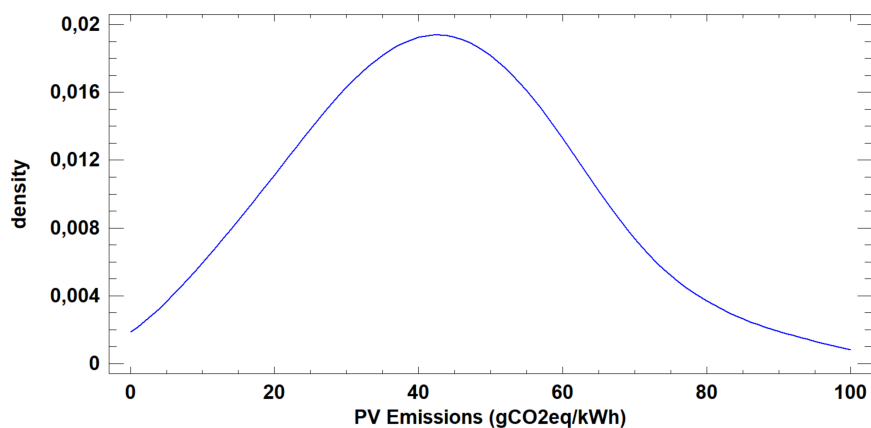


Figure 5.6: Probability density trace of solar PV emission values in gCO₂eq/kWh

The evaluation method consisted of Kolmogorov-Smirnov (KS) goodness-of-fit testing in combination with log-likelihood comparisons which evaluated twelve candidate distributions. The KS test used maximum separation (D_n) to measure differences between empirical and theoretical distribution cumulative curves and log-likelihood revealed distribution quality comparison. The analysis first removed distributions which showed p-values under 0.05 coupled with physically unacceptable alignments to emission constraints.

The top candidate distributions are summarized by the metrics presented in Table 5.4.

Table 5.4 summarizes the key metrics for the top candidate distributions:

Table 5.4: Goodness-of-fit metrics for PV emission distributions

Distribution	KS Statistic	p-value	Log-Likelihood	Parameters
Weibull	0.0657	0.9485	-267.887	$\alpha = 2.682, \beta = 48.765$
Gamma	0.1047	0.5053	-268.095	$k = 5.704, \theta = 0.132$
Normal	0.0593	0.9788	-269.352	$\mu = 43.901, \sigma = 17.539$
Lognormal	0.1293	0.2433	-269.954	$\mu = 3.678, \sigma = 0.448$
Triangular	0.1168	0.3599	-268.907	$a = 6.939, b = 36.540, c = 35.650$

The Weibull distribution emerged as the optimal parametric model, demonstrating:

- Non-significant KS test result ($p = 0.9485 > 0.05$)
- Best log-likelihood among candidates (-267.887)

- Excellent visual agreement in Quantile plot (Figure 5.7)
- Physical plausibility for positive, right-skewed emission data

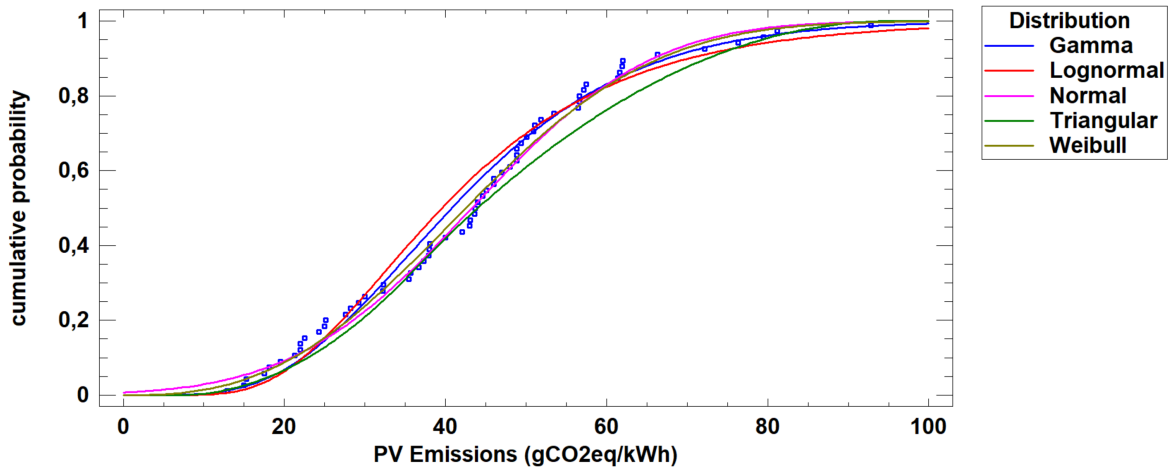


Figure 5.7: Quantile-quantile plot showing Weibull distribution fit with comparison to alternative distributions

The histogram in Figure 5.8 demonstrates how these parameters capture both the frequent moderate emissions (mean at 43.90 gCO₂eq/kWh) and rare higher values (up to 92.79 gCO₂eq/kWh).

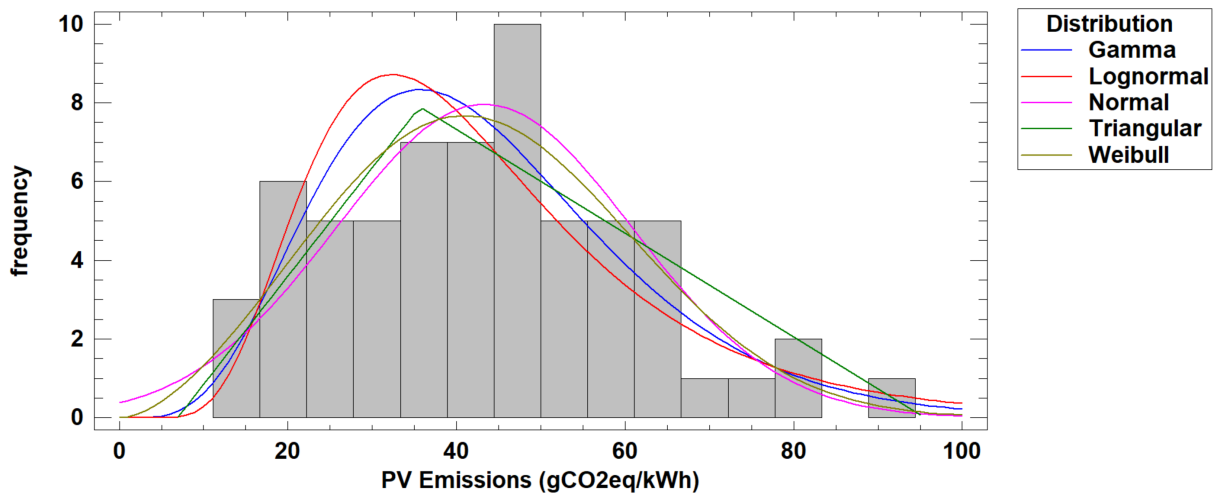


Figure 5.8: Frequency distribution with fitted Weibull density curve alongside possible candidates showing good agreement across all emission ranges

The Monte Carlo simulation (100,000 iterations) produced the statistical characteristics presented in Table 5.5.

The simulation results demonstrate:

Table 5.5: Descriptive statistics of PV Monte Carlo simulation

Statistic	Value (gCO ₂ eq/kWh)
Mean	43.70
Median	42.89
Standard Deviation	17.49
10th Percentile	21.31
25th Percentile (Q1)	30.94
75th Percentile (Q3)	55.51
90th Percentile	66.98
Interquartile Range	24.57
Minimum	6.94
Maximum	92.79

- **Central Tendency:** Median emissions of 42.89 gCO₂eq/kWh with similar mean (43.70), indicating symmetric distribution
- **Variability:** Standard deviation of 17.49 reflects significant technology and installation differences
- **Range:** 90% of simulated values fall between 21.31-66.98 gCO₂eq/kWh
- **Extremes:** Maximum observed value of 92.79 gCO₂eq/kWh confirms presence of high-emission cases

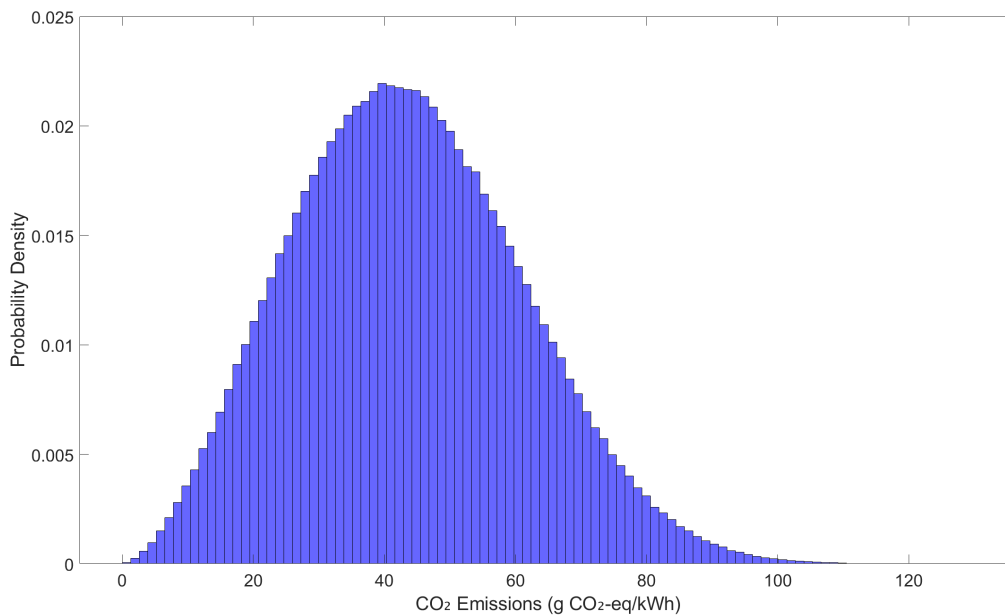


Figure 5.9: Empirical distribution of simulated PV emissions showing Weibull fit.

The cumulative distribution plot (Figure 5.10) confirms these findings, showing excellent agreement between theoretical and simulated distributions across all percentiles.

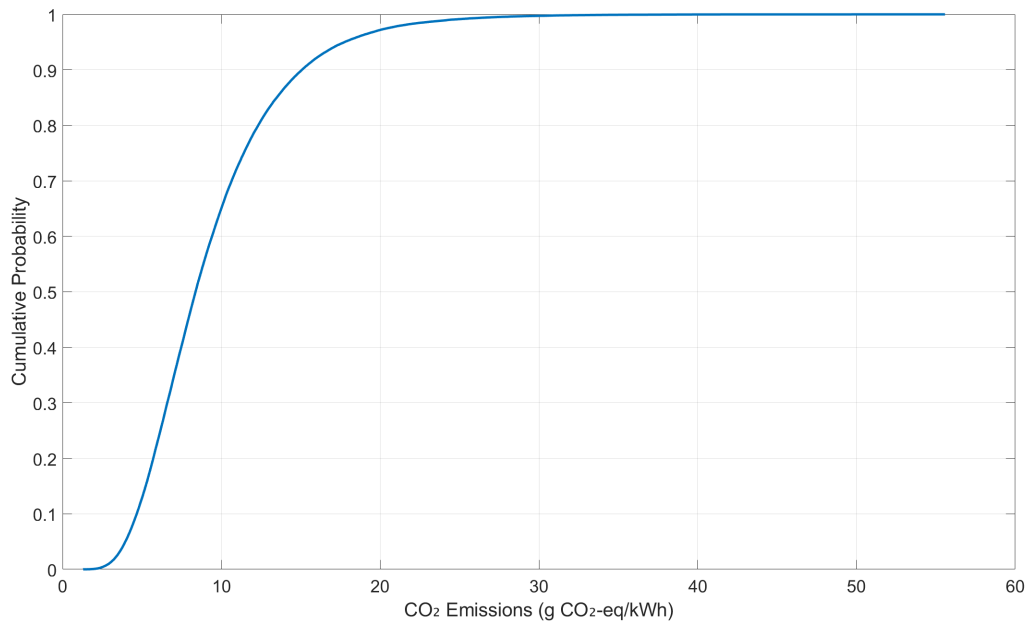


Figure 5.10: Cumulative distribution function for solar PV.

These results enable more nuanced PV lifecycle assessments by:

- Quantifying the 24.57 gCO₂eq/kWh interquartile range across installations
- Establishing 66.98 gCO₂eq/kWh as the 90th percentile benchmark
- Identifying the 10% best-performing systems below 21.31 gCO₂eq/kWh
- Supporting comparative analyses with other energy technologies

5.3.3 Hydropower: Emission Profile and Monte Carlo Analysis

The statistical modelling of hydropower lifecycle emissions required rigorous evaluation of parametric distributions to accurately represent the dataset’s underlying probability structure. Figure 5.11 depicts the density trace for the hydro distribution.

The evaluation method consisted of Kolmogorov-Smirnov (KS) goodness-of-fit testing in combination with log-likelihood comparisons which evaluated fourteen candidate distributions. The KS test used maximum separation (D_n) to measure differences between empirical and theoretical distribution cumulative curves and log-likelihood revealed distribution quality comparison. The analysis first removed distributions which showed p-values under 0.05 coupled with physically unacceptable alignments to emission constraints.

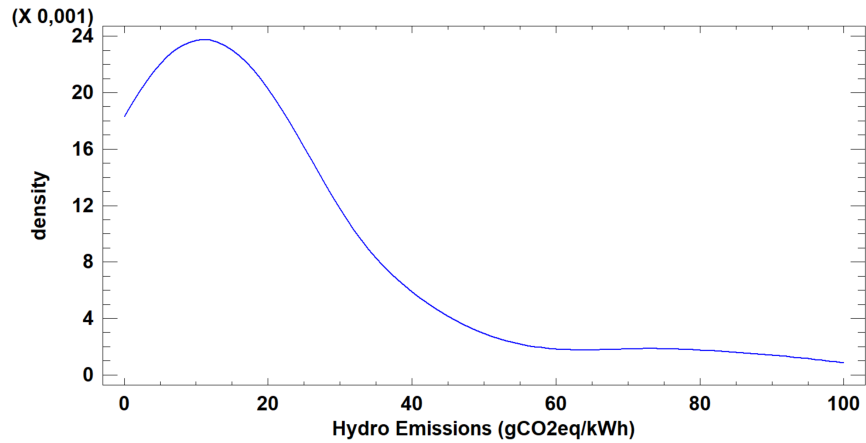


Figure 5.11: Probability density trace of hydro emission values showing a highly right-skewed distribution with most values below 20 gCO₂eq/kWh

The top candidate distributions are summarized by the metrics presented in Table 5.6.

Table 5.6: Goodness-of-fit metrics for hydro emission distributions

Distribution	KS Statistic	p-value	Log-Likelihood	Parameters
Lognormal	0.0778	0.9863	-133.746	$\mu = 2.445, \sigma = 1.089$
Weibull	0.1052	0.8459	-134.273	$\lambda = 19.343, k = 1.028$
Gamma	0.1117	0.7903	-134.145	$k = 1.128, \theta = 0.059$
Normal	0.2214	0.0744	-150.990	$\mu = 19.103, \sigma = 20.835$

Results showed the lognormal distribution was the best fitting model through its demonstration of:

- The KS test yielded a non-significant result with $p = 0.9863$ above 0.05.
- Near-optimal log-likelihood (-133.746)
- The distribution displays an excellent visual match according to Quantile plot in Figure 5.12.
- Positive skewed data placed within a physically reasonable framework.

The histogram in Figure 5.13 demonstrates how these parameters capture both the frequent lower emissions (median at 11.54 gCO₂eq/kWh) and rare higher values (up to 92.15 gCO₂eq/kWh).

The Monte Carlo simulation (100,000 iterations) produced the statistical characteristics presented in Table 5.7.

The simulation results demonstrate:

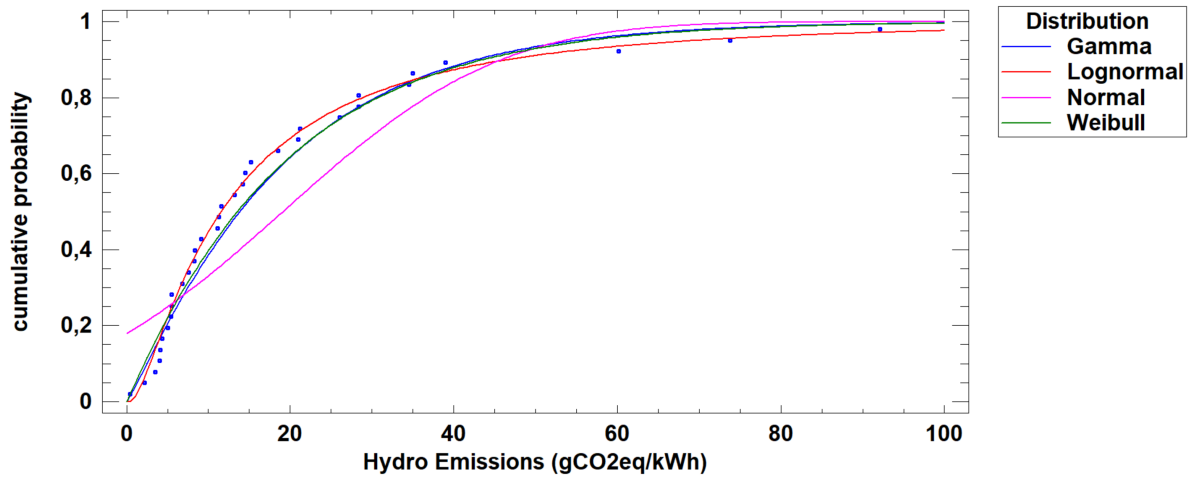


Figure 5.12: Quantile plot showing lognormal distribution fit alongside other candidate distributions.

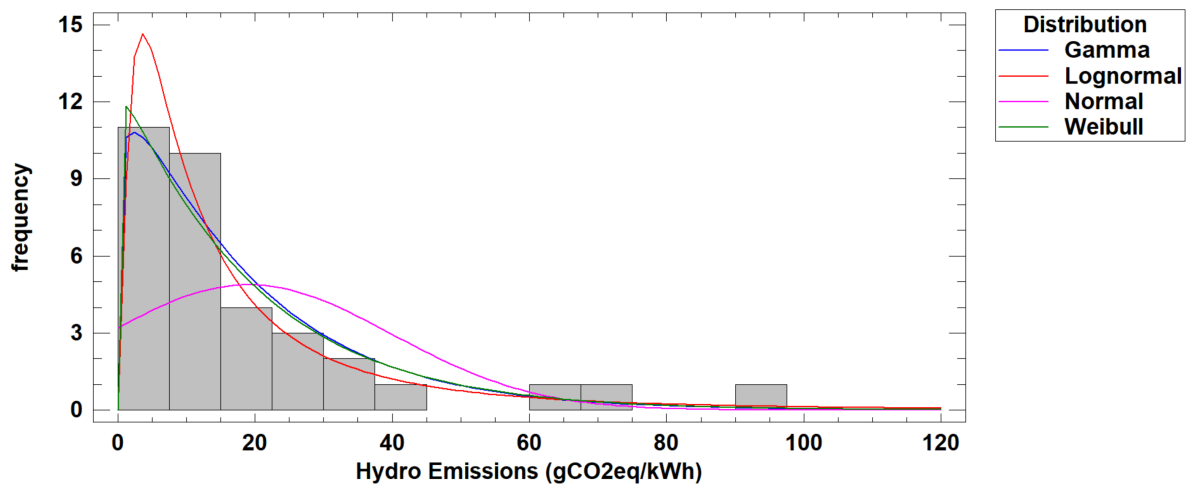


Figure 5.13: Frequency distribution with fitted lognormal density curve alongside possible candidates showing good agreement across all emission ranges

Table 5.7: Descriptive statistics of Hydropower Monte Carlo simulation

Statistic	Value (gCO ₂ eq/kWh)
Mean	20.91
Median	11.53
Standard Deviation	31.52
10th Percentile	2.84
25th Percentile (Q1)	5.54
75th Percentile (Q3)	24.18
90th Percentile	46.65
Interquartile Range	18.64
Minimum	0.12
Maximum	92.15

- **Central Tendency:** Median emissions of 11.53 gCO₂eq/kWh with substantially higher mean (20.91), indicating right-skewed distribution
- **Variability:** Standard deviation of 31.52 reflects extreme differences between low-impact and high-emission hydropower systems
- **Range:** 90% of simulated values fall between 2.84-46.65 gCO₂eq/kWh
- **Extremes:** Maximum observed value of 92.15 gCO₂eq/kWh confirms presence of rare high-emission cases

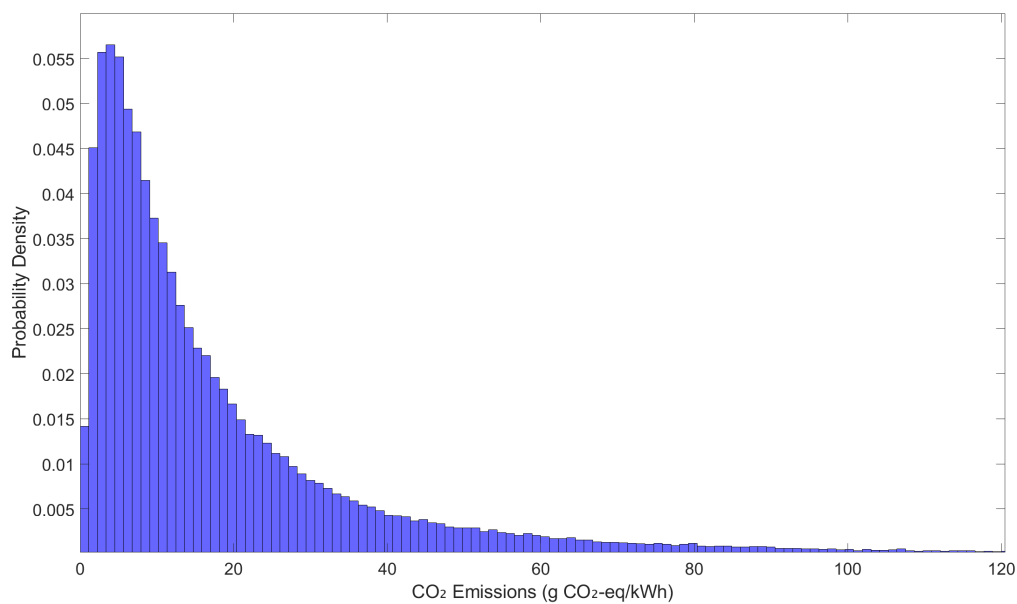


Figure 5.14: Empirical distribution of simulated Hydropower emissions showing Lognormal fit.

The cumulative distribution plot (Figure 5.15) confirms these findings, showing excellent agreement between theoretical and simulated distributions across all percentiles.

These results enable more nuanced Hydropower lifecycle assessments by:

- Quantifying the 18.64 gCO₂eq/kWh interquartile range across installations
- Establishing 46.65 gCO₂eq/kWh as the 90th percentile benchmark
- Identifying the 10% best-performing systems below 2.84 gCO₂eq/kWh
- Supporting comparative analyses with other energy technologies

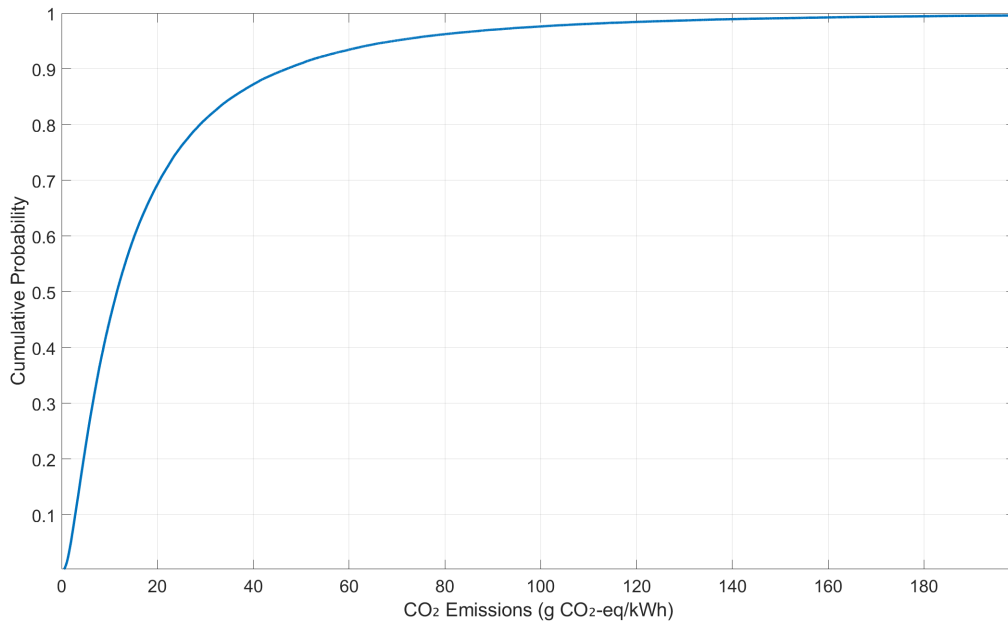


Figure 5.15: Cumulative distribution function for Hydropower emissions.

5.3.4 Biomass Power: Emission Profile and Monte Carlo Analysis

The statistical modelling of biomass lifecycle emissions required rigorous evaluation of parametric distributions to accurately represent the dataset's underlying probability structure. Figure 5.16 depicts the density trace for the biomass distribution.

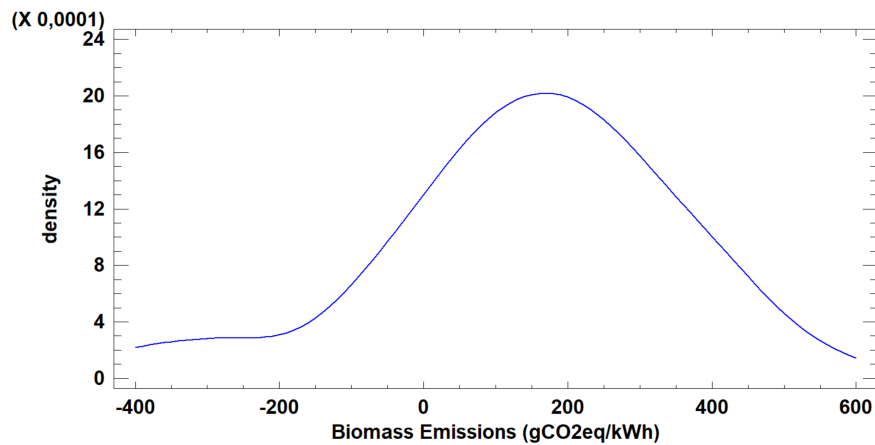


Figure 5.16: Probability density trace of biomass emission values showing extreme range (-395.0 to 510.0 gCO₂eq/kWh)

The evaluation method consisted of Kolmogorov-Smirnov (KS) goodness-of-fit testing in combination with log-likelihood comparisons which evaluated fourteen candidate distributions. The KS test used maximum separation (D_n) to measure differences between empirical and theoretical distribution cumulative curves and log-likelihood revealed distribution quality comparison. The

analysis first removed distributions which showed p-values under 0.05 coupled with physically unacceptable alignments to emission constraints.

The top candidate distributions are summarized by the metrics presented in Table 5.8.

Table 5.8: Goodness-of-fit metrics for biomass emission distributions

Distribution	KS Statistic	p-value	Log-Likelihood	Parameters
Smallest Ext. Val.	0.1175	0.5931	-285.52	$\mu = 231.324, \sigma = 161.200$
Logistic	0.0951	N/A	-286.90	$\mu = 141.479, s = 113.983$
Laplace	0.1562	0.2454	-287.49	$\mu = 127.0, b = 0.0068$
Normal	0.1498	0.2910	-287.83	$\mu = 141.479, \sigma = 197.626$

Results showed the smallest extreme value distribution was the best fitting model through its demonstration of:

- The KS test yielded a non-significant result with $p = 0.5931$ above 0.05.
- Optimal log-likelihood (-285.52)
- The distribution displays an excellent visual match according to Quantile plot in Figure 5.17.
- Physically reasonable handling of extreme values.

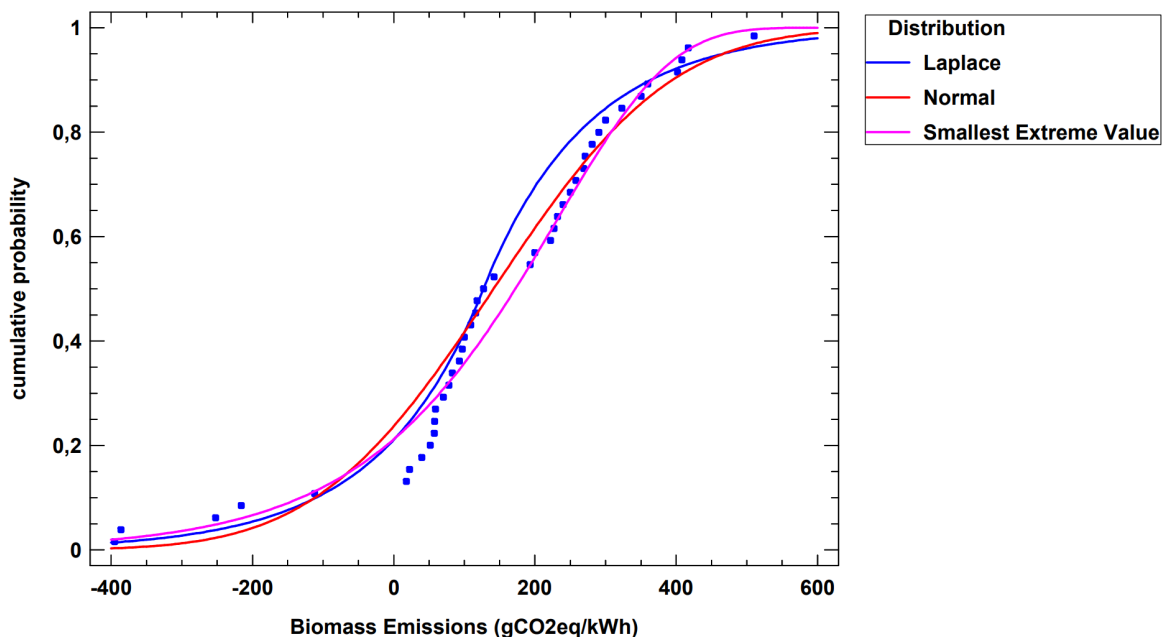


Figure 5.17: Quantile plot showing smallest extreme value distribution fit alongside other candidate distributions.

The histogram in Figure 5.18 demonstrates how these parameters capture both the central tendency (mode at 231.32 gCO₂eq/kWh) and extreme values (from -395.0 to 510.0 gCO₂eq/kWh).

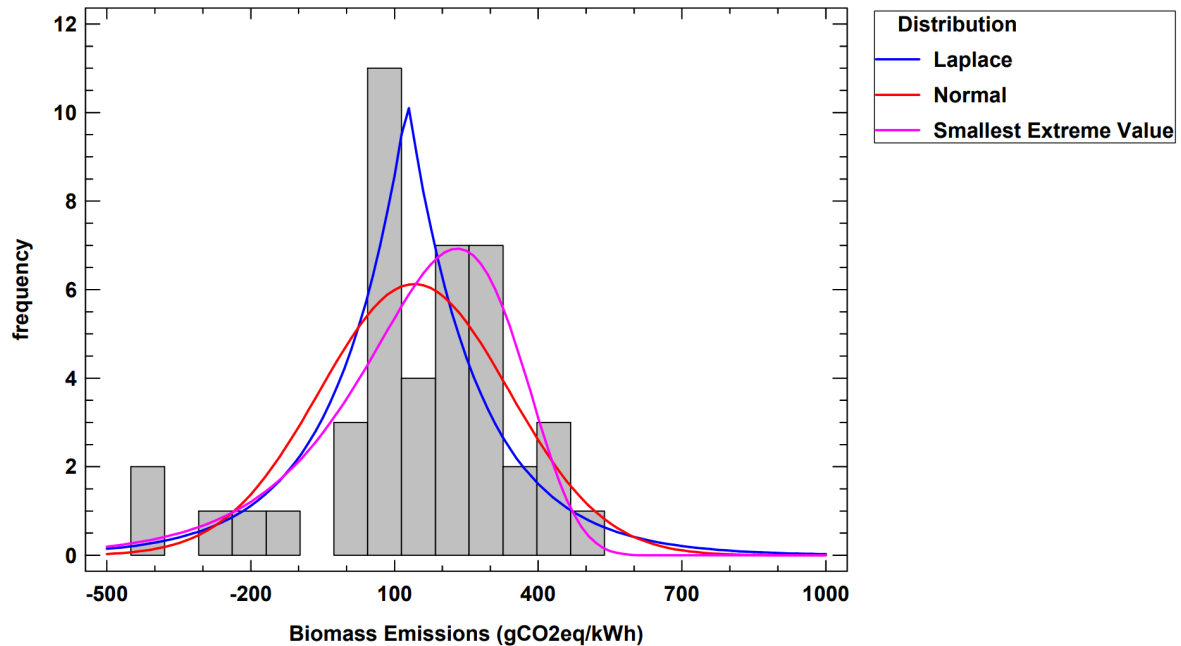


Figure 5.18: Frequency distribution with fitted smallest extreme value density curve showing agreement across the extreme emission ranges

The Monte Carlo simulation (100,000 iterations) produced the statistical characteristics presented in Table 5.9.

Table 5.9: Descriptive statistics of Biomass Monte Carlo simulation

Statistic	Value (gCO ₂ eq/kWh)
Mean	127.67
Median	163.70
Standard Deviation	219.81
10th Percentile	-159.80
25th Percentile (Q1)	11.80
75th Percentile (Q3)	283.19
90th Percentile	369.77
Interquartile Range	271.39
Minimum	-395.00
Maximum	510.00

The simulation results demonstrate:

- **Central Tendency:** Median emissions of 163.70 gCO₂eq/kWh with lower mean (127.67), indicating left-skewed distribution due to negative emission cases

- **Variability:** Standard deviation of 219.81 reflects extreme differences between carbon-negative and high-emission biomass systems
- **Range:** 90% of simulated values fall between -159.80-369.77 gCO₂eq/kWh, showing carbon-negative possibilities
- **Extremes:** Maximum observed value of 510.00 gCO₂eq/kWh confirms presence of high-emission cases

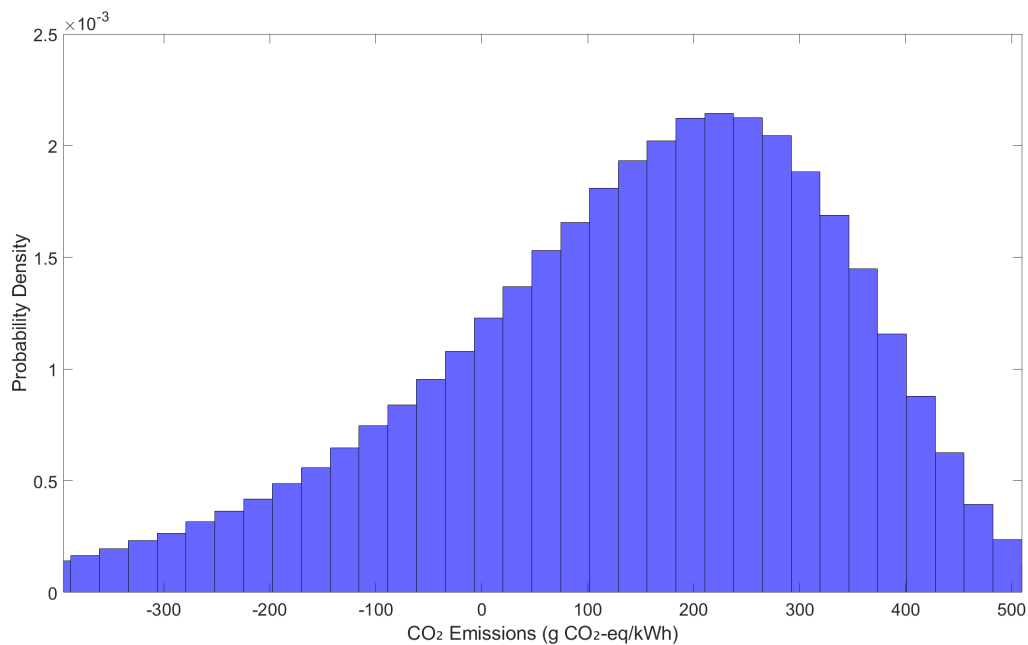


Figure 5.19: Empirical distribution of simulated Biomass emissions showing Smallest Extreme Value fit.

The cumulative distribution plot (Figure 5.20) confirms these findings, showing excellent agreement between theoretical and simulated distributions across all percentiles.

These results enable more nuanced Biomass lifecycle assessments by:

- Quantifying the 271.39 gCO₂eq/kWh interquartile range across systems
- Establishing 369.77 gCO₂eq/kWh as the 90th percentile benchmark
- Identifying the 10% best-performing systems below -159.80 gCO₂eq/kWh (carbon-negative cases)
- Supporting comparative analyses with other energy technologies

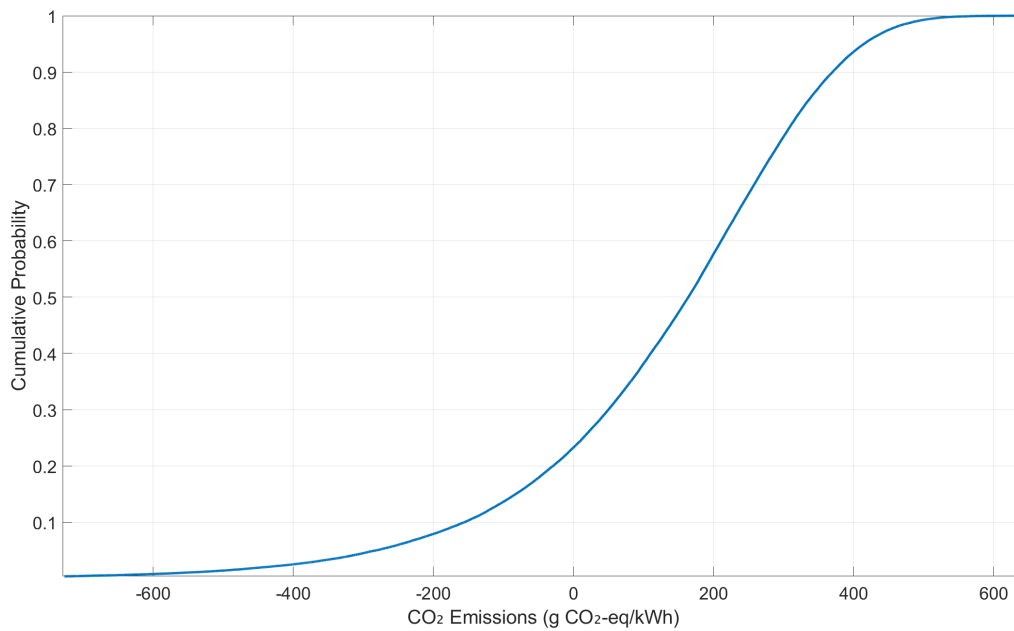


Figure 5.20: Cumulative distribution function for Biomass emissions.

5.3.5 Nuclear Power: Emission Profile and Monte Carlo Analysis

The statistical modelling of nuclear lifecycle emissions required rigorous evaluation of parametric distributions to accurately represent the dataset's underlying probability structure. Figure 5.21 depicts the density trace for the nuclear distribution.

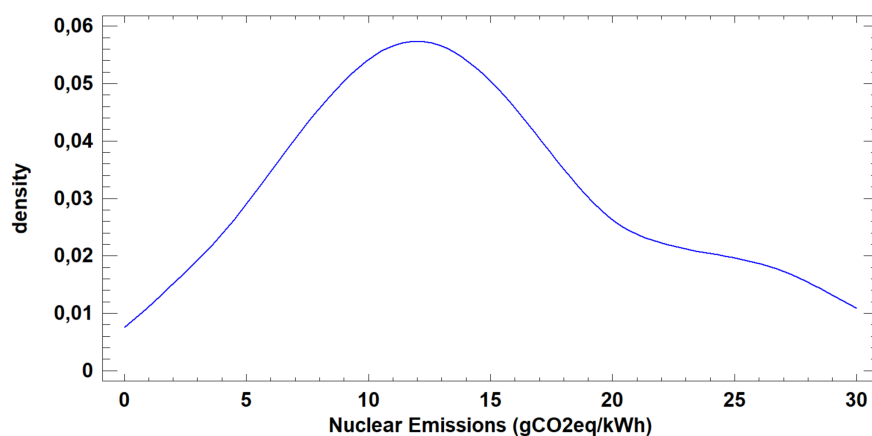


Figure 5.21: Probability density trace of nuclear emission values showing concentration between 5-20 gCO₂eq/kWh

The evaluation method consisted of Kolmogorov-Smirnov (KS) goodness-of-fit testing in combination with log-likelihood comparisons which evaluated fourteen candidate distributions. The KS test used maximum separation (D_n) to measure differences between empirical and theoretical distribution cumulative curves and log-likelihood revealed distribution quality comparison. The

analysis first removed distributions which showed p-values under 0.05 coupled with physically unacceptable alignments to emission constraints.

The top candidate distributions are summarized by the metrics presented in Table 5.10.

Table 5.10: Goodness-of-fit metrics for nuclear emission distributions

Distribution	KS Statistic	p-value	Log-Likelihood	Parameters
Gamma	0.1080	0.9220	-85.59	$k = 4.034, \theta = 0.283$
Laplace	0.1155	0.8784	-87.45	$\mu = 12.7, b = 0.082$
Lognormal	0.1409	0.6802	-86.30	$\mu = 2.529, \sigma = 0.543$
Normal	0.1487	0.6133	-87.09	$\mu = 14.27, \sigma = 7.028$
Uniform	0.2299	0.1282	-84.10	$a = 3.4, b = 28.8$

Results showed the Gamma distribution was the best fitting model through its demonstration of:

- The KS test yielded a non-significant result with $p = 0.9220$ above 0.05.
- Near-optimal log-likelihood (-85.59)
- The distribution displays an excellent visual match according to Quantile plot in Figure 5.22.
- Positive skewed data placed within a physically reasonable framework.

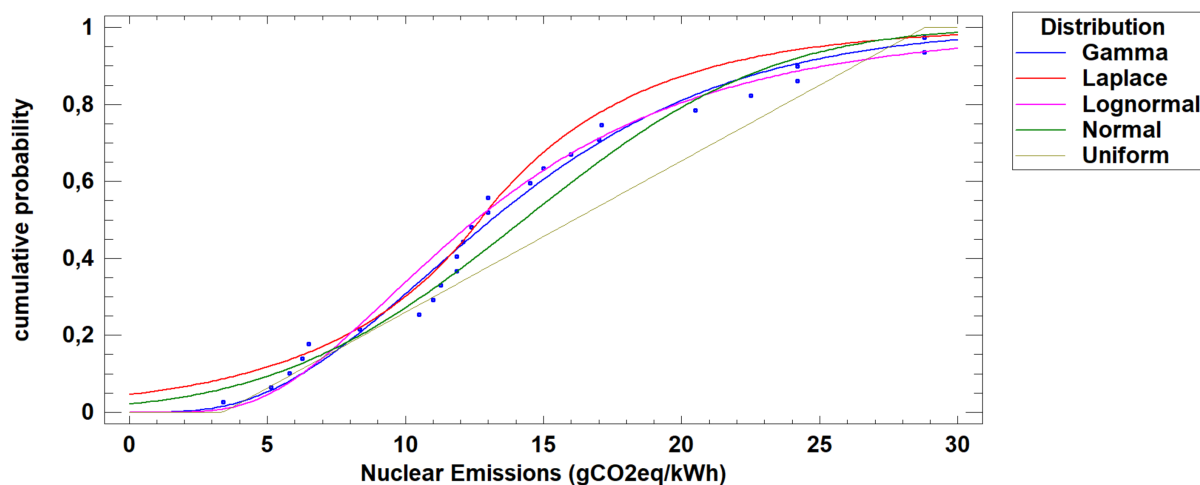


Figure 5.22: Quantile plot showing Gamma distribution fit alongside other candidate distributions.

The histogram in Figure 5.23 demonstrates how these parameters capture both the frequent lower emissions (mode at 12.1 gCO₂eq/kWh) and rare higher values (up to 28.8 gCO₂eq/kWh).

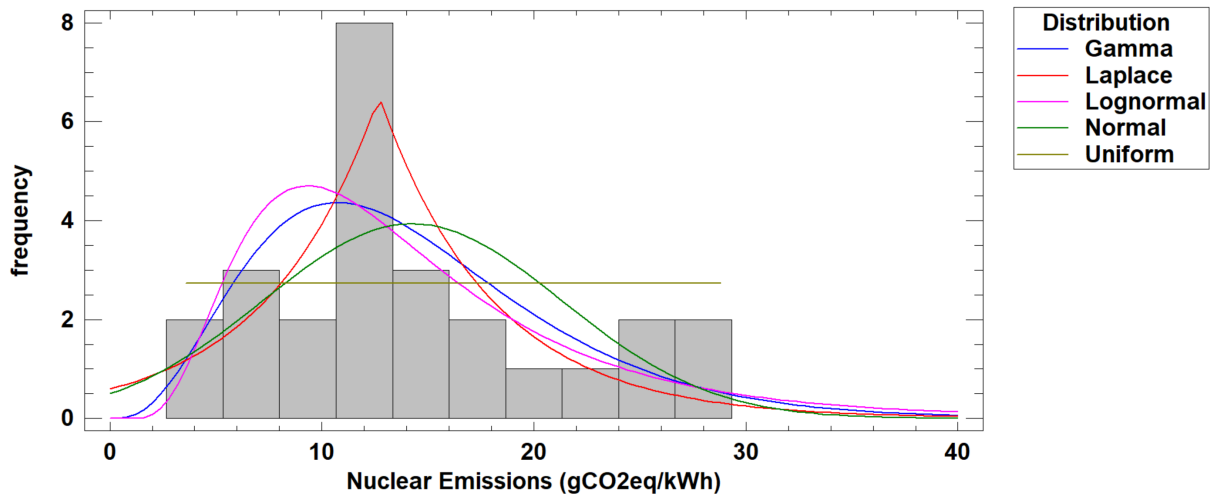


Figure 5.23: Frequency distribution with fitted Gamma density curve showing good agreement across all emission ranges

The Monte Carlo simulation (100,000 iterations) produced the statistical characteristics presented in Table 5.11.

Table 5.11: Descriptive statistics of Nuclear Monte Carlo simulation

Statistic	Value (gCO ₂ eq/kWh)
Mean	14.27
Median	13.14
Standard Deviation	7.18
10th Percentile	6.12
25th Percentile (Q1)	9.05
75th Percentile (Q3)	18.19
90th Percentile	22.84
Interquartile Range	9.14
Minimum	3.40
Maximum	28.80

The simulation results demonstrate:

- **Central Tendency:** Median emissions of 13.14 gCO₂eq/kWh with similar mean (14.27), indicating symmetric distribution
- **Variability:** Standard deviation of 7.18 reflects consistent emissions across nuclear technologies
- **Range:** 90% of simulated values fall between 6.12-22.84 gCO₂eq/kWh

- **Extremes:** Maximum observed value of 28.80 gCO₂eq/kWh confirms presence of high-emission cases

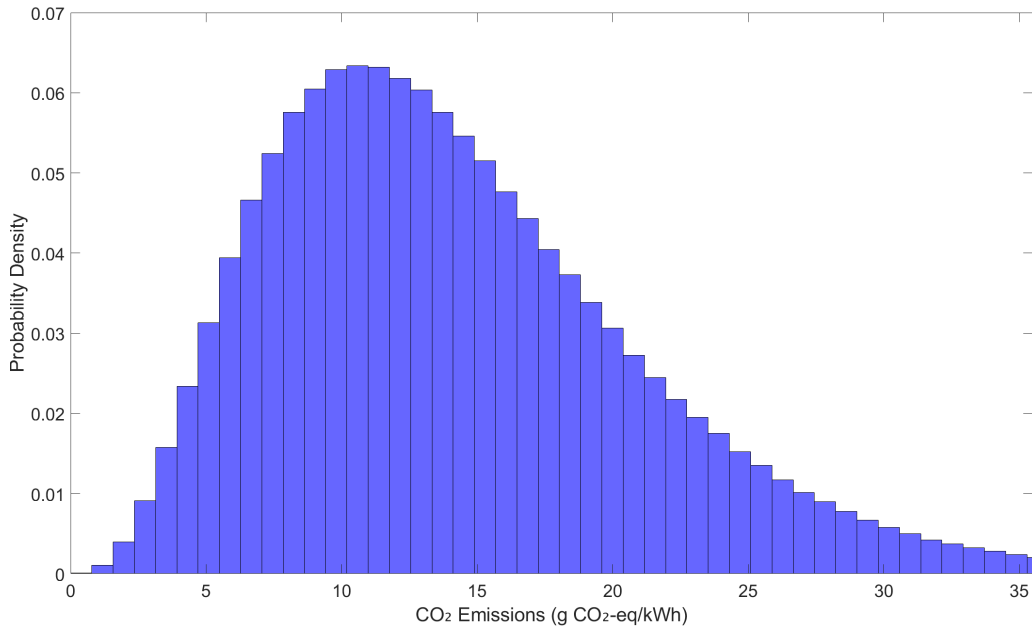


Figure 5.24: Empirical distribution of simulated Nuclear emissions showing Gamma fit.

The cumulative distribution plot (Figure 5.25) confirms these findings, showing excellent agreement between theoretical and simulated distributions across all percentiles.

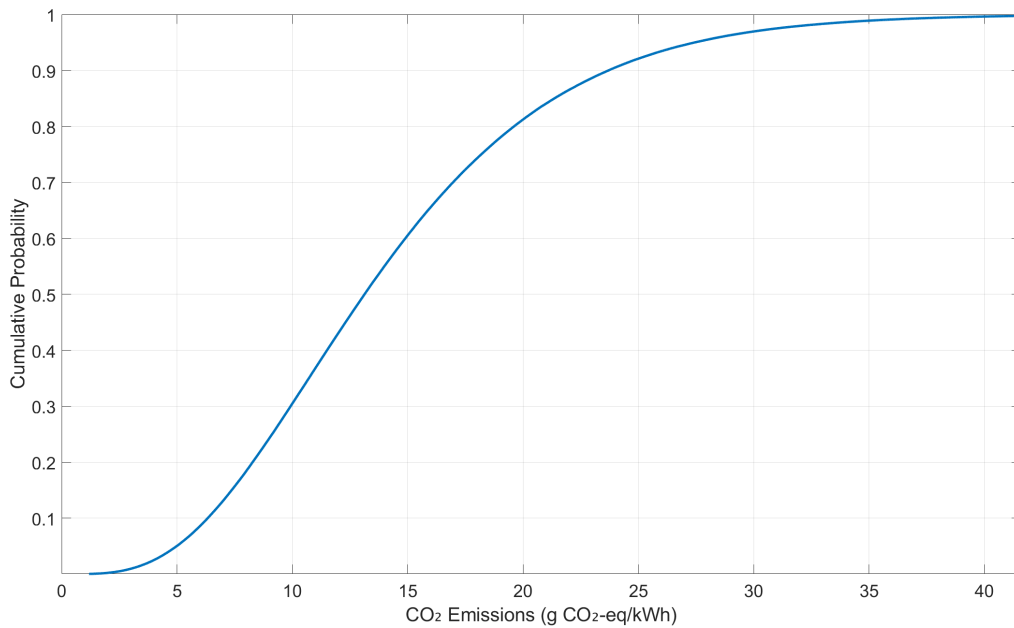


Figure 5.25: Cumulative distribution function for Nuclear emissions.

These results enable more nuanced Nuclear lifecycle assessments by:

- Quantifying the 9.14 gCO₂eq/kWh interquartile range across technologies
- Establishing 22.84 gCO₂eq/kWh as the 90th percentile benchmark
- Identifying the 10% best-performing systems below 6.12 gCO₂eq/kWh
- Supporting comparative analyses with other energy technologies

5.4 EnergyPLAN Simulation of the 100% RES Grid

This section presents the results from the simulations conducted using EnergyPLAN, assuming a 100% renewable energy system in Brazil by 2050. Simulations are carried out as two main phases, with each one depending on how much storage capacity is used and subsequently separated by whether storage is included.

At the beginning of the process, the model inputs were set up using the raw data from the PNE 2050 annex, with the installed capacity of each generation source listed in Table 4.1. For this initial stage, the capacity factors used were obtained from the TMY data explained in the previous section. The main purpose of this simulation is to observe the system results with all renewable resources being present with no changes made.

Both types of simulation are checked out in at least two different situations, using energy storage systems and without them. This includes having 11 GW of PHES and a sensitivity study on green hydrogen storage and Li-ion batteries both explained in Section 4.6. The aim is to find the correct capacity by trying out different configurations and reducing the possibility of wasting generated energy.

For each scenario, the findings are shown in two ways. The results are provided in two ways: potential (not limited) generation and actual generation that includes curtailment, export limits, and storage. The difference between the two graphs makes it clear how storage and system flexibility impact the use of renewable energy.

To better capture the variability during a year, generation profiles for a operational week have been included for each season (summer, autumn, winter, and spring). This way it is possible to identify the level of variations within the year, different stresses faced by the system, and the way storage operates with various climate and demand conditions.

5.4.1 Scenario 1: Simulation with TMY-Based Capacity Factors and without ESS

This subsection presents the simulation results using the capacity factors obtained from the TMY simulation dataset, without applying any correction factors. The use of unadjusted TMY values is based on the observation that the capacity factors reported in EPE’s PNE 2050 differ from those calculated in the TMY analysis. This difference will be further discussed in the section. The mismatch arises from the fact that the PNE 2050 projections include technological advancements in each energy source, whereas the TMY reflects historical performance data.

The information in Table 5.12 makes clear that the annual values from the simulation tend to be quite different from what the EPE aimed for in its 100% renewable grid scenario. Except for PCH, energy generation from all other sources is significantly higher than the predicted levels in the PNE scenario.

Table 5.12: Scenario 1: Comparison between EnergyPLAN simulation results and EPE’s PNE 2050 projections for annual generation without correction factor

Source	EnergyPLAN (TWh)	PNE (TWh)	Difference (%)
Electricity Generation			
Wind	758.09	811.94	-6.63%
PV (centralized)	153.27	199.20	-23.03%
Biomass	46.28	46.14	+0.30%
Nuclear	25.35	25.17	+0.72%
ROR Hydro	245.80	–	–
PCH	49.36	41.10	+20.10%
Reservoir Hydro	190.90	–	–
Hydro Total	436.70	451.73	-3.33%
Total DG	95.63	100.43	-4.78%
Demand and Balance			
Annual Generation	1564.68	1675.71	-6.62%
Annual Demand	1510.85	1510.85	0.00%
Import	29.15	–	–
Export	74.86	–	–

EnergyPLAN adds regional imports (29.15 TWh) and exports (74.86 TWh) to keep the system balanced, avoiding curtailments, unlike the PNE that does not mention regional interchange in electricity. As there are no ESS in this simulation, the system can only stay balanced by importing electricity. Consequently, EnergyPLAN uses 29.15 TWh of imported electricity to deal with demand which represents 1.93% of the total annual demand.

As this simulation does not reflect the best or most accurate situation for evaluating Brazil’s future energy system because it lacks both ESS and capacity factor corrections, the detailed

images are attached in the appendix. These include the pie chart of annual electricity generation and power flows (Figure A.6), as well as the typical operational week profiles for each season (Figure A.7), which help illustrate the system’s seasonal variability and dispatch behaviour under current limitations.

5.4.2 Scenario 2: Simulation of Potential Generation Using PNE-Based Capacity Factors

In this subsection, the capacity factors of the RES were adjusted using a EnergyPLAN’s correction factor tool to fit with the official projections of the PNE 2050 report. The correction was proposed to compensate the differences observed between historical capacity data from the TMY and the EPE’s predicted values. To calculate the correction factors, the expected annual generation values provided in Table 4.2 were divided by the corresponding installed capacity values from Table 4.1. By using these derived capacity factors, the input profiles in EnergyPLAN were modified to match the needs of a long-term planning approach.

EnergyPLAN applies this correction using a scalar factor applied to the hourly availability curve, as represented in Equation 5.1:

$$E_{\text{VRES}}(h) = \sum_{i=1}^N (C_{\text{VRES}_i} \cdot \delta_{\text{VRES}_i}(h) \cdot \text{CF}_{\text{corr}} \cdot \text{FAC}_{\text{curtail}}(h)) \quad (5.1)$$

Where C_{VRES_i} is the installed capacity, $\delta_{\text{VRES}_i}(h)$ is the normalized hourly profile, CF_{corr} is the correction factor, and $\text{FAC}_{\text{curtail}}(h)$ accounts for curtailment behaviour.

This simulation does not include any ESS or curtailment mechanisms, as a result, it does not try to replicate the real operation dynamics of the future Brazilian power system, which would require tools to balance supply and demand, mechanisms to deal with excess of power production, manage import and export capacities, and ensure overall system stability. Instead, the objective of the simulation is to estimate a maximum potential generation from each energy source when their capacity factors are adjusted to fit with the PNE projections. Therefore, the outcomes of this simulation can be seen as the maximum possible generation potential of each source, assuming unrestricted operational conditions. This scenario will be especially useful to compare its outputs with simulations that add in technical and operational restrictions.

Table 5.13 compares the capacity factors in the TMY dataset and the PNE 2050 report, as well as their relative variation.

The results of the simulation using the adjustment factors are presented in Table 5.14, that

Table 5.13: Comparison of Capacity Factors between TMY and PNE 2050

Source / Technology	CF (TMY)	CF (PNE)	Variation
Large Hydropower Plants (UHE)	0.42	0.42	0
Small Hydropower Plants (PCH)	0.32	0.29	-3%
Wind Power	0.41	0.44	+3%
Solar Power	0.24	0.28	+4%
Biomass	0.29	0.29	0
Nuclear	0.85	0.85	0
Distributed Generation (DG)	0.18	0.23	+5%

compares EnergyPLAN generated output with what is outlined in the PNE 2050 scenario.

Table 5.14: Comparison between EnergyPLAN simulation results (adjusted CF) and PNE 2050 projections

Source	EnergyPLAN (TWh)	PNE (TWh)	Difference (%)
Electricity Generation			
Wind	811.65	811.94	-0.04%
PV (centralized)	198.25	199.20	-0.48%
Biomass	46.28	46.14	+0.30%
Nuclear	25.35	25.17	+0.72%
ROR Hydro	270.78	–	–
PCH	46.09	41.10	+12.14%
Reservoir Hydro	191.92	–	–
Hydro Total	462.70	451.73	+2.43%
Total DG	99.43	100.43	-1.00%
Demand and Balance			
Annual Generation	1689.75	1675.71	+0.84%
Annual Demand	1510.85	1510.85	0.00%
Import	19.87	–	–
Export	198.16	–	–

5.4.3 Scenario 3: Simulation with Grid Operation Constraints and PHES

In contrast to previous simulations, which sought to estimate the maximum generation potential under ideal conditions and without restrictions, the current simulation incorporates real operational limitations, having greater accuracy of the effective functioning of the Brazilian electrical system. In this scenario, restrictions on energy import and export capacity, VRES curtailment mechanisms, ESS integration, and grid balancing strategies are implemented.

The first scenario considered involves the introduction of pumped-hydro energy storage (PHES), based on the technical survey carried out by GESEL (2021), which identified an installable potential of 11 GW in Brazil. This storage capacity is integrated into the EnergyPLAN

model as a solution to mitigate the variability of renewable sources, allowing the displacement of excess energy to times of greater demand or lower generation.

Table 5.15 represents the annual generation data of the system in the new observed context, reflecting the combined impacts of the operation control measures, curtailment of renewables and use of hydraulic storage.

Table 5.15: Comparison between EnergyPLAN results with grid constraints and PHES, and PNE 2050 projections

Source	EnergyPLAN (TWh)	PNE (TWh)	Difference (%)
Electricity Generation			
Wind	811.60	811.94	-0.04%
PV (centralized)	189.67	199.20	-4.79%
Biomass	46.28	46.14	+0.30%
Nuclear	25.35	25.17	+0.72%
ROR Hydro	249.29	–	–
PCH	46.09	41.10	+12.14%
Reservoir Hydro	158.06	–	–
Hydro Total	407.35	451.73	-9.82%
Total DG	99.43	100.43	-1.00%
Demand and Balance			
Annual Generation	1625.77	1675.71	-2.98%
Annual Demand	1510.85	1510.85	0.00%
Import	19.87	–	–
Export	109.56	–	–
PHES	13.13	–	–

When comparing the results of this simulation with those obtained in the previous scenario with correction of capacity factors, a reduction in electricity imports is observed, going from 19.87TWh to 15.86TWh — a decrease of approximately 18%. This drop is directly related to the introduction of the PHES, which allowed better use of surplus energy generation, reducing the need to resort to imports to meet times of deficit. Furthermore, there is a slight reduction in the total generation of the system (from 1689.75 TWh to 1625.77 TWh), while exports also decrease from 198.16 TWh to 109.56 TWh. This reduction in exports is not only due to the fact that part of the excess energy was consumed by the pumping process itself, but also to the restrictions imposed by the limits of international transmission lines, which were implemented in the simulation. These results indicate that the presence of PHES acts to help balance the system's operation, and also as an energy retention mechanism, avoiding waste due to excessive export and contributing to greater energy self-sufficiency.

Table 5.15, also demonstrates the occurrence of curtailment observed in all centralized renewable energy sources. The most impacted source was hydroelectric, which saw a reduction of almost 10% in its annual generation. This reduction is associated with its strategic role in controlling the system's operation, providing subsidiary services — such as frequency regulation and operating reserve — a role that it already established in the current Brazilian electrical system and that is expected to continue, given the operational flexibility of this technology. Centralized solar generation showed a slight reduction, less than 5%, reflecting the curtailment applied during peak generation periods, in which production exceeds instantaneous demand. On the other hand, wind generation showed practically no significant variation, indicating good compatibility with the demand profile and the control mechanisms employed in this operational scenario.

The functioning of the system under realistic operational constraints, including the implementation of pumped storage (PHES), grid balancing and renewable sources curtailment, can be better understood through the seasonal behavior of generation and demand. The figure 5.26 illustrates the hourly electricity generation by source and the corresponding demand curve during a representative operating week for each season. The results highlight the interaction between variable renewable generation, storage dispatch and import mechanisms, demonstrating how the system responds to seasonal variability and operational limitations.

The monthly behaviour of electricity imports throughout the year are also important data to be analyzed. As shown in Figure 5.27, it is observed that energy imports are concentrated mainly between the months of January and April, a period that corresponds to summer and early autumn in the Southern Hemisphere. This seasonal pattern indicates greater dependence on external supply during periods of higher demand and lower system flexibility, highlighting the importance of interconnections as a complementary mechanism for balancing the electricity grid in critical months for this specific scenario. However, this dependence on external resources is not desirable from an energy security perspective. This suggests, in the long term, a potential need to expand strategies to support the energy system in Brazil, such as the diversification of energy storage technologies, the strengthening of grid control mechanisms and the implementation of demand and response actions.

Figure 5.28 shows the monthly variation of the average capacity factors of the main renewable generation sources throughout the year. Analysis of these curves allows us to identify important seasonal patterns and assess the degree of complementarity between the different renewable technologies.

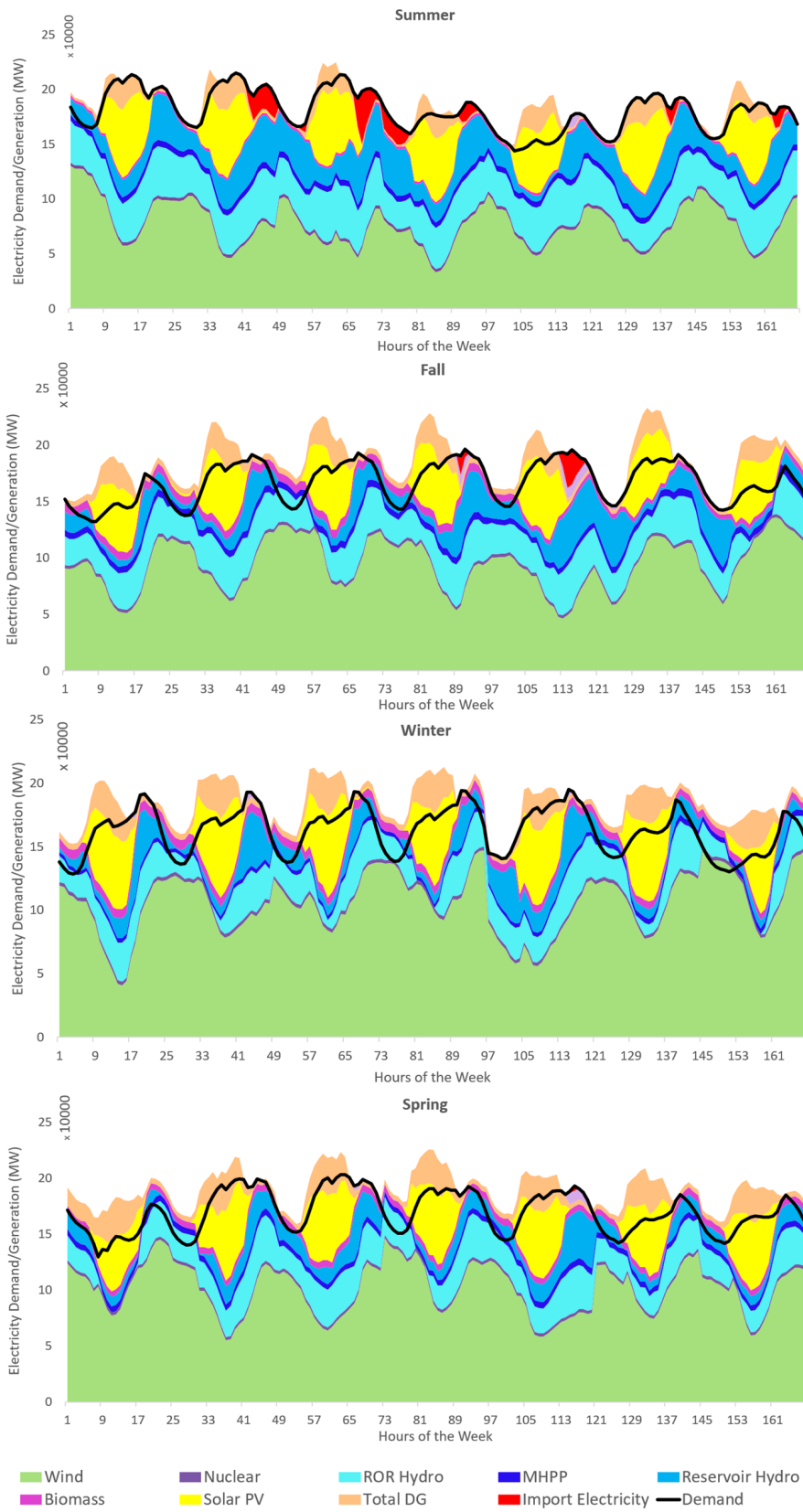


Figure 5.26: Hourly electricity generation and demand during a typical operational week for each season for Scenario 3.

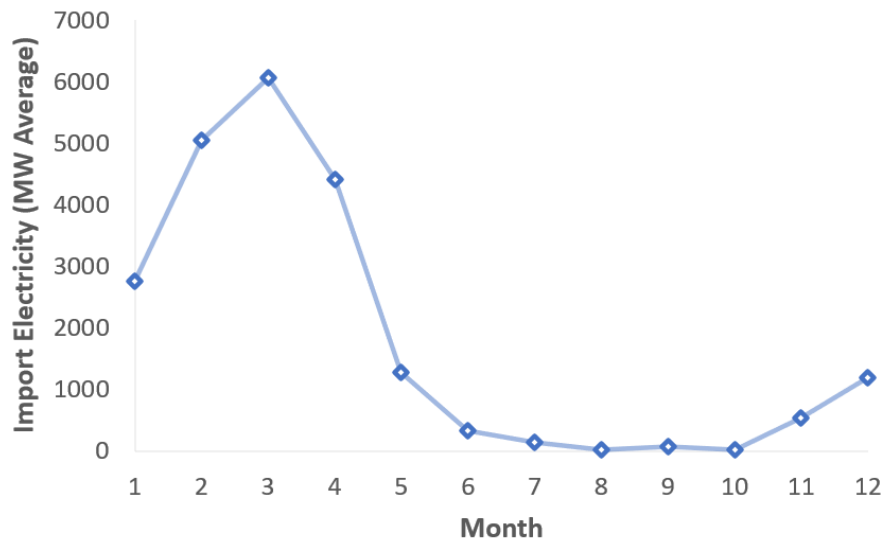


Figure 5.27: Average monthly electricity imports throughout the year for Scenario 3.

The seasonal analysis of system operation shows a clear mismatch between generation patterns and electricity demand in the 100% renewable scenario for Brazil. As shown in Figure 5.26, hydropower generation is higher in the first months of the year, especially during summer, when rainfall and reservoir inflows are greater. On the other hand, wind generation peaks later in the year, mainly from September to January. This inverse seasonality between the two main renewable sources creates a structural issue: even though hydropower provides plenty of energy early in the year, its flexibility and storage capacity are limited in the simulated scenario. At the same time, wind power is the main source in the mix, which leads to a critical gap during summer and early autumn. In this period, wind capacity factors drop and demand stays high, increasing dependence on electricity imports to meet system needs. Figure 5.27 shows that most imports occur between January and April, which reveals a seasonal vulnerability. These results reinforce the need for more storage capacity and better seasonal balancing strategies to reduce import dependence and improve energy security in a fully renewable grid.

It is possible to observe that the sources with the greatest seasonality are reservoir hydroelectric and wind. Generation from reservoirs hydroelectric peaks between February and April, with capacity factors above 0.60, and decrease sharply from May onwards, reaching its minimum value in September. However, wind generation reaches its lowest values in the months of May to August (with a capacity factor of around 0.29) and increases again from September onward, reaching peaks between November and January. These results indicate good complementarity between wind and reservoir hydroelectric sources, which contributes to the stability of the system throughout the year.

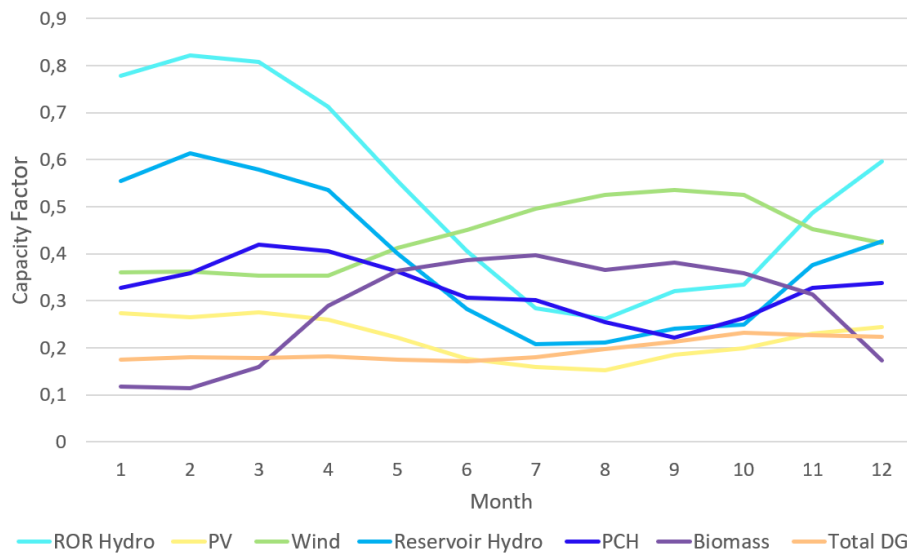


Figure 5.28: Monthly capacity factor variation for each renewable energy source, showing seasonal trends and resource complementarity.

Solar photovoltaic (PV) generation proved to be the most constant source throughout the year, with a capacity factor varying slightly between 0.25 and 0.28, which demonstrates its predictability and regularity. Total distributed generation (Total DG), which reflects the combination of decentralized technologies, follows a smoothed profile and shows gradual growth in the second half of the year. This result is due to the fact that distributed generation is composed, in its overwhelming majority, of photovoltaic systems. Distributed solar generation maintained good consistency in relation to centralized solar generation throughout the year, despite the former presenting a significantly lower capacity factor than the latter, which contributes to a stable production profile in the decentralized segment.

Biomass generation, in turn, presents a seasonal pattern strongly influenced by the sugarcane harvest calendar, which concentrates the availability of bagasse for burning between the months of April and November. As a result, biomass capacity factors increase significantly during this period, reaching their peak between July and October. This observed pattern results in good complementarity with wind energy, which tends to have lower performance in the middle months of the year (may to october), coinciding with hydroelectric generation from reservoirs, which also recovers its generation capacity from the second semester of the year. However, it is worth highlighting that, despite all its strategic complementary potential, biomass still represents a relatively small fraction of the system’s total generation when compared to the contribution of large hydroelectric reservoirs.

5.4.4 Scenario 4: Integration and Sensitivity Analysis of Lithium Battery and Green Hydrogen Storage

This section expands the previous simulation by integrating lithium-ion battery storage systems and performing a sensitivity analysis to assess their impact on the operation of the power system. The objective is to identify storage configurations that minimize the need for electricity imports and to observe how the system responds to variations in installed power capacity and energy storage capacity. Although this analysis will later be applied to green hydrogen, each storage alternative is initially explored separately to better understand its individual influence on system operation.

As discussed in the previous chapter, both lithium-ion batteries and green hydrogen have advantages and limitations. Lithium-ion batteries offer high efficiency and fast response time, which makes them suitable for grid balancing and short-term storage. However, its energy storage capacity is relatively limited. In contrast, green hydrogen can be stored in larger quantities and used for long-term balancing, although it has significantly lower efficiency and slower conversion dynamics.

The first sensitivity analysis focuses on lithium-ion battery storage. The baseline values used for modeling are derived from actual systems already in operation; according to the 2024 Statistical Report on Electrochemical Energy Storage Power Stations by the China Electricity Council (CEC), as of December 31, 2024, China has achieved a total installed capacity of 62GW and 141GWh of lithium-ion battery energy storage.

In California, lithium-ion battery storage systems have also been expanding rapidly. According to data from the California Energy Commission (CEC), as of April 2025, the total installed battery storage capacity in the state exceeded 15,700 MW, with an additional 8,600 MW planned by the end of 2027, bringing the total energy storage capacity estimated at approximately 40 GWh.

At this phase, a two-dimensional sensitivity analysis is performed to evaluate the impact of integrating lithium-ion batteries into the electrical system. Both installed power capacity (MW) and energy storage capacity (MWh) are input variables, and various combinations between these two parameters are simulated. This approach allows us to observe, in a more comprehensive way, how the system behaves under different technical configurations, as well as to identify which combinations minimize the need for imported electrical energy.

For each pair of installed power and energy storage values, the model is run and the annual amount of imported energy is recorded as the main performance indicator. This method allows

identifying more efficient operating regions, in addition to understanding the technical and operational limits of the system in response to the renewable variability.

Based on the literature and experimental data, it is assumed that lithium-ion batteries have a full-cycle efficiency of 90%, with 95% efficiency in charging and 95% in discharging. These values are consistent with commercial systems already in operation, including in second-life applications.

Table 5.16 presents the results of the two-dimensional sensitivity analysis for lithium-ion battery storage systems. The table shows the annual electricity imports (in TWh) resulting from different combinations of installed power capacity (GW) and energy storage capacity (GWh). The goal of this analysis is to identify the configurations that most effectively reduce import needs. As expected, increasing either parameter generally improves system self-sufficiency, with diminishing returns beyond certain thresholds.

Table 5.16: Annual electricity imports (TWh) as a function of lithium-ion storage power capacity (GW) and energy capacity (GWh).

Installed capacity (GW)	Energy Storage Capacity (GWh)										
	20	40	60	80	100	125	150	175	200	250	300
5	16.74	15.81	15.44	15.22	15.08	14.95	14.85	14.75	14.67	14.57	14.48
10	16.40	14.67	13.74	13.16	12.79	12.44	12.18	11.99	11.83	11.58	11.36
15	16.39	14.39	13.15	12.33	11.69	11.08	10.71	10.37	10.07	9.66	9.37
20	16.39	14.33	12.95	11.99	11.26	10.47	9.85	9.42	9.07	8.48	8.04
25	16.39	14.33	12.93	11.89	11.08	10.24	9.49	8.91	8.45	7.76	7.23
30	16.39	14.33	12.92	11.87	11.01	10.14	9.36	8.72	8.19	7.33	6.77
35	16.39	14.33	12.92	11.87	11.00	10.12	9.32	8.65	8.09	7.16	6.50
40	16.39	14.33	12.92	11.87	11.00	10.12	9.32	8.64	8.06	7.10	6.37
50	16.39	14.33	12.92	11.87	11.00	10.12	9.32	8.64	8.06	7.07	6.33
75	16.39	14.33	12.92	11.87	11.00	10.12	9.32	8.64	8.06	7.07	6.33

Based on the results of the simulation with the integration of lithium-ion battery storage systems, a detailed graphical analysis was performed to identify the most technically efficient configurations of energy storage (GWh) and installed power (GW) to reduce dependence on electricity imports in the Brazilian system.

The main appliance for this analysis was a contour plot as shown in Figures 5.29 and 5.30, which shows the levels of avoided imports (in TWh) as a function of storage capacity and installed power. To complement this visualization, technical gradient curves were superimposed (∇Z). These curves represent the magnitude of the variation in the benefit (avoided imports) for each additional unit of technical investment — that is, they show where the system responds with greater or lesser intensity to capacity increases.

The highest gradients ($\nabla Z > 2$, for example) indicate regions where small infrastructure expansions still provide large gains in terms of avoided imports. As they approach the line $\nabla Z = 1.0$, these gains become proportionally equivalent to the technical effort invested. However, in areas with $\nabla Z < 1.0$, the returns begin to decrease, characterizing regions of saturation, where there is lower incremental efficiency.

Based on this interpretation, two technical points were selected as strategic references:

- **Early Threshold Point (100 GWh, 15 GW)** This point is located exactly on the line $\nabla Z = 1.0$, corresponding to 7.52 TWh of avoided imports. It represents the limit of the region of high technical efficiency, where the system still delivers returns proportional to the effort invested. It is therefore an excellent reference for short and medium-term decisions, as it combines relevant gains with relatively contained infrastructure.
- **True Knee Point (60 GWh, 15 GW)** Identified by curvature analysis (Hessian-based method), this point provides 6.09 TWh of avoided imports — representing the location of maximum surface curvature. Although it lies within a more moderate benefit zone, it mathematically reflects the most abrupt inflection of the surface, where the system transitions from rapid benefit growth to diminishing returns. For this reason, it is interpreted as the *True Knee Point* — a critical technical reference that can guide system design choices with high mathematical precision.

This point was identified by treating the avoided import matrix as a continuous surface $Z(x, y)$, with x being the energy storage and y the installed power. The first order partial derivative were calculated s as:

$$\frac{\partial Z}{\partial x} = f_x, \quad \frac{\partial Z}{\partial y} = f_y \quad (5.2)$$

After that, the Hessian matrix was built using the second-order derivatives:

$$H = \begin{bmatrix} \frac{\partial^2 Z}{\partial x^2} & \frac{\partial^2 Z}{\partial x \partial y} & \frac{\partial^2 Z}{\partial y \partial x} & \frac{\partial^2 Z}{\partial y^2} \end{bmatrix} \quad (5.3)$$

The determinant of this matrix is used as an approximation of Gaussian curvature:

$$K = \frac{\partial^2 Z}{\partial x^2} \cdot \frac{\partial^2 Z}{\partial y^2} - \left(\frac{\partial^2 Z}{\partial x \partial y} \right)^2 \quad (5.4)$$

The point on the grid that has the highest value for K shows the place where returns start to decline after reaching a peak. The calculated values of K are present in Table A.7 in the appendix section.

The choice of the *True Knee Point* as the main planning reference is justified by its technical value and also by its robustness and precision considering possible future scenarios. This point represents a configuration in which the system still responds efficiently, even after the saturation threshold, giving a significant volume of avoided imports (more than 6 TWh), with a controlled level of infrastructure. As a result, it emerges as a particularly relevant option in energy transition strategies, where the objective is to balance technical expansion and energy security.

The combined analysis of isolines, gradient curves and performance points therefore provides a richer reading and a clearer understanding of the observed pattern in the simulated system. In addition to revealing areas of greatest stability and technical return, it provides clear guidelines for selecting configurations that maximize impact with optimized infrastructure. This type of graphical and analytical approach represents a powerful tool for efficiency-driven energy planning, especially in systems with a high participation of renewable sources and the need for storage support.

Following the analysis of lithium-ion battery storage, green hydrogen was added as a further option in the simulated electricity system, mainly examined as a storage option for medium and long-term solution due to the characteristics of hydrogen that can be stored in tanks and reservoirs. Unlike batteries, the systems used for green hydrogen requires two separate equipments to produce and convert the green hydrogen: an electrolyser to produce hydrogen and a fuel cell (or gas turbine) to reconvert it into electricity. These two components do not necessarily have to be sized the same, as their installed powers can be independently sized.

In order to address this characteristic, the sensitivity analysis was performed based on the (E/C) configuration grid that uses electrolyser capacity in GW represented as “E” and fuel cell capacity in GW labelled as “C”. Each row in the table stands for a certain E/C configuration, so the analysis reflects how such systems could really be scaled separately in practice. The results are display in Table 5.17.

The approach taken for lithium-ion batteries is also being used for hydrogen storage. A matrix of avoided electricity imports (TWh) was constructed as a function of energy storage capacity (GWh), and their gradients magnitude maps (∇Z) were calculated to determine areas of optimal technical response. Furthermore, a Hessian-based analysis of second-order derivatives

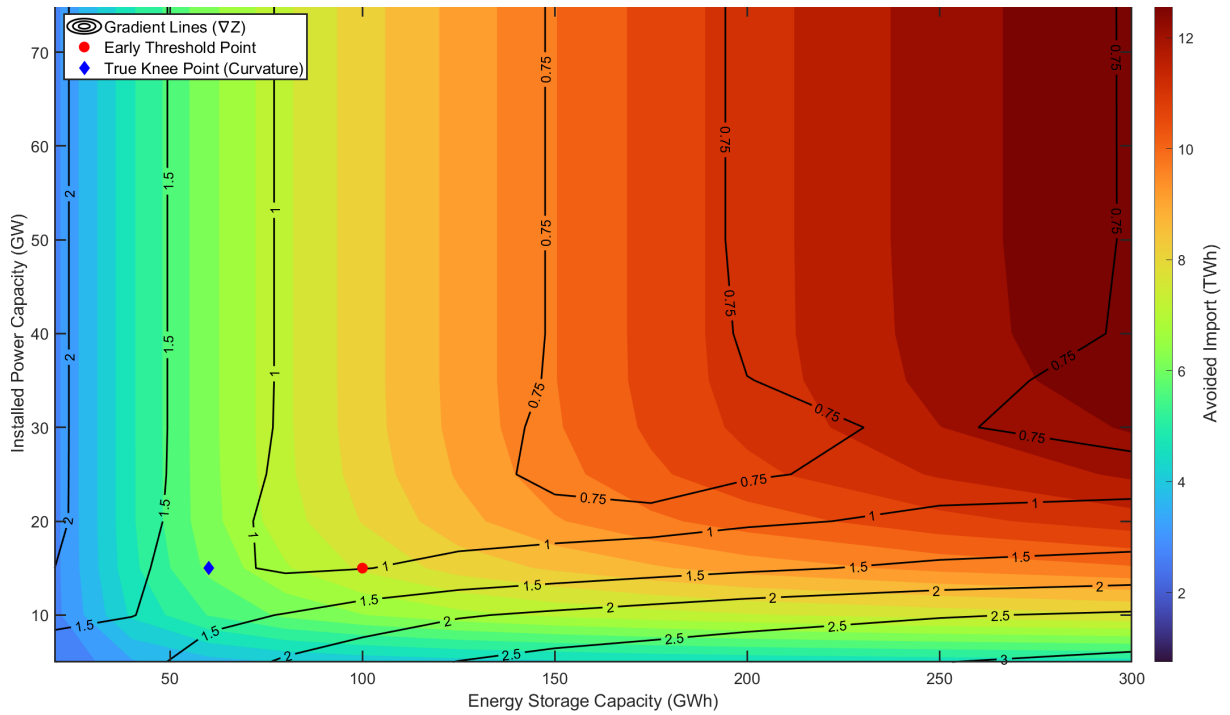


Figure 5.29: Isoline map of avoided electricity imports (TWh) as a function of energy storage capacity (GWh) and installed power capacity (GW) of Lithium-ion batteries, overlaid with technical gradient lines (∇Z). Two reference points are highlighted: the **Early Threshold Point** (100 GWh, 15 GW), located exactly on the $\nabla Z = 1.0$ gradient line, and the **True Knee Point** (60 GWh, 15 GW), identified by the Hessian determinant as the point of maximum curvature where the system begins to exhibit strong diminishing returns.

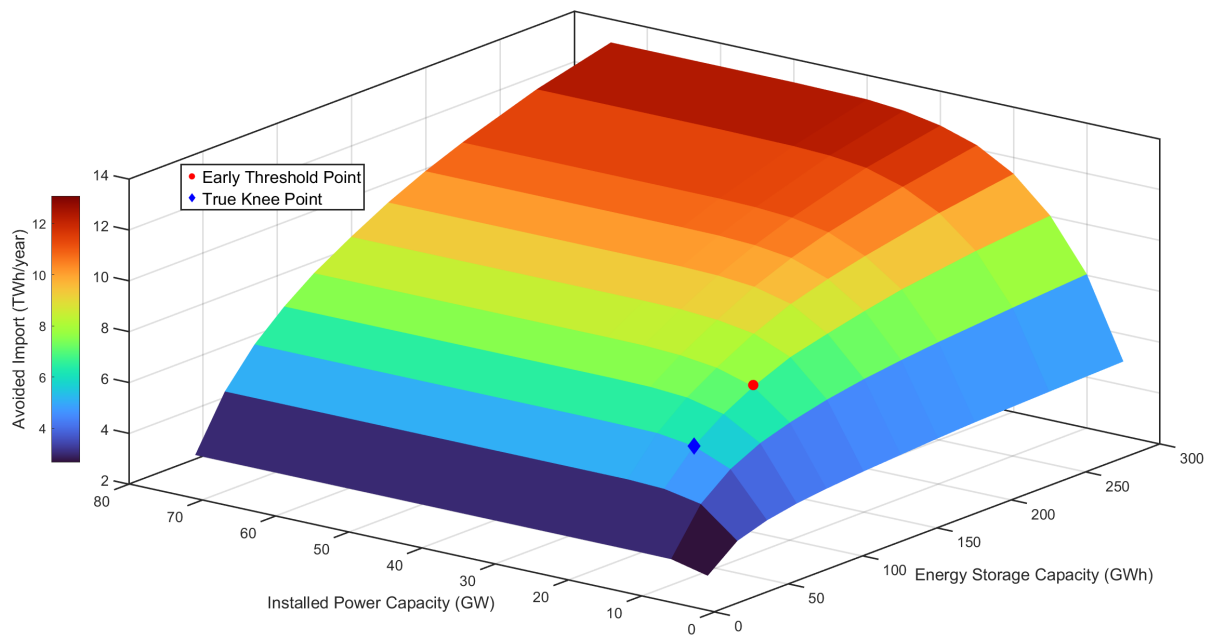


Figure 5.30: Three-dimensional surface of avoided electricity imports (TWh/year) as a function of energy storage capacity (GWh) and installed power capacity (GW) of Lithium-ion batteries. The surface illustrates the simulated system's response to different infrastructure configurations. Two reference points are highlighted: the **Early Threshold Point** (red circle), where the benefit-to-effort ratio reaches $\nabla Z = 1.0$, and the **True Knee Point** (blue diamond), mathematically identified through the Hessian determinant as the location of maximum curvature, representing the most critical inflection in the system's performance surface.

Table 5.17: Annual electricity imports (TWh) as a function of hydrogen storage system configuration — electrolyzer/fuel cell power capacity (GW) and storage energy capacity (GWh).

E/C Configuration (GW/GW)	Energy Storage Capacity (GWh)								
	100	200	300	500	700	900	1200	1500	2000
5/5	11.45	11.18	11.12	11.00	10.88	10.76	10.58	10.40	10.10
5/10	11.19	10.81	10.65	10.42	10.30	10.18	10.00	9.82	9.52
5/15	11.14	10.67	10.51	10.27	10.03	9.91	9.73	9.55	9.25
10/10	10.58	10.05	9.77	9.54	9.42	9.30	9.12	8.94	8.64
10/20	9.78	9.40	9.19	8.85	8.65	8.45	8.27	8.09	7.79
10/30	10.49	9.76	9.34	8.85	8.61	8.45	8.27	8.09	7.79
15/15	10.33	9.28	8.88	8.40	8.27	8.15	7.97	7.79	7.49
15/30	10.31	9.16	8.69	8.05	7.83	7.71	7.53	7.35	7.05
15/45	10.31	9.16	8.67	7.98	7.74	7.60	7.42	7.24	6.94
20/20	10.29	8.84	8.27	7.68	7.41	7.29	7.11	6.93	6.63
20/40	10.29	8.80	8.17	7.44	7.10	6.98	6.80	6.62	6.32
20/60	10.29	8.80	8.17	7.44	7.09	6.97	6.79	6.61	6.31

was used to pinpoint the point on the avoidance curve with the strongest curvature, the True Knee Point (TKP).

The same two strategic reference points were thus identified for the hydrogen system:

The initial Threshold Point is set at 100 GWh and 15/15 GW. This combination is on the $\nabla Z = 1.0$ gradient contour and shows a balanced mix of electrolyser and fuel cell capacity. This point manages to avoid 2.82 TWh of future imports and defines the boundary between the high-efficiency region. However, unlike batteries, hydrogen supplies have fewer regions where $\nabla Z > 1.0$, reflecting a more limited area of efficiency.

True Knee Point (200 GWh, 20/40 GW) Maximum concavity along the avoided import surface marks this point as a high-storage, high-power setting, providing about 4.19 TWh of avoided imports. It is where the surface of the curve shifts to mean that, starting here, more investments bring diminishing marginal benefits. From technical and planning perspective, this is the middle point between security of energy supply and the cost-effectiveness of hydrogen deployment. The H values of the Hessian determinant are presented in Table A.8 in the appendix section.

The results of the hydrogen system simulation are visualized in Figures 5.31 and 5.32. Figure 5.31 shows the avoided import levels and highlights the Early Threshold and True Knee Points with the technical gradient lines (∇Z). The 3D surface (Figure 5.32) offers a better visualization of the knee point and the system's response to different configurations.

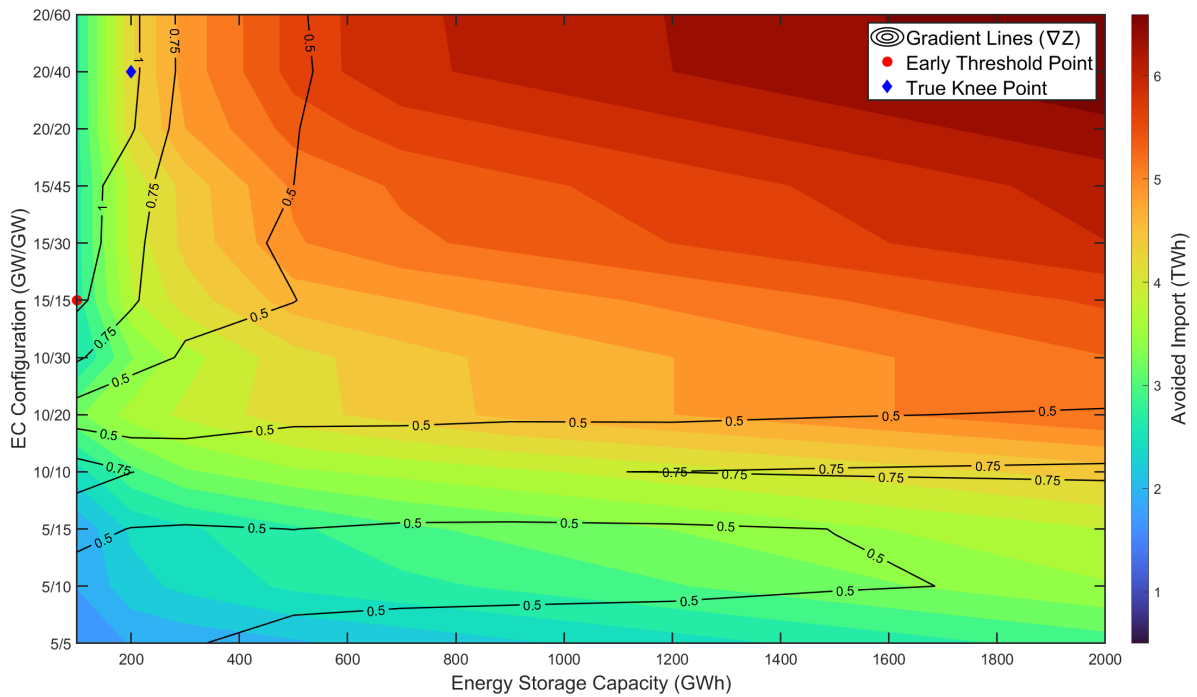


Figure 5.31: Isoline map of avoided electricity imports (TWh) for the hydrogen storage system as a function of energy storage capacity (GWh) and electrolyser/fuel cell configuration (GW) of green hydrogen storage system. Technical gradient lines (∇Z) are overlaid. The **Early Threshold Point** (100 GWh, 15/15 GW), where $\nabla Z = 1.0$, and the **True Knee Point** (200 GWh, 20/40 GW), identified by Gaussian curvature analysis, are highlighted.

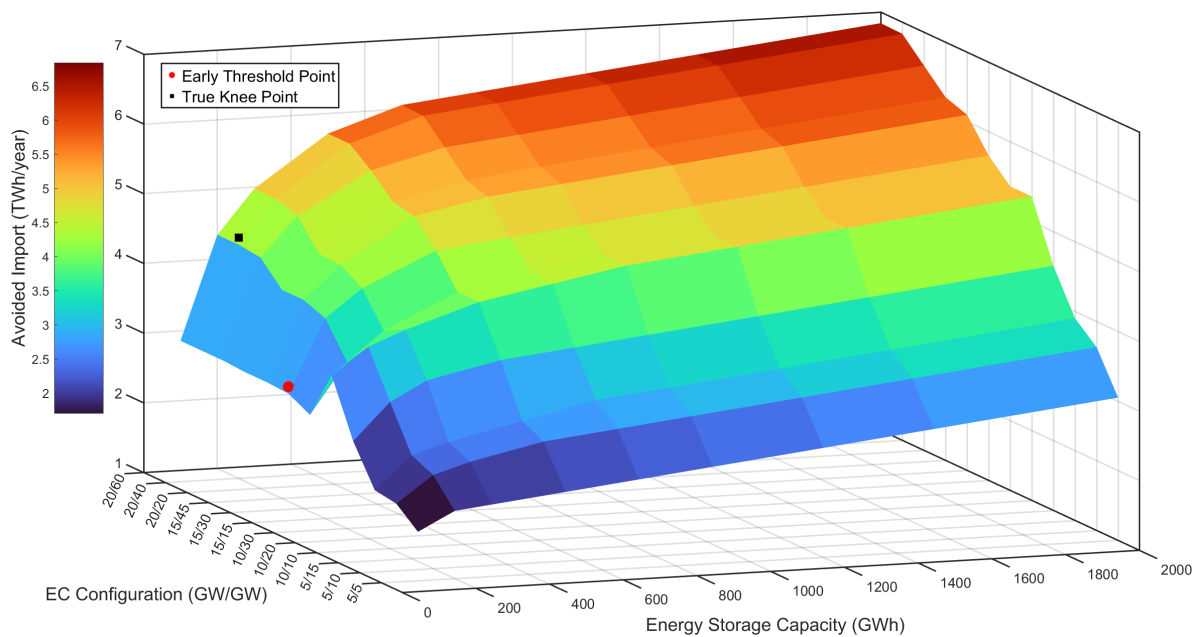


Figure 5.32: Three-dimensional surface of avoided electricity imports (TWh/year) for the hydrogen storage system. Axes represent energy storage capacity (GWh) and electrolyser/fuel cell configuration (GW) of green hydrogen storage system. The **Early Threshold Point** (red circle) marks the onset of diminishing returns ($\nabla Z = 1.0$), while the **True Knee Point** (black square) indicates the location of maximum curvature — the most significant inflection point in system performance.

5.4.5 Final Scenario: Full Storage System Integration

The final scenario presented demonstrates the full implementation of all energy storage technologies studied in this work. Including a Pumped Hydroelectric Energy Storage system (PHES) with 11 GW of installed capacity, a lithium-ion battery system with 8 GW of installed power and 48 GWh of energy capacity, in addition to a hydrogen storage system configured at the True Knee Point (TKP), with 15/45 GW (electrolyzer/fuel cell) and 1500 GWh of storage capacity.

The energy balance achieved in this scenario is summarized in Table 5.18, and is being compared to the baseline scenario — a system without the implementation of any storage technology. This comparison allows us to assess the systemic benefits provided by the integration of different storage technologies, especially in terms of demand coverage, use of renewable energy and reduction of electricity imports.

In the final scenario observed, total electricity generation reaches 1511.7 TWh/year, a lower value than in the base scenario. This reduction, however, is intentional and beneficial, as it results from restriction strategies adopted to balance supply and demand more effectively. Run-of-the-river hydropower (ROR Hydro) production, in particular, was reduced from its maximum potential, as it was redirected to provide frequency regulation and ancillary services, reinforcing system stability rather than maximizing production.

Electricity imports were reduced to just 8.8 TWh/year, a significant reduction from the 19.87 TWh/year observed in the scenario without energy storage — representing a drop of 55.7%. These results highlight the importance of energy storage to attend demand during periods of renewable variability and minimize dependence on external sources.

Each of the energy storage systems proved to be relevant in different and complementary ways within the final scenario. The PHES system provided an energy throughput of 13.13 TWh/year, demonstrating high efficiency and operational flexibility to attend medium-term balancing needs and rapid dispatch capacity. The lithium-ion battery system contributed 6.09 TWh/year, acting mainly in short-term balancing tasks, such as smoothing fluctuations, managing intraday variability and reducing peak demand. The hydrogen storage system, configured at True Knee Point with a capacity of 15/45 GW and 1500 GWh, provided 4.19 TWh/year. This system was optimized to handle long-term imbalances and seasonal mismatches, effectively complementing the faster response capabilities.

To assess the system operation dynamically, Figure 5.33 presents a representative operational week for each season. It can be seen that the integration of storage allows a smoother alignment between renewable generation and load profiles. During periods of high or low demand

(especially in summer and winter), the storage systems collectively compensate for fluctuations, significantly reducing the need for imports and ensuring stable demand satisfaction.

Table 5.18: Comparison between the final scenario results and PNE 2050 values for electricity generation and system balance.

Source	Final Scenario (TWh)	PNE 2050 (TWh)	Difference (%)
<i>Electricity Generation</i>			
Wind	811.60	811.94	-0.04%
PV (centralized)	190.13	199.20	-4.55%
Biomass	46.28	46.14	+0.30%
Nuclear	25.35	25.17	+0.72%
ROR Hydro	251.83	—	—
PCH	46.09	41.10	+12.14%
Reservoir Hydro	153.06	158.06	-3.16%
Hydro Total	404.89	451.73	-10.37%
Total DG	99.43	100.43	-1.00%
<i>Demand and Balance</i>			
Annual Generation	1623.77	1675.71	-3.10%
Annual Demand	1510.85	1510.85	0.00%
Import	8.80	19.87	-55.70%
Export	104.56	109.56	-4.56%
PHES	13.13	—	—
Lithium Battery	6.09	—	—
Hydrogen Storage	4.19	—	—

5.5 Monte Carlo Analysis of Indirect CO₂eq Emissions from RES in the Final Scenario

A Monte Carlo simulation with one million iterations was performed to estimate the uncertainty of indirect GHG emissions based on the outputs of the final scenario. As outlined in the methodology section, it took energy emissions from different technologies and different report in order to construct a LCA inventory for the five main technologies applied in the scenario (biomass, wind, solar PV, hydropower and nuclear) and then fitted with the distribution that better fit the density trace of each technology.

Figure 5.34 depicts the stacked histogram distribution of life cycle specific emissions (in gCO₂eq/kWh) by each RES., that illustrates how each technology influences the total emissions of the energy mix per unit of kWh produced.

Figure 5.35 illustrates the distribution of total annual indirect emissions for the full electricity

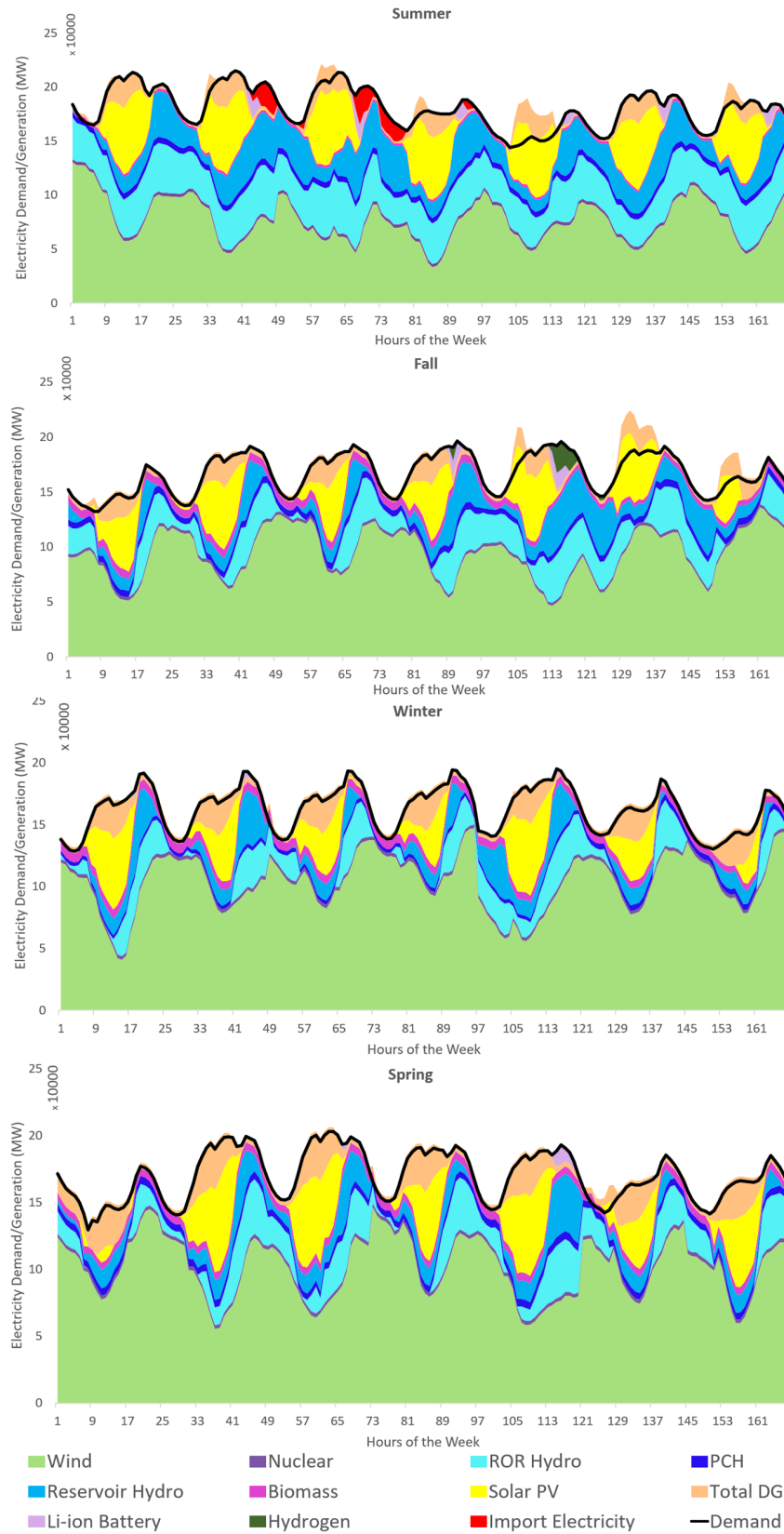


Figure 5.33: Typical operational week for each season in the final scenario with all storage systems implemented.

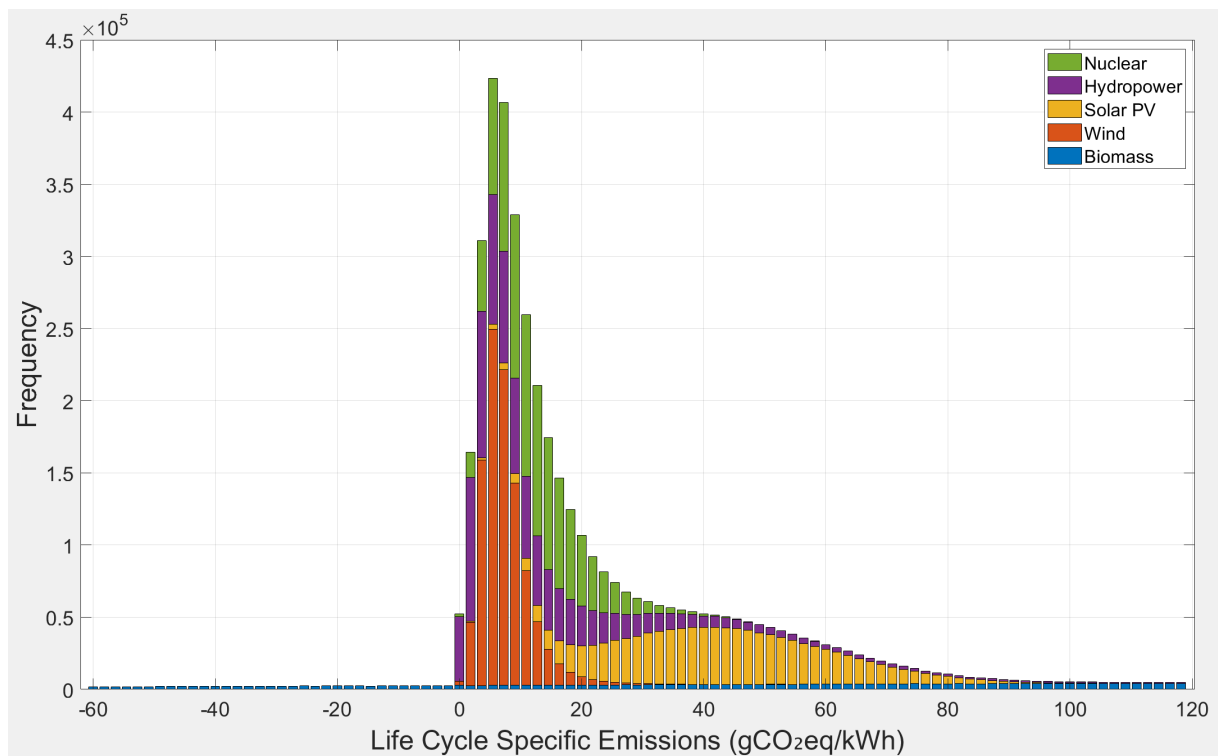


Figure 5.34: Stacked histogram showing the distribution of life cycle specific CO₂eq emissions (gCO₂eq/kWh) by energy source after Monte Carlo simulation. Each coloured segment corresponds to a technology's contribution to the total mix.

mix, expressed in MtCO₂eq/year. In this histogram, the energy generation contribution was taken into account together with the LCA emissions of each energy source in order to estimate the total CO₂eq indirect emissions for the final scenario. The histogram is normalized as a probability density function.

The simulation resulted in a mean value of 30.8 MtCO₂eq/year and a median of 28.9 MtCO₂eq/year, with the first and third quartiles positioned at 21.5 and 37.5 MtCO₂eq/year, respectively. The central 90% confidence interval (from the 5th to the 95th percentile) ranges from 10.5 a 57.0 MtCO₂eq/year.

These results challenge the frequent assumption that renewable electricity systems produce zero emissions. Although commonly regarded as emission-free—including in major national plans such as Brazil's PNE 2050, this analysis demonstrates that a fully renewable scenario still leads to significant levels of indirect CO₂ emissions when life cycle factors are accounted for.

To illustrate the significance of these findings, the 30.8 MtCO₂eq/year average indirect emissions found in this study are close to the PNE scenario "Repowering of Hydropower Plants" (32 MtCO₂eq/year), which includes almost 31 GW of installed capacity from natural gas power plants. While this renewable-based scenario studied here involves nearly 490 GW of installed

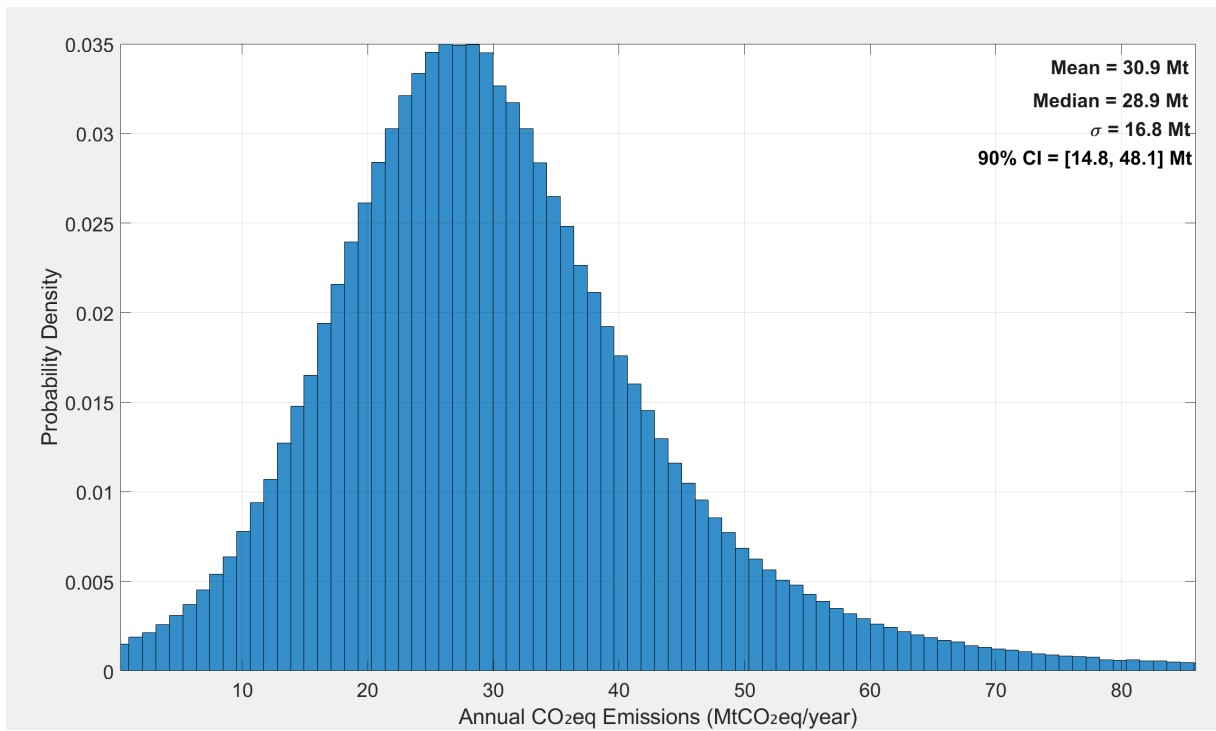


Figure 5.35: Probability density of total annual CO₂eq emissions (MtCO₂eq/year) for the 2050 fully renewable scenario. Results derived from 1,000,000 Monte Carlo simulations.

capacity, demonstrating a far lower emission intensity, these results highlight that the environmental impacts of renewable sources are not negligible.

Chapter 6

Conclusions

This research shows that, from a technical point of view, Brazil could reach a fully renewable electricity system by 2050. The system was able to deliver stable and reliable power at an hourly resolution through the integration of hydropower, wind, solar PV, biomass, and nuclear energy, combined with multiple energy storage technologies. No fossil fuels were needed.

One of the main contributions of this work is the development of a detailed life cycle inventory for the main electricity sources in Brazil. This database supported the use of a probabilistic methodology that produced a more realistic estimation of indirect greenhouse gas (GHG) emissions, acknowledging uncertainties that are often overlooked in traditional assessments. Besides, this approach can be applied to a wide range of issues, such as environmental impact assessments, policy scenario evaluations, and national decarbonization strategies.

Monte Carlo simulations showed that there is a wide range of possible outcomes depending on the technology, and that emissions vary significantly across different technologies. The results call into question the assumption that all renewable sources are 'zero-emission' and show that even with a fully renewable grid, the mean emissions are 30.8 MtCO₂eq/year, mostly from upstream processes and life cycle impacts. This suggests the need for more transparent and rigorous emission accounting in national energy reports and climate planning.

Energy storage showed to be essential for making the renewable system more reliable and flexible. The addition of 11 GW of pumped hydro storage (PHES) reduced electricity imports by 18%, from 19.87 TWh to 15.86 TWh. When combined with other storage systems, the imports dropped even more, down to 8.8 TWh. This highlights the role of storage in dealing with seasonal variation and improving energy security. Finding key points like the True Knee Point and looking at technical gradients helped in deciding how to size and prioritize each resource.

Still, despite the system's feasibility, important challenges remain. Achieving this transition

would require major capital investment, development of infrastructure (including grid expansions and control systems), and a strong policy framework. A full transition would also require long-term public policy coordination, transparent emissions disclosure, and mechanisms to support private investment. Policymakers must carefully weigh whether the benefits justify the technical and economic efforts involved.

Lastly, this study points to some paths for future research. Including demand response and adding sectors like heating and mobility into the electricity system could make the grid more flexible and reduce how much storage is needed. Better projections of electricity demand, especially with more electrification, would also help improve planning. Doing a full techno-economic analysis of the 100% renewable scenario could bring a clearer view of its financial viability and help guide future policy and investment decisions.

6.1 Limitations and future research

Despite the broad scope of this work, some limitations must be acknowledged. In the first place, EnergyPLAN is capable of high-resolution hourly simulations, but it adopts a deterministic approach for system operation and dispatch modelling. As such, it does not fully capture certain dynamic behaviours of real power systems, such as cascading failures, ramping constraints, or stochastic weather variability beyond the TMY. This could be addressed in future studies by coupling EnergyPLAN with stochastic or agent-based modelling frameworks.

Second, the life cycle assessment (LCA) was carried out separately from the energy system model and focused only on environmental impacts, using probabilistic Monte Carlo simulations. Although this method captured the uncertainty in indirect GHG emissions, the results were not integrated with system operations, such as storage dispatch or curtailment. Future work could integrate the LCA into the dispatch model through a feedback loop to allow a more complete assessment.

Third, the emission factors used in the LCA were obtained from international sources, since there is still a lack of Brazil-specific data. However, this can affect the accuracy of some results, particularly for technologies like hydropower and biomass, which have highly context-dependent life cycle impacts. Future research should focus even more on developing national LCA databases with regionally appropriate emission factors.

Finally, economic or policy aspects such as investment costs, financing models, political feasibility or public acceptance were not included in the study. The technical and environmental

sides were well covered, but a full 2050 roadmap would have to include these dimensions. Future research should seek to integrate techno-economic tools and participatory scenario development to support decision-making at the strategic level.

The importance of these results is not reduced by these limitations, but rather indicates areas where the work can be expanded. Achieving a fully renewable grid in Brazil will not be possible with technical solutions alone, but will require better data, more robust methods and collaboration between sectors.

Bibliography

- [1] E. Manirambona, S. M. Talai, and S. K. Kimutai, “A review of sustainable planning of Burundian energy sector in East Africa,” *Energy Strategy Reviews*, vol. 43, p. 100927, 2022. [Online]. Available: <https://www.sciencedirect.com/science/article/pii/S2211467X22001213>
- [2] UNSD, “Geoscheme,” <https://unstats.un.org/unsd/methodology/m49/#ftn13>, 2025, accessed: 2025-04-30.
- [3] UNECE, “Life Cycle Assessment of Electricity Generation Options,” <https://unece.org/sed/documents/2021/10/reports/life-cycle-assessment-electricity-generation-options>, 2021, accessed: 2025-04-30.
- [4] EPE, “Balanco Energético Nacional 2014,” <https://www.epe.gov.br/pt/publicacoes-dados-abertos/publicacoes/Balanco-Energetico-Nacional-2014>, 2015, accessed: 2025-04-17.
- [5] C. R. de Integração Energética, “Síntesis Informativa Energética de los Países de la CIER, Información del sector energético em países de América del Sul, América Central y Caribe (2010).”
- [6] W. B. Group, “Electric power consumption (kWh per capita) | Data,” <https://data.worldbank.org/indicator/EG.USE.ELEC.KH.PC>, 2015, accessed: 2025-04-24.
- [7] M. Prina, M. Lionetti, G. Manzolini, W. Sparber, and D. Moser, “Transition pathways optimization methodology through EnergyPLAN software for long-term energy planning,” *Applied Energy*, vol. 235, pp. 356–368, 2019. [Online]. Available: <https://www.sciencedirect.com/science/article/pii/S0306261918316672>
- [8] IRENA, “Renewable energy statistics 2023,” <https://www.irena.org/Publications/2023/Jul/Renewable-energy-statistics-2023>, 2024, accessed: 2025-04-24.

- [9] R. Loulou and M. Labriet, “ETSAP-TIAM: the TIMES integrated assessment model Part I: Model structure,” *Computational Management Science*, vol. 5, no. 1–2, p. 7–40, feb 2007. [Online]. Available: <http://dx.doi.org/10.1007/s10287-007-0046-z>
- [10] International Energy Agency, “MARKAL model Documentation,” IEA-ETSAP, Tech. Rep., 2005. [Online]. Available: https://IEA-etsap.org/docs/MARKAL_Documentation.pdf
- [11] M. Howells, H. Rogner, N. Strachan, C. Heaps, H. Huntington, S. Kypreos, A. Hughes, S. Silveira, J. DeCarolis, M. Bazillian, and A. Roehrl, “OSeMOSYS: The Open Source Energy Modeling System: An introduction to its ethos, structure and development,” *Energy Policy*, vol. 39, no. 10, pp. 5850–5870, 2011, sustainability of biofuels. [Online]. Available: <https://www.sciencedirect.com/science/article/pii/S0301421511004897>
- [12] H. Lund, J. Z. Thellufsen, P. A. Østergaard, P. Sorknæs, I. R. Skov, and B. V. Mathiesen, “EnergyPLAN – Advanced analysis of smart energy systems,” *Smart Energy*, vol. 1, p. 100007, 2021. [Online]. Available: <https://www.sciencedirect.com/science/article/pii/S2666955221000071>
- [13] Empresa de Pesquisa Energética, *Plano Nacional de Energia 2050*, 1st ed. Brasília, Brasil: Ministério de Minas e Energia, 2020, accessed: 2023-10-01. [Online]. Available: <https://www.gov.br/epe/pt-br/publicacoes/pne-2050>
- [14] R. Hanna and R. Gross, “How do energy systems model and scenario studies explicitly represent socio-economic, political and technological disruption and discontinuity? Implications for policy and practitioners,” *Energy Policy*, vol. 149, p. 111984, 2021. [Online]. Available: <https://www.sciencedirect.com/science/article/pii/S0301421520306959>
- [15] G. G. Dranka, P. Ferreira, and A. I. F. Vaz, “Integrating supply and demand-side management in renewable-based energy systems,” *Energy*, vol. 232, p. 120978, oct 2021. [Online]. Available: <http://dx.doi.org/10.1016/j.energy.2021.120978>
- [16] M. N. H. Shazon, Nahid-Al-Masood, and A. Jawad, “Frequency control challenges and potential countermeasures in future low-inertia power systems: A review,” *Energy Reports*, vol. 8, pp. 6191–6219, 2022. [Online]. Available: <https://www.sciencedirect.com/science/article/pii/S2352484722008289>

- [17] J. Andrade Guerra, L. Dutra, N. Schwinden, and S. F. de Andrade, “Future scenarios and trends in energy generation in Brazil: supply and demand and mitigation forecasts,” *Journal of Cleaner Production*, vol. 103, pp. 197–210, 2015, carbon Emissions Reduction: Policies, Technologies, Monitoring, Assessment and Modeling. [Online]. Available: <https://www.sciencedirect.com/science/article/pii/S095965261401021X>
- [18] G. Dranka and P. Ferreira, “Planning for a renewable future in the Brazilian power system,” *Energy*, vol. 164, pp. 496–511, 2018. [Online]. Available: <https://www.sciencedirect.com/science/article/pii/S0360544218317006>
- [19] G. de Moura, L. Legey, and M. Howells, “A Brazilian perspective of power systems integration using OSeMOSYS SAMBA – South America Model Base – and the bargaining power of neighbouring countries: A cooperative games approach,” *Energy Policy*, vol. 115, pp. 470–485, 2018. [Online]. Available: <https://www.sciencedirect.com/science/article/pii/S0301421518300521>
- [20] M. J. Santos, P. M. T. Ferreira, M. M. Araújo, J. Portugal-Pereira, A. Lucena, and R. Schaeffer, “Low-carbon scenarios for the Brazilian power system,” 2016, [Online]. Available: https://repositorium.sdum.uminho.pt/bitstream/1822/44898/1/Santos_et_al_2016b.pdf. [Online]. Available: https://repositorium.sdum.uminho.pt/bitstream/1822/44898/1/Santos_et_al_2016b.pdf
- [21] D. Connolly, H. Lund, and B. Mathiesen, “Smart Energy Europe: The technical and economic impact of one potential 100% renewable energy scenario for the European Union,” *Renewable and Sustainable Energy Reviews*, vol. 60, pp. 1634–1653, 2016. [Online]. Available: <https://www.sciencedirect.com/science/article/pii/S1364032116002331>
- [22] A. Franco and P. Salza, “Strategies for optimal penetration of intermittent renewables in complex energy systems based on techno-operational objectives,” *Renewable Energy*, vol. 36, no. 2, pp. 743–753, 2011. [Online]. Available: <https://www.sciencedirect.com/science/article/pii/S0960148110003460>
- [23] H. Lund, “Renewable energy strategies for sustainable development,” *Energy*, vol. 32, no. 6, pp. 912–919, 2007, third Dubrovnik Conference on Sustainable Development of Energy, Water and Environment Systems. [Online]. Available: <https://www.sciencedirect.com/science/article/pii/S036054420600301X>

- [24] L. Fernandes and P. Ferreira, “Renewable energy scenarios in the Portuguese electricity system,” *Energy*, vol. 69, p. 51–57, may 2014. [Online]. Available: <http://dx.doi.org/10.1016/j.energy.2014.02.098>
- [25] G. Krajačić, N. Duić, Z. Zmijarević, B. V. Mathiesen, A. A. Vučinić, and M. da Graça Carvalho, “Planning for a 100% independent energy system based on smart energy storage for integration of renewables and CO2 emissions reduction,” *Applied Thermal Engineering*, vol. 31, no. 13, pp. 2073–2083, 2011, selected Papers from the 13th Conference on Process Integration, Modelling and Optimisation for Energy Saving and Pollution Reduction. [Online]. Available: <https://www.sciencedirect.com/science/article/pii/S1359431111001463>
- [26] A. Júnior, *Planejamento energético: inserção da variável ambiental na expansão da oferta de energia elétrica*. Synergia, 2020. [Online]. Available: <https://biblioteca.aneel.gov.br/acervo/detalhe/242362>
- [27] Empresa de Pesquisa Energética (EPE), “Balanco Energético Nacional 2009,” <https://www.epe.gov.br/pt/publicacoes-dados-abertos/publicacoes/Balanco-Energetico-Nacional-2009>, 2009, accessed: 2025-04-24.
- [28] E. de Pesquisa Energética, “Balanco Energético Nacional 2019,” <https://www.epe.gov.br/pt/publicacoes-dados-abertos/publicacoes/balanco-energetico-nacional-2019>, 2019, accessed: 2025-04-24.
- [29] M. de Minas e Energia & Empresa de Pesquisa Energética, “Prólogo e Introdução do Plano Nacional de Energia 2050,” 2020, accessed: 2023-10-01. [Online]. Available: <https://www.epe.gov.br/pt/publicacoes-dados-abertos/publicacoes/Plano-Nacional-de-Energia-2050>
- [30] E. de Pesquisa Energética, “Plano Decenal de Expansão de Energia 2026,” <https://www.epe.gov.br/pt/publicacoes-dados-abertos/publicacoes/plano-decenal-de-expansao-de-energia-pde>, 2017, accessed: 2025-04-24.
- [31] EPE, “Plano Nacional de Energia - 2030,” <https://www.epe.gov.br/pt/publicacoes-dados-abertos/publicacoes/Plano-Nacional-de-Energia-PNE-2030>, 2007, accessed: 2025-04-24.
- [32] B. N. do Desenvolvimento, “Relatório Anual BNDES, 1999,” 1999. [Online]. Available: http://web.bndes.gov.br/bib/jspui/bitstream/1408/3867/1/RA_1999.pdf

- [33] D. da República, “Portaria n.º 6/2020 | DR,” <https://diariodarepublica.pt/dr/detalhe/portaria/6-2020-128071724>, 2020, accessed: 2025-04-24.
- [34] Government of Brazil, “Brazil’s NDC: National determination to contribute and transform,” https://unfccc.int/sites/default/files/2024-11/Brazil_Second%20Nationally%20Determined%20Contribution%20%28NDC%29_November2024.pdf, 2024, accessed: 2025-04-24.
- [35] B. Pinheiro, M. C. L. Velasquez, G. Faria, A. F. C. Aquino, D. Issicaba, and D. Dotta, “Evaluation of the Impact of IBR on the Frequency Dynamics in the Brazilian Power System,” 2025. [Online]. Available: <https://arxiv.org/abs/2503.11040>
- [36] C. N. d. S. Souza, D. de Pontes Souza, V. José, and M. F. Filho, “Criticality of rare earths for application in electric vehicles and wind energy in Brazil,” *Journal of Sustainable Energy Studies*, 2020.
- [37] M. Silva, T. Francisco, E. Torres, A. Rocha, F. Freires, S. Tito, and P. de Jong, “Biodiesel in Brazil: A Market Analysis and Its Economic Effects,” *Journal of Agricultural Science*, vol. 6, pp. 160–160, 07 2014.
- [38] A. Herbst, F. Toro, F. Reitze, and E. Jochem, “Introduction to energy systems modelling,” *Swiss journal of economics and statistics*, vol. 148, pp. 111–135, 2012.
- [39] N. Van Beeck, “Classification of Energy Models,” Tilburg University, Tilburg, Netherlands, Working Paper FEW 777, 1999, FEW 777 Working Paper Series. [Online]. Available: <https://research.tilburguniversity.edu/en/publications/classification-of-energy-models>
- [40] P. Pisciella, E. R. van Beesten, and A. Tomsgard, “Efficient coordination of top-down and bottom-up models for energy system design: An algorithmic approach,” *Energy*, vol. 284, p. 129320, 2023. [Online]. Available: <https://www.sciencedirect.com/science/article/pii/S0360544223027147>
- [41] D. P. Da Silva, “Sistemas Sustentáveis de Energia na Ilha Terceira: O Contributo da Modelação e Gestão da Procura,” Ph.D. dissertation, Instituto Superior Técnico, Universidade de Lisboa, Lisboa, Portugal, jul 2016, PhD Thesis in Sustainable Energy Systems. [Online]. Available: <http://hdl.handle.net/10400.5/12345>
- [42] IEEE Power & Energy Society, “IEEE Standard for Power System Dynamic Studies,” IEEE, Standard IEEE Std 1110-2013, 2013.

- [43] B. V. Mathiesen, H. Lund, D. Connolly, H. Wenzel, P. A. Østergaard, B. Möller, S. Nielsen, I. Ridjan, P. Karnøe, K. Sperling, and F. K. Hvelplund, “Smart Energy Systems for Coherent 100
- [44] S. Pfenninger, L. Hirth, I. Schlecht, E. Schmid, F. Wiese, T. Brown, C. Davis, M. Gidden, H. Heinrichs, C. Heuberger, S. Hilpert, U. Krien, C. Matke, A. Nebel, R. Morrison, F. Müsgens, P.-Y. Oei, B. Pickering, and C. Wingenbach, “Opening the Black Box of Energy Modelling: Strategies and Lessons Learned,” *Energy Strategy Reviews*, vol. 19, pp. 63–71, 2018.
- [45] J. F. DeCarolis, K. Hunter, and S. Sreepathi, “The Case for Repeatable Analysis with Energy Economy Optimization Models,” *Energy Economics*, vol. 64, pp. 440–447, 2017.
- [46] J. E. Bistline and G. J. Blanford, “Value of technology in the U.S. electric power sector: Impacts of full portfolios and technological change on the costs of meeting decarbonization goals,” *Energy Economics*, vol. 86, p. 104694, 2020. [Online]. Available: <https://www.sciencedirect.com/science/article/pii/S0140988320300335>
- [47] R. Loulou, G. Goldstein, and K. Noble, “Documentation for the MARKAL family of Models,” *Energy Technology Systems Analysis Programme*, 2005. [Online]. Available: https://IEA-etsap.org/docs/Documentation_for_the_MARKAL_Family.pdf
- [48] H. Lund, *EnergyPLAN Advanced Energy Systems Analysis Computer Model*, 2022, official documentation. [Online]. Available: <https://www.energyplan.eu/documentation/>
- [49] B. Mathiesen, H. Lund, D. Connolly, H. Wenzel, P. Østergaard, B. Möller, S. Nielsen, I. Ridjan, P. Karnøe, K. Sperling, and F. Hvelplund, “Smart Energy Systems for coherent 100
- [50] Stockholm Environment Institute, *LEAP: Long-range Energy Alternatives Planning System*, 2023, official website. [Online]. Available: <https://leap.sei.org/>
- [51] K. Wang, C. Wang, X. Lu, and J. Chen, “Scenario analysis on CO₂ emissions reduction potential in China’s iron and steel industry,” *Energy Policy*, vol. 35, no. 4, pp. 2320–2335, 2007. [Online]. Available: <https://www.sciencedirect.com/science/article/pii/S0301421506003181>

- [52] National Renewable Energy Laboratory, *HOMER Pro User Manual*, 2023, official documentation. [Online]. Available: <https://www.homerenergy.com/products/pro/docs/latest/index.html>
- [53] F. A. Farret and M. G. Simões, *Micropower System Modeling with HOMER*. John Wiley & Sons, Inc., 2006, pp. 379–418.
- [54] International Institute for Applied Systems Analysis, “MESSAGEix documentation,” 2022, official documentation. [Online]. Available: <https://docs.messageix.org/en/stable/>
- [55] D. Huppmann, M. Gidden, O. Fricko, P. Kolp, C. Orthofer, M. Pimmer, N. Kushin, A. Vinca, A. Mastrucci, K. Riahi, and V. Krey, “The MESSAGEix Integrated Assessment Model and the ix modeling platform (ixmp): An open framework for integrated and cross-cutting analysis of energy, climate, the environment, and sustainable development,” *Environmental Modelling & Software*, vol. 112, pp. 143–156, 2019. [Online]. Available: <https://www.sciencedirect.com/science/article/pii/S1364815218302330>
- [56] OSeMOSYS Community, *OSeMOSYS Documentation*, 2023, official website. [Online]. Available: <https://osemosys.org/>
- [57] IEA-ETSAP, “TIMES Model Documentation,” 2022, official documentation. [Online]. Available: https://www.iaea.org/etsap/docs/TIMES_Documentation.pdf
- [58] S. Pfenninger, A. Hawkes, and J. Keirstead, “Energy systems modeling for twenty-first century energy challenges,” *Renewable and Sustainable Energy Reviews*, vol. 33, pp. 74–86, 2014. [Online]. Available: <https://www.sciencedirect.com/science/article/pii/S1364032114000872>
- [59] R. Akpahou, L. D. Mensah, D. A. Quansah, and F. Kemausuor, “Energy planning and modeling tools for sustainable development: A systematic literature review,” *Energy Reports*, vol. 11, pp. 830–845, 2024. [Online]. Available: <https://www.sciencedirect.com/science/article/pii/S2352484723015688>
- [60] D. Connolly, H. Lund, B. Mathiesen, and M. Leahy, “A review of computer tools for analysing the integration of renewable energy into various energy systems,” *Applied Energy*, vol. 87, no. 4, pp. 1059–1082, 2010. [Online]. Available: <https://www.sciencedirect.com/science/article/pii/S0306261909004188>

- [61] P. Østergaard, H. Lund, J. Thellufsen, P. Sorknæs, and B. Mathiesen, “Review and validation of EnergyPLAN,” *Renewable and Sustainable Energy Reviews*, vol. 168, p. 112724, 2022. [Online]. Available: <https://www.sciencedirect.com/science/article/pii/S136403212200613X>
- [62] I. O. for Standardization, “ISO 14044:2006 - Environmental management — Life cycle assessment — Requirements and guidelines,” https://www.iso.org/standard/38498.html?utm_source=.com, 2006, accessed: 2025-04-17.
- [63] J. Pryshlakivsky and C. Searcy, “Fifteen years of ISO 14040: a review,” *Journal of Cleaner Production*, vol. 57, pp. 115–123, 2013. [Online]. Available: <https://www.sciencedirect.com/science/article/pii/S0959652613003764>
- [64] J. Kabayo, P. Marques, R. Garcia, and F. Freire, “Life-cycle sustainability assessment of key electricity generation systems in Portugal,” *Energy*, vol. 176, pp. 131–142, 2019. [Online]. Available: <https://www.sciencedirect.com/science/article/pii/S0360544219305869>
- [65] International Energy Agency, “Brazil - electricity,” <https://www.iea.org/countries/brazil/electricity>, 2023, accessed: 2025-04-17.
- [66] A. T. Dale, A. F. Pereira de Lucena, J. Marriott, B. S. M. C. Borba, R. Schaeffer, and M. M. Bilec, “Modeling Future Life-Cycle Greenhouse Gas Emissions and Environmental Impacts of electricity supplies in brazil,” *Energies*, vol. 6, no. 7, pp. 3182–3208, 2013. [Online]. Available: <https://www.mdpi.com/1996-1073/6/7/3182>
- [67] Chambile, Enock, “Assessment of grid electricity systems using the life-cycle carbon-emission model,” *Sci. Tech. Energ. Transition*, vol. 79, p. 73, 2024. [Online]. Available: <https://doi.org/10.2516/stet/2024077>
- [68] A.-S. Herbert, C. Azzaro-Pantel, and D. Le Boulch, “A typology for world electricity mix: Application for inventories in Consequential LCA (CLCA),” *Sustainable Production and Consumption*, vol. 8, pp. 93–107, 2016. [Online]. Available: <https://www.sciencedirect.com/science/article/pii/S2352550916300215>
- [69] M. Liu, G. Zhu, and Y. Tian, “The historical evolution and research trends of life cycle assessment,” *Green Carbon*, vol. 2, no. 4, pp. 425–437, 2024. [Online]. Available: <https://www.sciencedirect.com/science/article/pii/S2950155524000727>

- [70] Ecoinvent, “Ecoinvent - Data with purpose.” <https://ecoinvent.org/>, 2025, accessed: 2025-04-17.
- [71] M. Cellura, S. Longo, and M. Mistretta, “Sensitivity analysis to quantify uncertainty in Life Cycle Assessment: The case study of an Italian tile,” *Renewable and Sustainable Energy Reviews*, vol. 15, no. 9, pp. 4697–4705, 2011. [Online]. Available: <https://www.sciencedirect.com/science/article/pii/S1364032111003273>
- [72] Varun, I. Bhat, and R. Prakash, “LCA of renewable energy for electricity generation systems—A review,” *Renewable and Sustainable Energy Reviews*, vol. 13, no. 5, pp. 1067–1073, 2009. [Online]. Available: <https://www.sciencedirect.com/science/article/pii/S1364032108001093>
- [73] C. F. Blanco, S. Cucurachi, J. B. Guinée, M. G. Vijver, W. J. Peijnenburg, R. Trattnig, and R. Heijungs, “Assessing the sustainability of emerging technologies: A probabilistic LCA method applied to advanced photovoltaics,” *Journal of Cleaner Production*, vol. 259, p. 120968, 2020. [Online]. Available: <https://www.sciencedirect.com/science/article/pii/S0959652620310155>
- [74] C. D. Zuluaga-Ríos and C. Guarnizo-Lemus, “Data-driven approaches for generating probabilistic short-term renewable energy scenarios,” *Computers and Electrical Engineering*, vol. 120, p. 109817, 2024. [Online]. Available: <https://www.sciencedirect.com/science/article/pii/S0045790624007444>
- [75] E. J. da Silva Pereira, J. T. Pinho, M. A. B. Galhardo, and W. N. Macêdo, “Methodology of risk analysis by Monte Carlo Method applied to power generation with renewable energy,” *Renewable Energy*, vol. 69, pp. 347–355, 2014. [Online]. Available: <https://www.sciencedirect.com/science/article/pii/S0960148114002183>
- [76] A. D. Rollett and P. Manohar, “The Monte Carlo method,” *Continuum scale simulation of engineering materials: fundamentals–microstructures–process applications*, pp. 77–114, 2004.
- [77] S. LO, H. MA, and S. LO, “Quantifying and reducing uncertainty in life cycle assessment using the Bayesian Monte Carlo method,” *Science of The Total Environment*, vol. 340, no. 1–3, p. 23–33, mar 2005. [Online]. Available: <http://dx.doi.org/10.1016/j.scitotenv.2004.08.020>

- [78] M. H. Kalos and P. A. Whitlock, *Monte Carlo methods*. John Wiley & Sons, 2009.
- [79] C. Robert, “Monte Carlo Statistical Methods,” 1999.
- [80] DEISO, “Monte-Carlo Simulation, Uncertainty Analysis, and Sensitivity Analysis in Life Cycle Assessment,” <https://dei.so/monte-carlo-simulation-uncertainty-analysis-and-sensitivity-analysis-in-life-cycle-assessment/>, 2023, accessed: 2025-05-05.
- [81] S. Sun and M. Ertz, “Life cycle assessment and Monte Carlo simulation to evaluate the environmental impact of promoting LNG vehicles,” *MethodsX*, vol. 7, p. 101046, 2020. [Online]. Available: <http://dx.doi.org/10.1016/j.mex.2020.101046>
- [82] M. G. Pereira, C. F. Camacho, M. A. V. Freitas, and N. F. da Silva, “The renewable energy market in Brazil: Current status and potential,” *Renewable and Sustainable Energy Reviews*, vol. 16, no. 6, pp. 3786–3802, 2012. [Online]. Available: <https://www.sciencedirect.com/science/article/pii/S1364032112002079>
- [83] M. Tolmasquim, “As origens da crise energética brasileira,” *Ambiente & Sociedade*, no. 6–7, p. 179–183, jun 2000. [Online]. Available: <http://dx.doi.org/10.1590/S1414-753X2000000100012>
- [84] H.-T. Pao, Y.-Y. Li, and H.-C. Fu, “Causality Relationship between Energy Consumption and Economic Growth in Brazil,” *Smart Grid and Renewable Energy*, vol. 05, no. 08, p. 198–205, 2014. [Online]. Available: <http://dx.doi.org/10.4236/sgre.2014.58019>
- [85] M. Mele, “Economic growth and energy consumption in Brazil: cointegration and causality analysis,” *Environmental Science and Pollution Research*, vol. 26, no. 29, p. 30069–30075, aug 2019. [Online]. Available: <http://dx.doi.org/10.1007/s11356-019-06161-3>
- [86] National Congress of Brazil, “Law no. 14,299 of january 3, 2022,” http://www.planalto.gov.br/ccivil_03/_ato2019-2022/2022/lei/L14299.htm, 2022, establishes the legal framework for renewable energy expansion, mandating 85% renewable sources in Brazil’s electricity matrix. Official Portuguese version; no official English translation available. [Online]. Available: http://www.planalto.gov.br/ccivil_03/_ato2019-2022/2022/lei/L14299.htm
- [87] Government of Brazil, “Brazil’s nationally determined contribution (NDC) - updated submission,” <https://unfccc.int/sites/default/files/NDC/2022-11/Updated%20NDC%20-%>

- 20BRAZIL%20-%20english%20-FINAL.pdf, 2022, commits to 48% reduction in greenhouse gas emissions by 2025 compared to 2005 levels. Official English version submitted to UNFCCC. [Online]. Available: <https://unfccc.int/sites/default/files/NDC/2022-11/Updated%20NDC%20-%20BRAZIL%20-%20english%20-FINAL.pdf>
- [88] Operador Nacional do Sistema (ONS), “Histórico da Operação,” <https://www.ONS.org.br/paginas/resultados-da-operacao/historico-da-operacao>, 2025, accessed: 2025-05-08.
- [89] M. de Minas e Energia–Empresa de Pesquisa Energética, “Plano decenal de expansão de energia 2033,” Brasília, 2023.
- [90] S. Pfenninger and I. Staffell, “Renewables.ninja,” Available: <https://www.renewables.ninja>, 2016, accessed: September 12, 2024.
- [91] I. Staffell and S. Pfenninger, “Using bias-corrected reanalysis to simulate current and future wind power output,” *Energy*, vol. 114, pp. 1224–1239, 2016. [Online]. Available: <https://www.sciencedirect.com/science/article/pii/S0360544216311811>
- [92] European Commission’s Joint Research Centre (JRC), “PVGIS - Photovoltaic Geographical Information System,” <https://ec.europa.eu/jrc/en/pvgis>, 2024.
- [93] Z. Zeng, P. Stackhouse, J.-H. J. Kim, and R. T. Muehleisen, “Development of typical solar years and typical wind years for efficient assessment of renewable energy systems across the U.S.” *Applied Energy*, vol. 377, p. 124698, jan 2025. [Online]. Available: <http://dx.doi.org/10.1016/j.apenergy.2024.124698>
- [94] S. Wilcox and W. Marion, “Users manual for TMY3 data sets,” 2008.
- [95] S. Janjai and P. Deeyai, “Comparison of methods for generating typical meteorological year using meteorological data from a tropical environment,” *Applied Energy*, vol. 86, no. 4, p. 528–537, apr 2009. [Online]. Available: <http://dx.doi.org/10.1016/j.apenergy.2008.08.008>
- [96] S. S. Seyed Salehi, T. Kalamees, J. Kurnitski, and M. Thalfeldt, “New typical meteorological year generation method based on long-term building energy simulations,” *Building and Environment*, vol. 256, p. 111504, may 2024. [Online]. Available: <http://dx.doi.org/10.1016/j.buildenv.2024.111504>
- [97] A. A. Juárez, A. M. Araújo, J. S. Rohatgi, and O. D. Q. de Oliveira Filho, “Development of the wind power in Brazil: Political, social and technical issues,” *Renewable*

- and Sustainable Energy Reviews*, vol. 39, p. 828–834, nov 2014. [Online]. Available: <http://dx.doi.org/10.1016/j.rser.2014.07.086>
- [98] K. B. Oebels and S. Pacca, “Life cycle assessment of an onshore wind farm located at the northeastern coast of Brazil,” *Renewable Energy*, vol. 53, pp. 60–70, 2013. [Online]. Available: <https://www.sciencedirect.com/science/article/pii/S0960148112006714>
- [99] B. Guezuraga, R. Zauner, and W. Pölz, “Life cycle assessment of two different 2 MW class wind turbines,” *Renewable Energy*, vol. 37, no. 1, pp. 37–44, 2012. [Online]. Available: <https://www.sciencedirect.com/science/article/pii/S0960148111002254>
- [100] ABEEólica, “Boletim de Geração Eólica,” <https://abeeolica.org.br/energia-eolica/dados-abeeolica/>, 2023, accessed: 2025-05-01.
- [101] J. C. de Bona, J. C. E. Ferreira, and J. F. Ordoñez Duran, “Analysis of scenarios for repowering wind farms in Brazil,” *Renewable and Sustainable Energy Reviews*, vol. 135, p. 110197, 2021. [Online]. Available: <https://www.sciencedirect.com/science/article/pii/S1364032120304871>
- [102] L. Stamford and A. Azapagic, “Environmental Impacts of Photovoltaics: The Effects of Technological Improvements and Transfer of Manufacturing from Europe to China,” *Energy Technology*, vol. 6, no. 6, p. 1148–1160, may 2018. [Online]. Available: <http://dx.doi.org/10.1002/ente.201800037>
- [103] D. D. Hsu, P. O’Donoughue, V. Fthenakis, G. A. Heath, H. C. Kim, P. Sawyer, J. Choi, and D. E. Turney, “Life Cycle Greenhouse Gas Emissions of Crystalline Silicon Photovoltaic Electricity Generation: Systematic Review and Harmonization,” *Journal of Industrial Ecology*, vol. 16, no. s1, mar 2012. [Online]. Available: <http://dx.doi.org/10.1111/j.1530-9290.2011.00439.x>
- [104] B. Vicari Stefani, M. Kim, Y. Zhang, B. Hallam, M. A. Green, R. S. Bonilla, C. Fell, G. J. Wilson, and M. Wright, “Historical market projections and the future of silicon solar cells,” *Joule*, vol. 7, no. 12, p. 2684–2699, dec 2023. [Online]. Available: <http://dx.doi.org/10.1016/j.joule.2023.11.006>
- [105] A. Müller, L. Friedrich, C. Reichel, S. Herceg, M. Mittag, and D. H. Neuhaus, “A comparative life cycle assessment of silicon PV modules: Impact of module design,

- manufacturing location and inventory,” *Solar Energy Materials and Solar Cells*, vol. 230, p. 111277, sep 2021. [Online]. Available: <http://dx.doi.org/10.1016/j.solmat.2021.111277>
- [106] L. La Picirelli de Souza, E. Eduardo Silva Lora, S. Rajabi Hamedani, J. C. Escobar Palacio, L. Cioccolanti, M. Villarini, G. Comodi, and A. Colantoni, “Life cycle assessment of prospective scenarios maximizing renewable resources in the Brazilian electricity matrix,” *Renewable Energy Focus*, vol. 44, p. 1–18, mar 2023. [Online]. Available: <http://dx.doi.org/10.1016/j.ref.2022.11.002>
- [107] D. J. Bertassoli, H. O. Sawakuchi, K. R. de Araújo, M. G. P. de Camargo, V. A. T. Alem, T. S. Pereira, A. V. Krusche, D. Bastviken, J. E. Richey, and A. O. Sawakuchi, “How green can Amazon hydropower be? Net carbon emission from the largest hydropower plant in Amazonia,” *Science Advances*, vol. 7, no. 26, jun 2021. [Online]. Available: <http://dx.doi.org/10.1126/sciadv.abe1470>
- [108] A. Fusi, J. Bacenetti, M. Fiala, and A. Azapagic, “Life Cycle Environmental Impacts of Electricity from Biogas Produced by Anaerobic Digestion,” *Frontiers in Bioengineering and Biotechnology*, vol. 4, mar 2016. [Online]. Available: <http://dx.doi.org/10.3389/fbioe.2016.00026>
- [109] E. Beagle and E. Belmont, “Comparative life cycle assessment of biomass utilization for electricity generation in the European Union and the United States,” *Energy Policy*, vol. 128, p. 267–275, may 2019. [Online]. Available: <http://dx.doi.org/10.1016/j.enpol.2019.01.006>
- [110] M. d. C. O. Pavan, D. S. Ramos, M. Y. Soares, C. Barufi, and M. M. d. Carvalho, “Barriers to broaden the electricity production from biomass and biogas in Brazil,” *Production*, vol. 31, 2021. [Online]. Available: <http://dx.doi.org/10.1590/0103-6513.20210064>
- [111] T. Sinigaglia, T. E. Freitag, A. Machado, V. B. Pedrozo, F. F. Rovai, R. T. Gondim Guilherme, T. D. Metzka Lanza Nova, M. Dalla Nora, and M. E. Santos Martins, “Current scenario and outlook for biogas and natural gas businesses in the mobility sector in Brazil,” *International Journal of Hydrogen Energy*, vol. 47, no. 24, p. 12074–12095, mar 2022. [Online]. Available: <http://dx.doi.org/10.1016/j.ijhydene.2022.01.234>
- [112] B. H. M. Silveira, H. K. M. Costa, and E. M. Santos, “Bioenergy with Carbon Capture and Storage (BECCS) in Brazil: A Review,” *Energies*, vol. 16, no. 4, p. 2021, feb 2023. [Online]. Available: <http://dx.doi.org/10.3390/en16042021>

- [113] I. L. Wiesberg, J. L. de Medeiros, R. V. Paes de Mello, J. G. Santos Maia, J. B. V. Bastos, and O. d. Q. F. Araújo, “Bioenergy production from sugarcane bagasse with carbon capture and storage: Surrogate models for techno-economic decisions,” *Renewable and Sustainable Energy Reviews*, vol. 150, p. 111486, oct 2021. [Online]. Available: <http://dx.doi.org/10.1016/j.rser.2021.111486>
- [114] G. Dehner, M. K. McBeth, R. Moss, and I. van Woerden, “A Zero-Carbon Nuclear Energy Future? Lessons Learned from Perceptions of Climate Change and Nuclear Waste,” *Energies*, vol. 16, no. 4, p. 2025, feb 2023. [Online]. Available: <http://dx.doi.org/10.3390/en16042025>
- [115] R. S. El-Emam, A. Constantin, R. Bhattacharyya, H. Ishaq, and M. E. Ricotti, “Nuclear and renewables in multipurpose integrated energy systems: A critical review,” *Renewable and Sustainable Energy Reviews*, vol. 192, p. 114157, mar 2024. [Online]. Available: <http://dx.doi.org/10.1016/j.rser.2023.114157>
- [116] F. Pomponi and J. Hart, “The greenhouse gas emissions of nuclear energy – Life cycle assessment of a European pressurised reactor,” *Applied Energy*, vol. 290, p. 116743, may 2021. [Online]. Available: <http://dx.doi.org/10.1016/j.apenergy.2021.116743>
- [117] M. Maestrini, M. Vargas, L. Losekann, and P. M. Senra, “Energy transition and innovative choices of Brazilian electricity distribution utilities,” *Utilities Policy*, vol. 95, p. 101913, aug 2025. [Online]. Available: <http://dx.doi.org/10.1016/j.jup.2025.101913>
- [118] E. de Pesquisa Energética, “PNE 2050 - Anexo,” <https://www.epe.gov.br/pt/publicacoes-dados-abertos/publicacoes/Plano-Nacional-de-Energia-2050>, 2020, accessed: 2025-05-12.
- [119] ONS, “Reservatórios,” <https://www.ONS.org.br/paginas/energia-agora/reservatorios>, 2020, accessed: 2025-05-12.
- [120] CIER, “Síntesis Informativa Energética de los Países de la CIER - datos del año 2014,” 2017.
- [121] International Energy Agency, “Energy Storage: Tracking Report,” 2020, accessed: 2024-05-13. [Online]. Available: <https://www.IEA.org/reports/energy-storage>

- [122] GESEL - Grupo de Estudos do Setor Elétrico, “Potencial Técnico e Econômico de Usinas Hidrelétricas Reversíveis no Brasil,” 2021, accessed: 2024-05-13. [Online]. Available: <http://www.nuca.ie.ufrj.br/gesel/>
- [123] D. Pashchenko, “Green hydrogen as a power plant fuel: What is energy efficiency from production to utilization?” *Renewable Energy*, vol. 223, p. 120033, mar 2024. [Online]. Available: <http://dx.doi.org/10.1016/j.renene.2024.120033>
- [124] W. N. Association, “Electricity and Energy Storage,” https://world-nuclear.org/information-library/current-and-future-generation/electricity-and-energy-storage?utm_source=.com, 2022, accessed: 2025-05-19.
- [125] A. A. Kebede, M. S. Hosen, T. Kalogiannis, H. A. Behabtu, M. Z. Assefa, T. Jemal, V. Ramayya, J. Van Mierlo, T. Coosemans, and M. Bercibar, “Optimal sizing and lifetime investigation of second life lithium-ion battery for grid-scale stationary application,” *Journal of Energy Storage*, vol. 72, p. 108541, nov 2023. [Online]. Available: <http://dx.doi.org/10.1016/j.est.2023.108541>
- [126] International Energy Agency, “World Energy Outlook 2022,” Paris, 2022, licence: CC BY 4.0 (report); CC BY NC SA 4.0 (Annex A). [Online]. Available: <https://www.{IEA}.org/reports/world-energy-outlook-2022>
- [127] S. Orangi, N. Manjong, D. P. Clos, L. Usai, O. S. Burheim, and A. H. Strømman, “Historical and prospective lithium-ion battery cost trajectories from a bottom-up production modeling perspective,” *Journal of Energy Storage*, vol. 76, p. 109800, jan 2024. [Online]. Available: <http://dx.doi.org/10.1016/j.est.2023.109800>
- [128] International Energy Agency, “Critical Minerals Market Review 2023,” Paris, 2023, licence: CC BY 4.0. [Online]. Available: <https://www.{IEA}.org/reports/critical-minerals-market-review-2023>
- [129] Reuters, “Chile has 28% more lithium than previous estimates, studies find,” https://www.reuters.com/markets/commodities/chile-has-28-more-lithium-than-previous-estimates-studies-find-2025-04-07/?utm_source=.com, 2025, accessed: 2025-05-19.

- [130] Empresa de Pesquisa Energética (EPE), “Hydropower,” <https://www.epe.gov.br/en/areas-of-expertise/electricity/generation-capacity-expansion/source>, 2025, accessed: 2025-05-14.
- [131] D. Newbery, “Implications of renewable electricity curtailment for delivered costs,” *Energy Economics*, vol. 145, p. 108472, may 2025. [Online]. Available: <http://dx.doi.org/10.1016/j.eneco.2025.108472>
- [132] G. Roma, G. Dranka, and A. Ferreira, “Computer modeling for high-RES systems: Exploring the applicability of EnergyPLAN,” in *Proceedings of the 2024 International Conference on Electrical, Computer, Communications and Mechatronics Engineering (ICECCME)*, 11 2024, pp. 1–7.
- [133] K. Feng, K. Hubacek, Y. L. Siu, and X. Li, “The energy and water nexus in Chinese electricity production: A hybrid life cycle analysis,” *Renewable and Sustainable Energy Reviews*, vol. 39, pp. 342–355, 2014. [Online]. Available: <https://www.sciencedirect.com/science/article/pii/S1364032114005322>
- [134] L. Gagnon, C. Bélanger, and Y. Uchiyama, “Life-cycle assessment of electricity generation options: The status of research in year 2001,” *Energy Policy*, vol. 30, no. 14, pp. 1267–1278, 2002, hydropower, Society, and the Environment in the 21st Century. [Online]. Available: <https://www.sciencedirect.com/science/article/pii/S0301421502000885>
- [135] IPCC, “Renewable Energy Sources and Climate Change Mitigation,” <https://www.ipcc.ch/report/renewable-energy-sources-and-climate-change-mitigation/>, 2012, accessed: 2025-04-30.
- [136] L. La Picirelli de Souza, E. Eduardo Silva Lora, S. Rajabi Hamedani, J. C. Escobar Palacio, L. Cioccolanti, M. Villarini, G. Comodi, and A. Colantoni, “Life cycle assessment of prospective scenarios maximizing renewable resources in the Brazilian electricity matrix,” *Renewable Energy Focus*, vol. 44, pp. 1–18, 2023. [Online]. Available: <https://www.sciencedirect.com/science/article/pii/S1755008422000904>
- [137] O. Siddiqui and I. Dincer, “Comparative assessment of the environmental impacts of nuclear, wind and hydro-electric power plants in Ontario: A life cycle assessment,” *Journal of Cleaner Production*, vol. 164, pp. 848–860, 2017. [Online]. Available: <https://www.sciencedirect.com/science/article/pii/S0959652617314063>

- [138] NREL, “Life Cycle Greenhouse Gas Emissions from Electricity Generation,” U.S. Department of Energy Technical Report, NREL, Golden, CO, United States, Tech. Rep., 2013, accessed: 2025-04-30. [Online]. Available: <https://www.osti.gov/servlets/purl/1338444>
- [139] H. Hondo, “Life cycle GHG emission analysis of power generation systems: Japanese case,” *Energy*, vol. 30, no. 11, pp. 2042–2056, 2005, international Symposium on CO₂ Fixation and Efficient Utilization of Energy (CandE 2002) and the International World Energy System Conference (WESC-2002). [Online]. Available: <https://www.sciencedirect.com/science/article/pii/S0360544204003652>
- [140] N. Jungbluth, C. Bauer, R. Dones, and R. Frischknecht, “Life Cycle Assessment for Emerging Technologies: Case Studies for Photovoltaic and Wind Power (11 pp),” *The International Journal of Life Cycle Assessment*, vol. 10, no. 1, p. 24–34, nov 2004. [Online]. Available: <http://dx.doi.org/10.1065/lca2004.11.181.3>
- [141] M. Ozoemena, W. M. Cheung, and R. Hasan, “Comparative LCA of technology improvement opportunities for a 1.5-MW wind turbine in the context of an onshore wind farm,” *Clean Technologies and Environmental Policy*, vol. 20, no. 1, p. 173–190, nov 2017. [Online]. Available: <http://dx.doi.org/10.1007/s10098-017-1466-2>
- [142] L. Wang, Y. Wang, H. Du, J. Zuo, R. Yi Man Li, Z. Zhou, F. Bi, and M. P. Garvlehn, “A comparative life-cycle assessment of hydro-, nuclear and wind power: A China study,” *Applied Energy*, vol. 249, pp. 37–45, 2019. [Online]. Available: <https://www.sciencedirect.com/science/article/pii/S0306261919307664>
- [143] Ecoinvent, “ecoquery,” <https://ecoquery.ecoinvent.org/3.11/cutoff>, 2018, accessed: 2025-04-30.
- [144] J. Chipindula, V. S. V. Botlaguduru, H. Du, R. R. Kommalapati, and Z. Huque, “Life cycle environmental impact of onshore and offshore wind farms in texas,” *Sustainability*, vol. 10, no. 6, 2018. [Online]. Available: <https://www.mdpi.com/2071-1050/10/6/2022>
- [145] V. L. C. Assessments, “Life cycle assessment of electricity production from an onshore V116-2.0 MW wind plant,” <https://www.vestas.com/en/sustainability/environment/lifecycle-assessments>, 2018, accessed: 2025-04-30.

- [146] Vestas, “Life cycle assessment of electricity production from an onshore V110-2.0 MW wind plant (mark 10B),” <https://www.vestas.com/en/sustainability/environment/lifecycle-assessments>, 2015, accessed: 2025-04-30.
- [147] EPD, “Electricity from an Indian onshore wind farm using SG 2.1-122 wind turbines,” <https://www.environdec.com/library>, 2018, accessed: 2025-04-30.
- [148] A. Bonou, A. Laurent, and S. I. Olsen, “Life cycle assessment of onshore and offshore wind energy-from theory to application,” *Applied Energy*, vol. 180, pp. 327–337, 2016. [Online]. Available: <https://www.sciencedirect.com/science/article/pii/S0306261916309990>
- [149] EPD, “Electricity from European G114-2.5 MW On-shore Wind Farm,” <https://www.environdec.com/library>, 2017, accessed: 2025-04-30.
- [150] EPD, “Electricity from a european onshore wind farm using SG 2.6-114 wind turbines,” <https://www.environdec.com/library>, 2020, accessed: 2025-04-30.
- [151] EPD, “Electricity from european G126-2.625 MW on-shore wind farm,” <https://www.environdec.com/library>, 2017, accessed: 2025-04-30.
- [152] J.-A. Vélez-Henao and D. F. Vivanco, “Hybrid life cycle assessment of an onshore wind farm including direct and indirect services: A case study in Guajira, Colombia,” *Journal of Environmental Management*, vol. 284, p. 112058, 2021. [Online]. Available: <https://www.sciencedirect.com/science/article/pii/S0301479721001201>
- [153] EPD, “Electricity from an Indian onshore wind farm using SG 3.4-145 wind turbines,” <https://www.environdec.com/library>, 2021, accessed: 2025-04-30.
- [154] V. L. C. Assessments, “Life cycle assessment of electricity production from an onshore V136-3.45 MW wind plant (Mark 3A),” <https://www.vestas.com/en/sustainability/environment/lifecycle-assessments>, 2017, accessed: 2025-04-30.
- [155] EPD, “Electricity from European SG 3.4-132 On-shore Wind Farm,” <https://www.environdec.com/library>, 2017, accessed: 2025-04-30.
- [156] V. L. C. Assessments, “Life cycle assessment of electricity production from an onshore V126-3.45 MW wind plant (Mark 3A),” <https://www.vestas.com/en/sustainability/environment/lifecycle-assessments>, 2017, accessed: 2025-04-30.

- [157] Vestas, “Life cycle assessment of electricity production from an onshore V117-3.45 MW wind plant (mark 3A),” <https://www.vestas.com/en/sustainability/environment/lifecycle-assessments>, 2017, accessed: 2025-04-30.
- [158] Nordex Report, “EPD of a Nordex wind farm with Delta4000 N149/4.0-4.5 turbines – LCA Report,” <https://www.environdec.com/library>, 2020, accessed: 2025-04-30.
- [159] V. L. C. Assessments, “Life cycle assessment of electricity production from an onshore V150-4.2 MW wind plant,” <https://www.vestas.com/en/sustainability/environment/lifecycle-assessments>, 2022, accessed: 2025-04-30.
- [160] Vestas, “Life cycle assessment of electricity production from an onshore V136-4.2 MW wind plant,” <https://www.vestas.com/en/sustainability/environment/lifecycle-assessments>, 2022, accessed: 2025-04-30.
- [161] V. L. C. Assessments, “Life cycle assessment of electricity production from an onshore V117-4.2 MW wind plant (Mark 3A),” <https://www.vestas.com/en/sustainability/environment/lifecycle-assessments>, 2019, accessed: 2025-04-30.
- [162] EPD, “Goldwind GW136-4.2 wind turbine Life Cycle Assessment,” <https://www.environdec.com/library>, 2020, accessed: 2025-04-30.
- [163] EPD, “Electricity from a European onshore wind farm using SG 4.5-145 wind turbines,” <https://www.environdec.com/library>, 2019, accessed: 2025-04-30.
- [164] V. L. C. Assessments, “LCA of Electricity Production from an onshore EnVentus V162-6.2,” <https://www.vestas.com/en/sustainability/environment/lifecycle-assessments>, 2025, accessed: 2025-04-30.
- [165] EPD Italy, “Goldwind GW136-4.5 wind turbine Life Cycle Assessment,” <https://www.environdec.com/library>, 2020, accessed: 2025-04-30.
- [166] EPD, “Electricity from a European onshore wind farm using SG 5.0-132 wind turbines,” <https://www.environdec.com/library>, 2020, accessed: 2025-04-30.
- [167] EPD, “Electricity from a european onshore wind farm using SG 5.0-145 wind turbines,” <https://www.environdec.com/library>, 2020, accessed: 2025-04-30.
- [168] Nordex Report, “EPD of a Nordex wind farm with Delta4000 N149/5.X turbines – LCA Report,” <https://www.environdec.com/library>, 2024, accessed: 2025-04-30.

- [169] Nordex, “EPD of a Nordex wind farm with Delta4000 N155/5.X turbines – LCA Report,” <https://www.environdec.com/library>, 2023, accessed: 2025-04-30.
- [170] Nordex Report, “EPD of a Nordex wind farm with Delta4000 N163/5.X turbines – LCA Report,” <https://www.environdec.com/library>, 2023, accessed: 2025-04-30.
- [171] EPD Italy, “Goldwind GW165-5.2/5.6/6.0 Wind Turbine Life Cycle Assessment,” <https://www.environdec.com/library>, 2022, accessed: 2025-04-30.
- [172] EPD, “Goldwind GWH182-5.3/6.2/7.2/7.5 wind turbine Wind Turbine Life Cycle Assessment,” <https://www.environdec.com/library>, 2022, accessed: 2025-04-30.
- [173] Nordex, “EPD of a Nordex wind farm with Delta4000 N163/6.X turbines – LCA Report,” <https://www.environdec.com/library>, 2024, accessed: 2025-04-30.
- [174] V. L. C. Assessments, “Life cycle assessment of electricity production from an onshore EnVentus V150-6.0 MW wind plant,” <https://www.vestas.com/en/sustainability/environment/lifecycle-assessments>, 2023, accessed: 2025-04-30.
- [175] EPD, “Electricity from a European onshore wind farm using SG 6.2-170 / 6.6-170 wind turbines,” <https://www.environdec.com/library>, 2022, accessed: 2025-04-30.
- [176] EPD, “Electricity from a european onshore wind farm using SG 6.6-155 wind turbines,” <https://www.environdec.com/library>, 2022, accessed: 2025-04-30.
- [177] EPD, “Electricity from a European offshore wind farm using SG 11-200 wind turbines,” <https://www.environdec.com/library>, 2023, accessed: 2025-04-30.
- [178] EPD, “Electricity from a european offshore wind farm using SG 14-222 wind turbines,” <https://www.environdec.com/library>, 2023, accessed: 2025-04-30.
- [179] EPD, “Electricity from a European offshore wind farm using SG 14-236 wind turbines,” <https://www.environdec.com/library>, 2023, accessed: 2025-04-30.
- [180] V. L. C. Assessments, “Life Cycle Assessment of electricity production from an offshore V236-15 MW wind plant,” <https://www.vestas.com/en/sustainability/environment/lifecycle-assessments>, 2024, accessed: 2025-04-30.
- [181] L. Ferraz de Paula and B. S. Carmo, “Environmental Impact Assessment and Life Cycle Assessment for a Deep Water floating offshore wind turbine on the brazilian

- continental shelf,” *Wind*, vol. 2, no. 3, pp. 495–512, 2022. [Online]. Available: <https://www.mdpi.com/2674-032X/2/3/27>
- [182] J. Yang, Y. Chang, L. Zhang, Y. Hao, Q. Yan, and C. Wang, “The life-cycle energy and environmental emissions of a typical offshore wind farm in China,” *Journal of Cleaner Production*, vol. 180, pp. 316–324, 2018. [Online]. Available: <https://www.sciencedirect.com/science/article/pii/S0959652618300969>
- [183] M. Ito, K. Komoto, and K. Kurokawa, “Life-cycle analyses of very-large scale PV systems using six types of PV modules,” *Current Applied Physics*, vol. 10, no. 2, Supplement, pp. S271–S273, 2010, the Proceeding of the International Renewable Energy Conference and Exhibition 2008 (RE2008). [Online]. Available: <https://www.sciencedirect.com/science/article/pii/S1567173909005240>
- [184] H. C. Kim, V. Fthenakis, J. Choi, and D. E. Turney, “Life Cycle Greenhouse Gas Emissions of Thin-film Photovoltaic Electricity Generation: Systematic Review and Harmonization,” *Journal of Industrial Ecology*, vol. 16, no. s1, mar 2012. [Online]. Available: <http://dx.doi.org/10.1111/j.1530-9290.2011.00423.x>
- [185] A. Louwen, W. van Sark, R. Schropp, W. Turkenburg, and A. Faaij, “Life-cycle greenhouse gas emissions and energy payback time of current and prospective silicon heterojunction solar cell designs,” *Progress in Photovoltaics: Research and Applications*, vol. 23, no. 10, p. 1406–1428, aug 2014. [Online]. Available: <http://dx.doi.org/10.1002/pip.2540>
- [186] F. Querini, S. Dagostino, S. Morel, and P. Rousseaux, “Greenhouse Gas Emissions of Electric Vehicles Associated with Wind and Photovoltaic Electricity,” *Energy Procedia*, vol. 20, pp. 391–401, 2012, technoport 2012 - Sharing Possibilities and 2nd Renewable Energy Research Conference (RERC2012). [Online]. Available: <https://www.sciencedirect.com/science/article/pii/S1876610212007680>
- [187] U. Desideri, F. Zepparelli, V. Morettini, and E. Garroni, “Comparative analysis of concentrating solar power and photovoltaic technologies: Technical and environmental evaluations,” *Applied Energy*, vol. 102, p. 765–784, feb 2013. [Online]. Available: <http://dx.doi.org/10.1016/j.apenergy.2012.08.033>
- [188] B.-j. Kim, J.-y. Lee, K.-h. Kim, and T. Hur, “Evaluation of the environmental performance of sc-Si and mc-Si PV systems in Korea,” *Solar Energy*, vol. 99, p. 100–114, jan 2014. [Online]. Available: <http://dx.doi.org/10.1016/j.solener.2013.10.038>

- [189] D. Nugent and B. K. Sovacool, “Assessing the lifecycle greenhouse gas emissions from solar PV and wind energy: A critical meta-survey,” *Energy Policy*, vol. 65, p. 229–244, feb 2014. [Online]. Available: <http://dx.doi.org/10.1016/j.enpol.2013.10.048>
- [190] Operador Nacional do Sistema (ONS), “Adoption of Photovoltaic Systems Along a Sure Path: A Life-Cycle Assessment (LCA) Study Applied to the Analysis of GHG Emission Impacts,” *Energies*, vol. 11, no. 10, p. 2806, oct 2018. [Online]. Available: <http://dx.doi.org/10.3390/en11102806>
- [191] M. M. Lunardi, J. Alvarez-Gaitan, N. L. Chang, and R. Corkish, “Life cycle assessment on PERC solar modules,” *Solar Energy Materials and Solar Cells*, vol. 187, p. 154–159, dec 2018. [Online]. Available: <http://dx.doi.org/10.1016/j.solmat.2018.08.004>
- [192] M. Salibi, F. Schonberger, Q. Makolli, E. Bousi, S. Almajali, and L. Friedrich, “Energy Payback Time of Photovoltaic Electricity Generated by Passivated Emitter and Rear Cell (PERC) Solar Modules: A Novel Methodology Proposal,” *38th European PV Solar Energy Conference and Exhibition*, pp. 1–6, September 2021, presented at the 38th European PV Solar Energy Conference and Exhibition, 6-10 September 2021. [Online]. Available: <https://www.eupvsec-proceedings.com/proceedings?fulltext=Salibi&paper=45153>
- [193] H. S. Schultz and M. Carvalho, “Design, Greenhouse Emissions, and Environmental Payback of a Photovoltaic Solar Energy System,” *Energies*, vol. 15, no. 16, p. 6098, aug 2022. [Online]. Available: <http://dx.doi.org/10.3390/en15166098>
- [194] P. C. Pupin, M. T. B. Perazzini, M. L. Grillo Renó, H. Perazzini, J. Haddad, and R. A. Yamachita, “Life cycle assessment for producing monocrystalline photovoltaic panels: a case study of Brazil,” *Energy Sources, Part A: Recovery, Utilization, and Environmental Effects*, vol. 45, no. 4, p. 12924–12937, oct 2023. [Online]. Available: <http://dx.doi.org/10.1080/15567036.2023.2278724>
- [195] G. Hou, H. Sun, Z. Jiang, Z. Pan, Y. Wang, X. Zhang, Y. Zhao, and Q. Yao, “Life cycle assessment of grid-connected photovoltaic power generation from crystalline silicon solar modules in China,” *Applied Energy*, vol. 164, p. 882–890, feb 2016. [Online]. Available: <http://dx.doi.org/10.1016/j.apenergy.2015.11.023>
- [196] N. Jungbluth, R. Dones, and R. Frischknecht, “Life Cycle Assessment of Photovoltaics; Update of the ecoinvent Database,” *MRS Proceedings*, vol. 1041, 2007. [Online]. Available: <http://dx.doi.org/10.1557/PROC-1041-R01-03>

- [197] M. (Mariska) de Wild-Scholten, “Energy payback time and carbon footprint of commercial photovoltaic systems,” *Solar Energy Materials and Solar Cells*, vol. 119, p. 296–305, dec 2013. [Online]. Available: <http://dx.doi.org/10.1016/j.solmat.2013.08.037>
- [198] D. Yue, F. You, and S. B. Darling, “Domestic and overseas manufacturing scenarios of silicon-based photovoltaics: Life cycle energy and environmental comparative analysis,” *Solar Energy*, vol. 105, p. 669–678, jul 2014. [Online]. Available: <http://dx.doi.org/10.1016/j.solener.2014.04.008>
- [199] E. Leccisi, M. Raugei, and V. Fthenakis, “The Energy and Environmental Performance of Ground-Mounted Photovoltaic Systems—A Timely Update,” *Energies*, vol. 9, no. 8, p. 622, aug 2016. [Online]. Available: <http://dx.doi.org/10.3390/en9080622>
- [200] Norsus, “Life cycle GHG emissions of renewable and non-renewable electricity generation technologies,” <https://norsus.no/en/publikasjon/life-cycle-ghg-emissions-of-renewable-and-non-renewable-electricity-generation-technologies/>, 2019, accessed: 2025-05-01.
- [201] G. C. d. Lima, A. L. L. Toledo, and L. Bourikas, “The Role of National Energy Policies and Life Cycle Emissions of PV Systems in Reducing Global Net Emissions of Greenhouse Gases,” *Energies*, vol. 14, no. 4, p. 961, feb 2021. [Online]. Available: <http://dx.doi.org/10.3390/en14040961>
- [202] M. C. Pamponet, H. L. Maranduba, J. A. Almeida Neto, and L. B. Rodrigues, “Energy balance and carbon footprint of very<scp>large-scale</scp>photovoltaic power plant,” *International Journal of Energy Research*, vol. 46, no. 5, p. 6901–6918, dec 2021. [Online]. Available: <http://dx.doi.org/10.1002/er.7529>
- [203] P. Olczak, A. Zelazna, K. Stecula, D. Matuszewska, and L. Lelek, “Environmental and economic analyses of different size photovoltaic installation in poland,” *Energy for Sustainable Development*, vol. 70, p. 160–169, oct 2022. [Online]. Available: <http://dx.doi.org/10.1016/j.esd.2022.07.016>
- [204] F. Asdrubali, G. Baldinelli, F. D’Alessandro, and F. Scrucca, “Life cycle assessment of electricity production from renewable energies: Review and results harmonization,” *Renewable and Sustainable Energy Reviews*, vol. 42, p. 1113–1122, feb 2015. [Online]. Available: <http://dx.doi.org/10.1016/j.rser.2014.10.082>

- [205] K. Feng, K. Hubacek, Y. L. Siu, and X. Li, “The energy and water nexus in Chinese electricity production: A hybrid life cycle analysis,” *Renewable and Sustainable Energy Reviews*, vol. 39, p. 342–355, nov 2014. [Online]. Available: <http://dx.doi.org/10.1016/j.rser.2014.07.080>
- [206] L. Gagnon, C. Bélanger, and Y. Uchiyama, “Life-cycle assessment of electricity generation options: The status of research in year 2001,” *Energy Policy*, vol. 30, no. 14, p. 1267–1278, nov 2002. [Online]. Available: [http://dx.doi.org/10.1016/S0301-4215\(02\)00088-5](http://dx.doi.org/10.1016/S0301-4215(02)00088-5)
- [207] T. H. Mehedi, E. Gemechu, and A. Kumar, “Life cycle greenhouse gas emissions and energy footprints of utility-scale solar energy systems,” *Applied Energy*, vol. 314, p. 118918, may 2022. [Online]. Available: <http://dx.doi.org/10.1016/j.apenergy.2022.118918>
- [208] A. H. Mohd Nordin, S. I. Sulaiman, S. Shaari, and R. F. Mustapa, “Energy and environmental impacts of a 37.57 MW dc ground-mounted large-scale photovoltaic system in Malaysia: A life-cycle approach,” *Journal of Cleaner Production*, vol. 335, p. 130326, feb 2022. [Online]. Available: <http://dx.doi.org/10.1016/j.jclepro.2021.130326>
- [209] M. Ito, K. Komoto, and K. Kurokawa, “Life-cycle analyses of very-large scale PV systems using six types of PV modules,” *Current Applied Physics*, vol. 10, no. 2, p. S271–S273, mar 2010. [Online]. Available: <http://dx.doi.org/10.1016/j.cap.2009.11.028>
- [210] A. Beylot, J. Payet, C. Puech, N. Adra, P. Jacquin, I. Blanc, and D. Beloin-Saint-Pierre, “Environmental impacts of large-scale grid-connected ground-mounted PV installations,” *Renewable Energy*, vol. 61, p. 2–6, jan 2014. [Online]. Available: <http://dx.doi.org/10.1016/j.renene.2012.04.051>
- [211] P. Wu, X. Ma, J. Ji, and Y. Ma, “Review on Life Cycle Assessment of Energy Payback of Solar Photovoltaic Systems and a Case Study,” *Energy Procedia*, vol. 105, p. 68–74, may 2017. [Online]. Available: <http://dx.doi.org/10.1016/j.egypro.2017.03.281>
- [212] W. Luo, Y. S. Khoo, A. Kumar, J. S. C. Low, Y. Li, Y. S. Tan, Y. Wang, A. G. Aberle, and S. Ramakrishna, “A comparative life-cycle assessment of photovoltaic electricity generation in Singapore by multicrystalline silicon technologies,” *Solar Energy Materials and Solar Cells*, vol. 174, p. 157–162, jan 2018. [Online]. Available: <http://dx.doi.org/10.1016/j.solmat.2017.08.040>

- [213] J. G. Lasso, D. Castelo Branco, A. Magrini, and D. Matos, “Environmental life cycle-based analysis of fixed and single-axis tracking systems for photovoltaic power plants: A case study in Brazil,” *Cleaner Engineering and Technology*, vol. 11, p. 100586, dec 2022. [Online]. Available: <http://dx.doi.org/10.1016/j.clet.2022.100586>
- [214] H. Hondo, “Life cycle GHG emission analysis of power generation systems: Japanese case,” *Energy*, vol. 30, no. 11–12, p. 2042–2056, aug 2005. [Online]. Available: <http://dx.doi.org/10.1016/j.energy.2004.07.020>
- [215] F. d. M. Ribeiro and G. A. da Silva, “Life-cycle inventory for hydroelectric generation: a Brazilian case study,” *Journal of Cleaner Production*, vol. 18, no. 1, p. 44–54, jan 2010. [Online]. Available: <http://dx.doi.org/10.1016/j.jclepro.2009.09.006>
- [216] Norsus, “Life Cycle Data for Hydroelectric Generation at Embretsfoss 4 (E4) Power Station,” <https://norsus.no/en/publikasjon/life-cycle-ghg-emissions-of-renewable-and-non-renewable-electricity-generation-technologies/>, 2013, accessed: 2025-05-01.
- [217] S. Zhang, B. Pang, and Z. Zhang, “Carbon footprint analysis of two different types of hydropower schemes: comparing earth-rockfill dams and concrete gravity dams using hybrid life cycle assessment,” *Journal of Cleaner Production*, vol. 103, p. 854–862, sep 2015. [Online]. Available: <http://dx.doi.org/10.1016/j.jclepro.2014.06.053>
- [218] M. Pang, L. Zhang, C. Wang, and G. Liu, “Environmental life cycle assessment of a small hydropower plant in China,” *The International Journal of Life Cycle Assessment*, vol. 20, no. 6, p. 796–806, may 2015. [Online]. Available: <http://dx.doi.org/10.1007/s11367-015-0878-7>
- [219] L. Oliveira, M. Messagie, J. Mertens, H. Laget, T. Coosemans, and J. Van Mierlo, “Environmental performance of electricity storage systems for grid applications, a life cycle approach,” *Energy Conversion and Management*, vol. 101, p. 326–335, sep 2015. [Online]. Available: <http://dx.doi.org/10.1016/j.enconman.2015.05.063>
- [220] B. Atilgan and A. Azapagic, “Renewable electricity in Turkey: Life cycle environmental impacts,” *Renewable Energy*, vol. 89, p. 649–657, apr 2016. [Online]. Available: <http://dx.doi.org/10.1016/j.renene.2015.11.082>

- [221] M. Geller and A. Meneses, “Life Cycle Assessment of a Small Hydropower Plant in the Brazilian Amazon,” *Journal of Sustainable Development of Energy, Water and Environment Systems*, vol. 4, pp. 379–391, 12 2016.
- [222] Z. Li, H. Du, Y. Xiao, and J. Guo, “Carbon footprints of two large hydro-projects in China: Life-cycle assessment according to ISO/TS 14067,” *Renewable Energy*, vol. 114, p. 534–546, dec 2017. [Online]. Available: <http://dx.doi.org/10.1016/j.renene.2017.07.073>
- [223] O. Siddiqui and I. Dincer, “Comparative assessment of the environmental impacts of nuclear, wind and hydro-electric power plants in Ontario: A life cycle assessment,” *Journal of Cleaner Production*, vol. 164, p. 848–860, oct 2017. [Online]. Available: <http://dx.doi.org/10.1016/j.jclepro.2017.06.237>
- [224] I. H. Association, “2018 Hydropower Status Report,” <https://www.hydropower.org/publications/2018-hydropower-status-report>, 2018, accessed: 2025-05-02.
- [225] S. Arnøy and I. S. Modahl, “Life Cycle Data for Hydroelectric Generation at Trollheim Power Station: Background Data for Updating Environmental Product Declaration (EPD),” 2013, commissioned by Statkraft Energi AS. [Online]. Available: www.{EPD}-norge.no
- [226] L. Wang, Y. Wang, H. Du, J. Zuo, R. Yi Man Li, Z. Zhou, F. Bi, and M. P. Garvlehn, “A comparative life-cycle assessment of hydro-, nuclear and wind power: A China study,” *Applied Energy*, vol. 249, p. 37–45, sep 2019. [Online]. Available: <http://dx.doi.org/10.1016/j.apenergy.2019.04.099>
- [227] M. A. P. Mahmud, N. Huda, S. H. Farjana, and C. Lang, “A strategic impact assessment of hydropower plants in alpine and non-alpine areas of Europe,” *Applied Energy*, vol. 250, p. 198–214, sep 2019. [Online]. Available: <http://dx.doi.org/10.1016/j.apenergy.2019.05.007>
- [228] R. M. Almeida, Q. Shi, J. M. Gomes-Selman *et al.*, “Reducing greenhouse gas emissions of Amazon hydropower with strategic dam planning,” *Nature Communications*, vol. 10, no. 1, sep 2019. [Online]. Available: <http://dx.doi.org/10.1038/s41467-019-12179-5>
- [229] T. K. Yuguda, Y. Li, W. Xiong, and W. Zhang, “Life cycle assessment of options for retrofitting an existing dam to generate hydro-electricity,” *The International Journal of Life Cycle Assessment*, vol. 25, no. 1, p. 57–72, aug 2019. [Online]. Available: <http://dx.doi.org/10.1007/s11367-019-01671-1>

- [230] A. Levasseur, S. Mercier-Blais, Y. Prairie, A. Tremblay, and C. Turpin, “Improving the accuracy of electricity carbon footprint: Estimation of hydroelectric reservoir greenhouse gas emissions,” *Renewable and Sustainable Energy Reviews*, vol. 136, p. 110433, feb 2021. [Online]. Available: <http://dx.doi.org/10.1016/j.rser.2020.110433>
- [231] X. Liu, X. Zheng, L. Wu, S. Deng, H. Pan, J. Zou, X. Zhang, and Y. Luo, “Techno-ecological synergies of hydropower plants: Insights from GHG mitigation,” *Science of The Total Environment*, vol. 853, p. 158602, dec 2022. [Online]. Available: <http://dx.doi.org/10.1016/j.scitotenv.2022.158602>
- [232] Y. Chu, Y. Pan, H. Zhan, W. Cheng, L. Huang, Z. Wu, and L. Shao, “Systems Accounting for Carbon Emissions by Hydropower Plant,” *Sustainability*, vol. 14, no. 11, p. 6939, jun 2022. [Online]. Available: <http://dx.doi.org/10.3390/su14116939>
- [233] D. Goswami, A. Bhattacharjee, P. Basak, U. Das, and C. Nandi, “Life cycle assessment: A perspective of improvement of hydro-plants for intensify “green electricity”,” *Energy Nexus*, vol. 10, p. 100201, jun 2023. [Online]. Available: <http://dx.doi.org/10.1016/j.nexus.2023.100201>
- [234] X. Liu, Y. Jiang, X. Zheng, W. Hou, X. Chen, S. Xiao, X. Zhang, S. Deng, J. Hao, H. Luo, and H. Pan, “Moving towards co-benefits of hydropower: Ecological efficiency evaluation based on LCA and DEA,” *Environmental Impact Assessment Review*, vol. 102, p. 107208, sep 2023. [Online]. Available: <http://dx.doi.org/10.1016/j.eiar.2023.107208>
- [235] H. Chen, H. Pan, S. Xiao, and S. Deng, “Nitrous oxide dominates greenhouse gas emissions from hydropower’s reservoirs in China from 2020 to 2060,” *Water Research*, vol. 279, p. 123420, jul 2025. [Online]. Available: <http://dx.doi.org/10.1016/j.watres.2025.123420>
- [236] C. Chevalier and F. Meunier, “Environmental assessment of biogas co- or tri-generation units by life cycle analysis methodology,” *Applied Thermal Engineering*, vol. 25, no. 17–18, p. 3025–3041, dec 2005. [Online]. Available: <http://dx.doi.org/10.1016/j.applthermaleng.2005.03.011>
- [237] J. Bacenetti, M. Negri, M. Fiala, and S. González-García, “Anaerobic digestion of different feedstocks: Impact on energetic and environmental balances of biogas process,” *Science of The Total Environment*, vol. 463–464, p. 541–551, oct 2013. [Online]. Available: <http://dx.doi.org/10.1016/j.scitotenv.2013.06.058>

- [238] K. Manninen, S. Koskela, A. Nuppenen, J. Sorvari, O. Nevalainen, and S. Siitonen, “The applicability of the renewable energy directive calculation to assess the sustainability of biogas production,” *Energy Policy*, vol. 56, p. 549–557, may 2013. [Online]. Available: <http://dx.doi.org/10.1016/j.enpol.2013.01.040>
- [239] T. L. T. Nguyen, J. E. Hermansen, and L. Mogensen, “Environmental performance of crop residues as an energy source for electricity production: The case of wheat straw in Denmark,” *Applied Energy*, vol. 104, p. 633–641, apr 2013. [Online]. Available: <http://dx.doi.org/10.1016/j.apenergy.2012.11.057>
- [240] A. Whiting and A. Azapagic, “Life cycle environmental impacts of generating electricity and heat from biogas produced by anaerobic digestion,” *Energy*, vol. 70, p. 181–193, jun 2014. [Online]. Available: <http://dx.doi.org/10.1016/j.energy.2014.03.103>
- [241] V. Fantin, A. Giuliano, M. Manfredi, G. Ottaviano, M. Stefanova, and P. Masoni, “Environmental assessment of electricity generation from an Italian anaerobic digestion plant,” *Biomass and Bioenergy*, vol. 83, p. 422–435, dec 2015. [Online]. Available: <http://dx.doi.org/10.1016/j.biombioe.2015.10.015>
- [242] L. E. Arteaga-Pérez, M. Vega, L. C. Rodríguez, M. Flores, C. A. Zaror, and Y. Casas Ledón, “Life-Cycle Assessment of coal–biomass based electricity in Chile: Focus on using raw vs torrefied wood,” *Energy for Sustainable Development*, vol. 29, p. 81–90, dec 2015. [Online]. Available: <http://dx.doi.org/10.1016/j.esd.2015.10.004>
- [243] J. Portugal-Pereira, R. Soria, R. Rathmann, R. Schaeffer, and A. Szklo, “Agricultural and agro-industrial residues-to-energy: Techno-economic and environmental assessment in Brazil,” *Biomass and Bioenergy*, vol. 81, p. 521–533, oct 2015. [Online]. Available: <http://dx.doi.org/10.1016/j.biombioe.2015.08.010>
- [244] F. Van Stappen, M. Mathot, V. Decruyenaere, A. Loriers, A. Delcour, V. Planchon, J.-P. Goffart, and D. Stilmant, “Consequential environmental life cycle assessment of a farm-scale biogas plant,” *Journal of Environmental Management*, vol. 175, p. 20–32, jun 2016. [Online]. Available: <http://dx.doi.org/10.1016/j.jenvman.2016.03.020>
- [245] R. Rana, C. Ingrao, M. Lombardi, and C. Tricase, “Greenhouse gas emissions of an agro-biogas energy system: Estimation under the Renewable Energy Directive,” *Science of The Total Environment*, vol. 550, p. 1182–1195, apr 2016. [Online]. Available: <http://dx.doi.org/10.1016/j.scitotenv.2015.10.164>

- [246] F. C. Ertem, J. Martínez-Blanco, M. Finkbeiner, P. Neubauer, and S. Junne, “Life cycle assessment of flexibly fed biogas processes for an improved demand-oriented biogas supply,” *Bioresource Technology*, vol. 219, p. 536–544, nov 2016. [Online]. Available: <http://dx.doi.org/10.1016/j.biortech.2016.07.123>
- [247] E. Rillo, M. Gandiglio, A. Lanzini, S. Bobba, M. Santarelli, and G. Blengini, “Life Cycle Assessment (LCA) of biogas-fed Solid Oxide Fuel Cell (SOFC) plant,” *Energy*, vol. 126, p. 585–602, may 2017. [Online]. Available: <http://dx.doi.org/10.1016/j.energy.2017.03.041>
- [248] M. V. Barros, C. M. Piekarski, and A. C. De Francisco, “Carbon Footprint of Electricity Generation in Brazil: An Analysis of the 2016–2026 Period,” *Energies*, vol. 11, no. 6, p. 1412, jun 2018. [Online]. Available: <http://dx.doi.org/10.3390/en11061412>
- [249] H. K. Jeswani, A. Whiting, A. Martin, and A. Azapagic, “Environmental and economic sustainability of poultry litter gasification for electricity and heat generation,” *Waste Management*, vol. 95, p. 182–191, jul 2019. [Online]. Available: <http://dx.doi.org/10.1016/j.wasman.2019.05.053>
- [250] M. Carvalho, V. B. D. S. Segundo, M. G. D. Medeiros, N. A. D. Santos, and L. M. C. Junior, “Carbon footprint of the generation of bioelectricity from sugarcane bagasse in a sugar and ethanol industry,” *International Journal of Global Warming*, vol. 17, no. 3, p. 235, 2019. [Online]. Available: <http://dx.doi.org/10.1504/IJGW.2019.098495>
- [251] F. M. de Melo, A. Silvestre, and M. Carvalho, “Carbon Footprints Associated with Electricity Generation from Biomass Syngas and Diesel,” *Environmental Engineering and Management Journal*, vol. 18, no. 7, pp. 1391–1397, 2019. [Online]. Available: <http://www.eemj.eu>
- [252] G. Zang, J. Zhang, J. Jia, E. S. Lora, and A. Ratner, “Life cycle assessment of power-generation systems based on biomass integrated gasification combined cycles,” *Renewable Energy*, vol. 149, p. 336–346, apr 2020. [Online]. Available: <http://dx.doi.org/10.1016/j.renene.2019.12.013>
- [253] H. Lin, A. Borrion, W. A. da Fonseca-Zang, J. W. Zang, W. M. Leandro, and L. C. Campos, “Life cycle assessment of a biogas system for cassava processing in Brazil to close the loop in the water-waste-energy-food nexus,” *Journal of Cleaner Production*, vol. 299, p. 126861, may 2021. [Online]. Available: <http://dx.doi.org/10.1016/j.jclepro.2021.126861>

- [254] E. A. Ocampo Batlle, J. C. Escobar Palacio, E. E. Silva Lora, E. Da Costa Bortoni, L. A. Horta Nogueira, G. E. Carrillo Caballero, A. A. Vitoriano Julio, and Y. C. Escorcía, “Energy, economic, and environmental assessment of the integrated production of palm oil biodiesel and sugarcane ethanol,” *Journal of Cleaner Production*, vol. 311, p. 127638, aug 2021. [Online]. Available: <http://dx.doi.org/10.1016/j.jclepro.2021.127638>
- [255] E. S. Warner and G. A. Heath, “Life Cycle Greenhouse Gas Emissions of Nuclear Electricity Generation: Systematic Review and Harmonization,” *Journal of Industrial Ecology*, vol. 16, no. s1, apr 2012. [Online]. Available: <http://dx.doi.org/10.1111/j.1530-9290.2012.00472.x>
- [256] C. C. Committee, “Current and future lifecycle emissions of key low-carbon technologies and alternatives,” <https://www.theccc.org.uk/publication/current-future-lifecycle-emissions-key-low-carbon-technologies-alternatives/>, 2013, accessed: 2025-05-03.
- [257] M. Seier and T. Zimmermann, “Environmental impacts of decommissioning nuclear power plants: methodical challenges, case study, and implications,” *The International Journal of Life Cycle Assessment*, vol. 19, no. 12, p. 1919–1932, sep 2014. [Online]. Available: <http://dx.doi.org/10.1007/s11367-014-0794-2>
- [258] N. Y. Amponsah, M. Troldborg, B. Kington, I. Aalders, and R. L. Hough, “Greenhouse gas emissions from renewable energy sources: A review of lifecycle considerations,” *Renewable and Sustainable Energy Reviews*, vol. 39, p. 461–475, nov 2014. [Online]. Available: <http://dx.doi.org/10.1016/j.rser.2014.07.087>
- [259] V. Nian, “Change impact analysis on the life cycle carbon emissions of energy systems – The nuclear example,” *Applied Energy*, vol. 143, p. 437–450, apr 2015. [Online]. Available: <http://dx.doi.org/10.1016/j.apenergy.2015.01.003>
- [260] A. Kadiyala, R. Kommalapati, and Z. Huque, “Quantification of the Lifecycle Greenhouse Gas Emissions from Nuclear Power Generation Systems,” *Energies*, vol. 9, no. 11, p. 863, oct 2016. [Online]. Available: <http://dx.doi.org/10.3390/en9110863>
- [261] P. Koltun, A. Tsykalo, and V. Novozhilov, “Life Cycle Assessment of the New Generation GT-MHR Nuclear Power Plant,” *Energies*, vol. 11, no. 12, p. 3452, dec 2018. [Online]. Available: <http://dx.doi.org/10.3390/en11123452>

Appendix A

Table A.1: Life Cycle Assessment Data for Wind Power Technologies

Ref.	Year	Type	Technology	Emissions ¹	Location
[133]	2015	SLA	Multiple	9.40	Global
[134]	2002	SLA	Multiple	9.00	Global
[135]	2012	IOG	Multiple	12.00	Global
[136]	2023	SLA	Multiple	20.26	Brazil
[137]	2017	SLA	Multiple	12.05	Canada
[138]	2013	IOG	Onshore	12.00	USA
[3]	2021	IOG	Offshore	14.20	Europe
[139]	2005	SLA	Onshore 0.3 MW	29.50	Japan
[140]	2005	SLA	Onshore 0.8 MW	11.00	Switzerland
[98]	2013	SLA	Onshore 1.5 MW	7.10	Brazil
[141]	2018	SLA	Onshore 1.5 MW	10.30	UK
[141]	2018	SLA	Onshore 1.5 MW	16.60	UK
[142]	2019	SLA	Onshore 1.5 MW	28.60	China
[143]	2018	EED	Onshore 1-3 MW	15.25	Brazil

Continued on next page

Continued from previous page

Ref.	Year	Type	Technology	Emissions	Location
[144]	2018	SLA	Onshore 1 MW	7.35	USA
[145]	2018	IOG	Onshore 2 MW	5.10	USA
[146]	2015	IOG	Onshore 2 MW	7.20	USA
[147]	2018	IOG	Onshore 2.1 MW	10.61	India
[148]	2016	SLA	Onshore 2.3 MW	6.00	Europe
[144]	2018	SLA	Onshore 2.3 MW	5.84	USA
[149]	2017	IOG	Onshore 2.5 MW	9.24	Europe
[150]	2020	IOG	Onshore 2.6 MW	8.64	Europe
[151]	2017	IOG	Onshore 2.625 MW	9.62	Europe
[144]	2018	SLA	Onshore 2 MW	7.09	USA
[148]	2016	SLA	Onshore 3.2 MW	5.00	Europe
[152]	2021	SLA	Onshore 3.3 MW	12.93	Colombia
[153]	2021	IOG	Onshore 3.4 MW	10.10	India
[154]	2017	IOG	Onshore 3.4 MW	7.60	Europe
[155]	2017	IOG	Onshore 3.4 MW	7.60	Europe

Continued on next page

Continued from previous page

Ref.	Year	Type	Technology	Emissions	Location
[156]	2017	IOG	Onshore 3.45 MW	6.40	Europe
[157]	2017	IOG	Onshore 3.45 MW	5.10	Europe
[158]	2020	IOG	Onshore 4 - 4.5 MW	6.50	Sweden
[159]	2022	IOG	Onshore 4.2 MW	7.30	Germany
[160]	2022	IOG	Onshore 4.2 MW	5.60	Germany
[161]	2019	IOG	Onshore 4.2 MW	4.40	Germany
[162]	2020	IOG	Onshore 4.2 MW	8.04	Canada
[163]	2019	IOG	Onshore 4.5 MW	7.80	Europe
[164]	2025	IOG	Onshore 4.5 MW	5.09	USA
[165]	2020	IOG	Onshore 4.5 MW	7.25	Canada
[166]	2020	IOG	Onshore 5 MW	5.48	Europe
[167]	2020	IOG	Onshore 5 MW	7.03	Europe
[168]	2024	IOG	Onshore 5 MW	9.97	Poland
[169]	2023	IOG	Onshore 5 MW	9.33	Spain
[170]	2023	IOG	Onshore 5 MW	5.66	Brazil

Continued on next page

Continued from previous page

Ref.	Year	Type	Technology	Emissions	Location
[171]	2022	IOG	Onshore 5.2 MW	6.25	Uzbekistan
[172]	2023	IOG	Onshore 5.3 MW	4.41	Egypt
[171]	2022	IOG	Onshore 5.6 MW	5.99	Uzbekistan
[173]	2024	IOG	Onshore 6 MW	9.56	Finland
[171]	2022	IOG	Onshore 6 MW	5.74	Uzbekistan
[174]	2023	IOG	Onshore 6 MW	5.60	Germany
[175]	2022	IOG	Onshore 6.2 MW	8.05	Sweden
[173]	2023	IOG	Onshore 6.2 MW	5.09	Germany
[172]	2023	IOG	Onshore 6.2 MW	4.05	Egypt
[176]	2022	IOG	Onshore 6.6 MW	6.59	Sweden
[172]	2023	IOG	Onshore 7.2 MW	3.82	Egypt
[172]	2023	IOG	Onshore 7.5 MW	3.72	Egypt
[3]	2021	IOG	Offshore	14.20	Europe
[177]	2023	IOG	Offshore 11 MW	9.49	Denmark
[178]	2023	IOG	Offshore 14 MW	9.88	Denmark

Continued on next page

Continued from previous page

Ref.	Year	Type	Technology	Emissions	Location
[179]	2023	IOG	Offshore 14 MW	9.58	Denmark
[180]	2024	IOG	Offshore 15 MW	7.00	Europe
[140]	2005	SLA	Offshore 2 MW	13.00	Switzerland
[148]	2016	SLA	Offshore 4 MW	10.90	Europe
[181]	2022	SLA	Offshore 5 MW	21.61	Brazil
[148]	2016	SLA	Offshore 6 MW	7.80	Europe
[182]	2018	SLA	Offshore 3.6 MW	25.50	China
[144]	2018	SLA	Offshore 5 MW	7.28	USA
[144]	2018	SLA	Offshore 2.3 MW	6.49	USA

Table A.2: Life Cycle Assessment Data for Photovoltaic Technologies

Ref.	Year	Type	Technology	Emissions¹	Location
[183]	2010	SLA	a-Si	45.05	China
[184]	2012	SLA	a-Si	28.24	Global
[103]	2012	SLA	Mono-Si	40.00	Global
[185]	2015	SLA	Mono-Si	38.00	Europe
[185]	2020	SLA	Mono-Si	25.00	Europe
[183]	2010	SLA	Mono-Si	51.06	China

Continued on next page

¹All emission values represented in gCO₂eq/kWh

Continued from previous page

Ref.	Year	Type	Technology	Emissions¹	Location
[186]	2012	SLA	Mono-Si	21.25	Global
[103]	2012	SLA	Mono-Si	66.35	Global
[187]	2013	SLA	Mono-Si	30.00	Italy
[188]	2014	SLA	Mono-Si	32.18	S.Korea
[189]	2018	SLA	Mono-Si	79.50	Global
[190]	2018	SLA	Mono-Si	57.43	Brazil
[191]	2018	SLA	Mono-Si	19.50	China
[102]	2018	SLA	Mono-Si	22.50	Spain
[102]	2018	SLA	Mono-Si	25.16	UK
[192]	2021	SLA	Mono-Si	18.16	Europe
[192]	2021	SLA	Mono-Si	35.47	Europe
[105]	2021	SLA	Mono-Si	17.51	Germany
[192]	2021	SLA	Mono-Si	12.92	Norway
[193]	2022	SLA	Mono-Si	48.84	Brazil
[194]	2023	SLA	Mono-Si	32.30	Brazil
[195]	2016	SLA	Mono-Si	61.36	China
[195]	2016	SLA	Mono-Si	61.60	China
[196]	2008	EED	Multiple	47.97	China
[196]	2008	EED	Multiple	49.36	Germany
[196]	2008	EED	Multiple	61.17	Italy
[196]	2008	EED	Multiple	51.88	Japan
[196]	2008	EED	Multiple	48.82	Spain
[196]	2008	EED	Multiple	43.70	US
[197]	2013	SLA	Multiple	38.10	Europe
[197]	2013	SLA	Multiple	81.20	China
[198]	2014	SLA	Multiple	37.30	Europe
[198]	2014	SLA	Multiple	72.20	China
[199]	2016	SLA	Multiple	37.88	Europe
[199]	2016	SLA	Multiple	48.82	China
[200]	2019	IOG	Multiple	50.90	Global

Continued on next page

Continued from previous page

Ref.	Year	Type	Technology	Emissions¹	Location
[201]	2021	SLA	Multiple	61.92	Brazil
[52]	2021	IOG	Multiple	46.00	US
[202]	2022	SLA	Multiple	43.99	Brazil
[203]	2022	SLA	Multiple	62.00	Poland
[204]	2015	SLA	Multiple	29.20	Global
[205]	2014	SLA	Multiple	76.30	Global
[206]	2002	SLA	Multiple	15.00	Global
[138]	2013	IOG	Multiple	43.00	USA
[3]	2021	IOG	Multiple	36.70	Europe
[135]	2012	IOG	Multiple	46.00	Global
[106]	2023	SLA	Multiple	92.79	Brazil
[207]	2022	SLA	Multi-Si	42.09	Global
[208]	2022	SLA	Multi-Si	35.65	Malaysia
[70]	2018	EED	Multi-Si	15.25	Brazil
[209]	2010	SLA	Multi-Si	43.05	China
[103]	2012	SLA	Multi-Si	47.00	Global
[210]	2014	SLA	Multi-Si	53.50	Global
[188]	2014	SLA	Multi-Si	24.30	S.Korea
[3]	2021	IOG	Multi-Si	50.08	Europe
[211]	2017	SLA	Multi-Si	43.60	China
[212]	2018	SLA	Multi-Si	27.60	Singapore
[103]	2012	SLA	Mult-Si	56.47	Global
[213]	2022	SLA	Muti-Si	44.64	Brazil

¹All emission values represented in gCO₂eq/kWh

Table A.3: Life Cycle Assessment Data for Hydropower Technologies

Ref.	Year	Type	Technology	Emissions ¹	Location
[214]	2005	SLA	Run-of-river/small reservoir	11.30	Japan
[215]	2010	SLA	Run-of-river/small reservoir	4.33	Brazil
[135]	2012	IOG	Hybrid	4.00	Global
[216]	2013	IOG	Run-of-river	2.19	Norway
[138]	2013	IOG	Hybrid	21.00	USA
[205]	2014	SLA	Hybrid	13.20	Global
[217]	2015	SLA	Reservoir	11.11	China
[218]	2015	SLA	Reservoir	28.4	China
[217]	2015	SLA	Reservoir	8.36	China
[219]	2015	SLA	Reservoir/pumped	5.46	Belgium
[204]	2015	SLA	Hybrid	11.60	Global
[220]	2016	SLA	Run-of-river	4.10	Turkey
[221]	2016	SLA	Run-of-river	5.47	Brazil
[220]	2016	SLA	Reservoir	8.30	Turkey
[222]	2017	SLA	Reservoir	0.434	China
[222]	2017	SLA	Reservoir	7.60	China
[222]	2017	SLA	Reservoir	9.12	China
[223]	2017	SLA	Reservoir	15.20	Canada
[70]	2018	EED	Reservoir	73.78	Brazil
[224]	2018	IOG	Hybrid	18.50	Global
[225]	2019	IOG	Reservoir	6.81	Norway
[226]	2019	SLA	Reservoir	3.50	China
[227]	2019	SLA	Reservoir	28.4	Switzerland
[228]	2019	SLA	Reservoir	39.00	Brazil
[229]	2020	SLA	Reservoir	5.51	Nigeria

Continued on next page

Continued from previous page

Ref.	Year	Type	Technology	Emissions¹	Location
[3]	2021	IOG	Hybrid	14.20	Europe
[107]	2021	SLA	Run-of-river	35.00	Brazil
[230]	2021	SLA	Run-of river/ small reservoir	34.50	Canada
[231]	2022	SLA	Hybrid	21.22	China
[232]	2022	SLA	Reservoir/pumped	26.06	China
[233]	2023	SLA	Run-of- river/small reservoir	5.01	Brazil
[234]	2023	SLA	Hybrid	14.52	China
[233]	2023	SLA	Hybrid	92.15	Brazil
[235]	2025	SLA	Reservoir	60.19	China

Table A.4: Life Cycle Assessment Data for Wind Power Technologies

Ref.	Year	Type	Technology	Emissions¹	Location
[206]	2002	SLA	Multiple	118.00	Global
[236]	2005	SLA	Biogas	78.00	Europe
[236]	2005	SLA	Biogas	281.00	Germany
[236]	2005	SLA	Biogas	142.00	France
[236]	2005	SLA	Biogas	193.00	Austria
[236]	2005	SLA	Biogas	-112.00	Europe
[135]	2012	IOG	Multiple	18.00	Global
[237]	2013	SLA	Biogas	323.00	Italy
[237]	2013	SLA	Biogas	-386.00	Italy
[238]	2013	SLA	Biogas	116.00	Finland
[239]	2013	SLA	Biomass	83.00	Denmark
[138]	2013	IOG	Multiple	52.00	USA

Continued on next page

¹All emission values represented in gCO₂eq/kWh

Continued from previous page

Ref.	Year	Type	Technology	Emissions	Location
[240]	2014	SLA	Biogas	222.00	UK
[205]	2014	SLA	Multiple	97.30	Global
[241]	2015	SLA	Biogas	290.52	Italy
[242]	2015	SLA	Biomass	232.00	Chile
[242]	2015	SLA	Biomass	258.00	Chile
[243]	2015	SLA	Multiple	39.90	Brazil
[108]	2016	SLA	Biogas	408.00	Italy
[108]	2016	SLA	Biogas	-395.00	Italy
[244]	2016	SLA	Biogas	-252.00	Belgium
[244]	2016	SLA	Biogas	-216.00	Belgium
[245]	2016	SLA	Biogas	402.00	Italy
[246]	2016	SLA	Biogas	93.00	Germany
[246]	2016	SLA	Biogas	127.00	Germany
[108]	2016	SLA	Biogas	58.00	Global
[247]	2017	SLA	Biogas	200.00	Italy
[247]	2017	SLA	Biogas	360.00	Italy
[247]	2017	SLA	Biogas	57.40	Norway
[248]	2018	EED	Biomass	417.10	Brazil
[248]	2018	EED	Biomass	59.06	Brazil
[249]	2019	SLA	Biomass	22.50	UK
[109]	2019	SLA	Biomass	250.00	USA/Europe
[109]	2019	SLA	Biomass	510.00	USA/Europe
[250]	2019	SLA	Biomass	227.00	Brazil
[251]	2019	SLA	Biogas	269.00	Brazil
[252]	2020	SLA	Biomass	240.00	Global
[253]	2021	SLA	Biogas	300.00	Brazil
[254]	2021	SLA	Biodiesel	70.29	Brazil
[254]	2021	SLA	Bioethanol	271.23	Brazil
[106]	2023	SLA	Multiple	109.29	Brazil

¹All emission values represented in gCO₂eq/kWh

Table A.5: Life Cycle Assessment Data for Nuclear Power Technologies

Ref.	Year	Type	Technology	Emissions¹	Location
[206]	2002	SLA	Multiple	15.00	Global
[214]	2005	SLA	Uranium	24.20	Japan
[135]	2012	IOG	Multiple	16.00	Global
[255]	2012	SLA	Multiple	11.00	Global
[255]	2012	SLA	Multiple	13.00	Global
[138]	2013	IOG	Multiple	13.00	USA
[256]	2013	IOG	Uranium	5.80	UK
[257]	2014	SLA	Uranium	11.27	Germany
[205]	2014	SLA	Multiple	17.10	China
[258]	2014	SLA	Multiple	24.20	Global
[259]	2015	SLA	Uranium	22.50	China
[260]	2016	SLA	Uranium	14.52	Global
[260]	2016	SLA	Uranium	11.87	Global
[260]	2016	SLA	Uranium	11.87	Global
[260]	2016	SLA	Uranium	20.50	Global
[260]	2016	SLA	Uranium	28.80	Global
[260]	2016	SLA	Uranium	28.80	Global
[260]	2016	SLA	Uranium	8.35	Global
[260]	2016	SLA	Plutonium	6.26	Global
[223]	2017	SLA	Uranium	3.40	Canada
[70]	2018	EED	Uranium	12.09	Brazil
[261]	2018	SLA	Uranium	6.50	Global
[226]	2019	SLA	Uranium	12.40	China
[3]	2021	IOG	Multiple	5.13	Europe
[116]	2021	SLA	Uranium	17.00	Europe
[106]	2023	SLA	Multiple	10.50	Brazil

¹All emission values represented in gCO₂eq/kWh

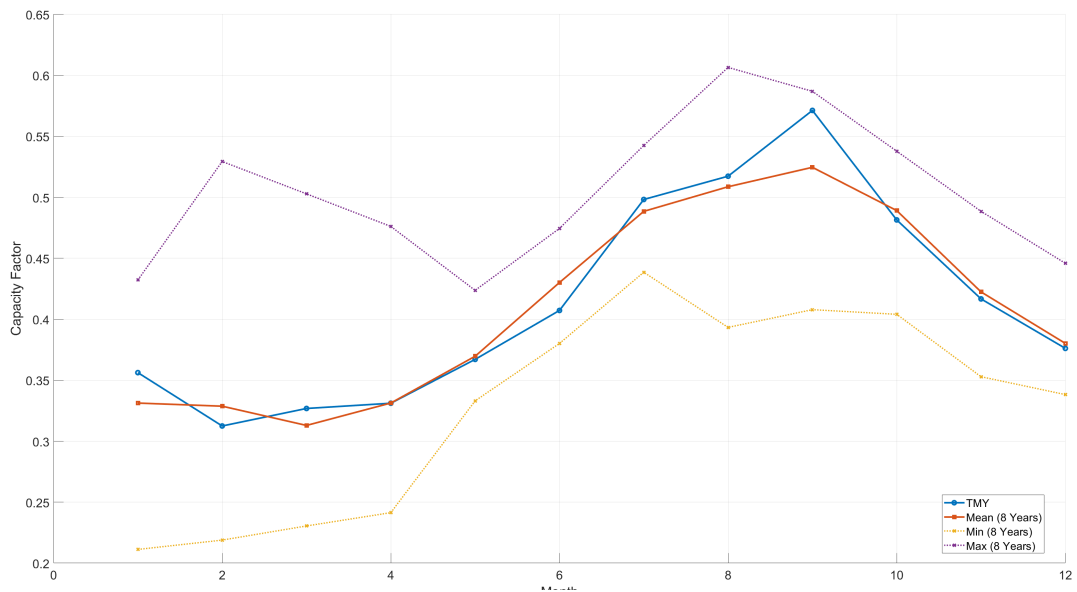


Figure A.1: Monthly capacity factor comparison for Wind Power: TMY vs. Historical min, max, and average

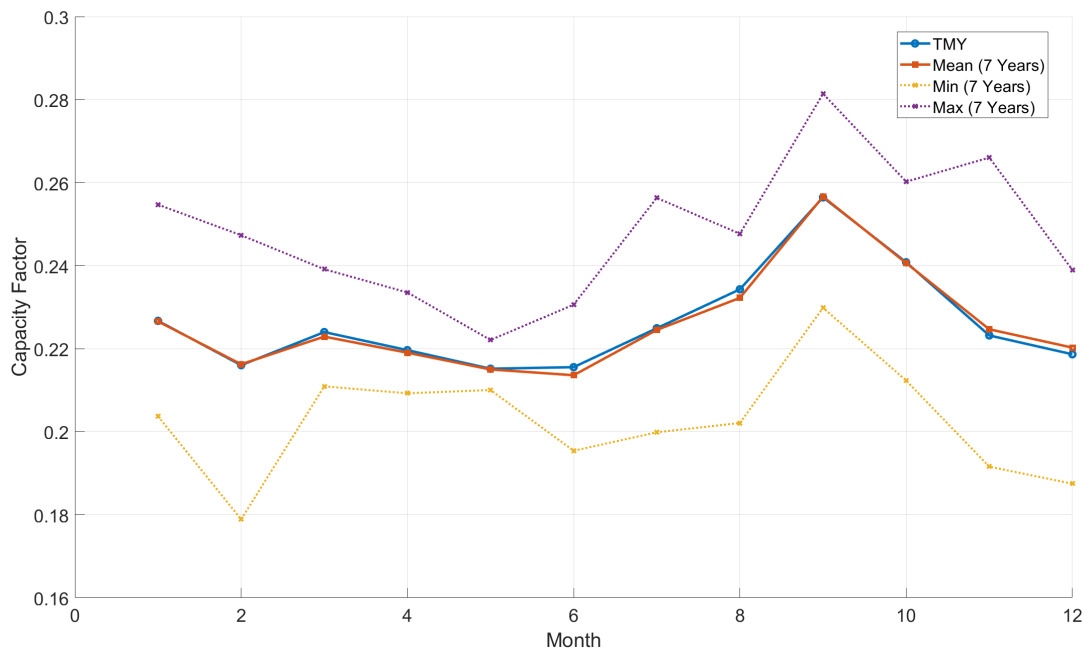


Figure A.2: Monthly capacity factor comparison for Solar PV: TMY vs. Historical min, max, and average.

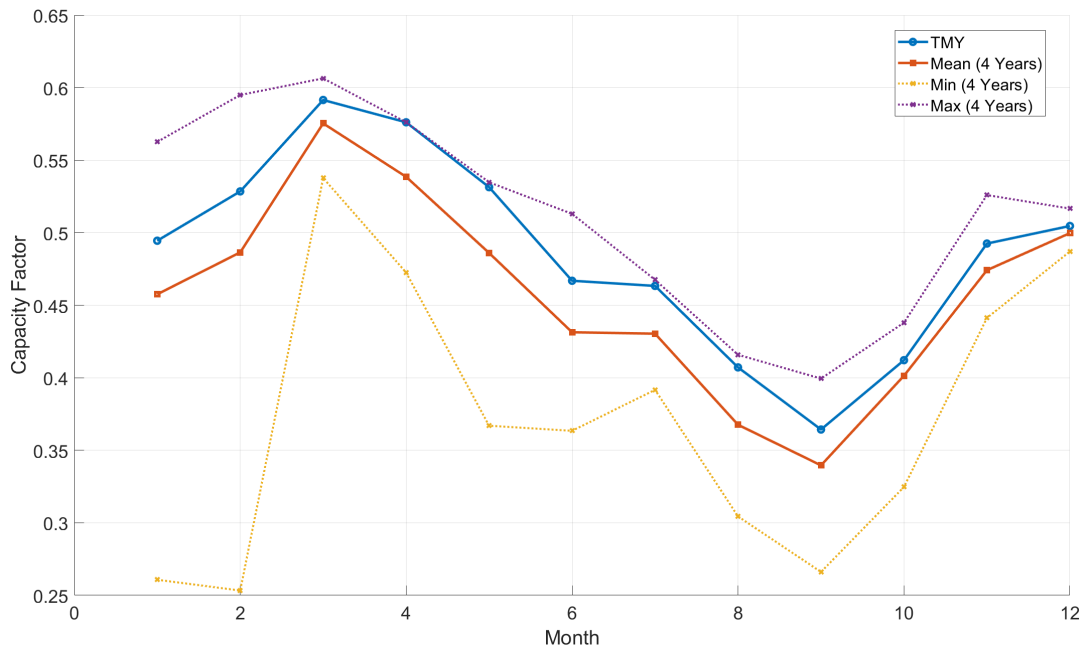


Figure A.3: Monthly capacity factor comparison for PCH Hydro: TMY vs. Historical min, max, and average.

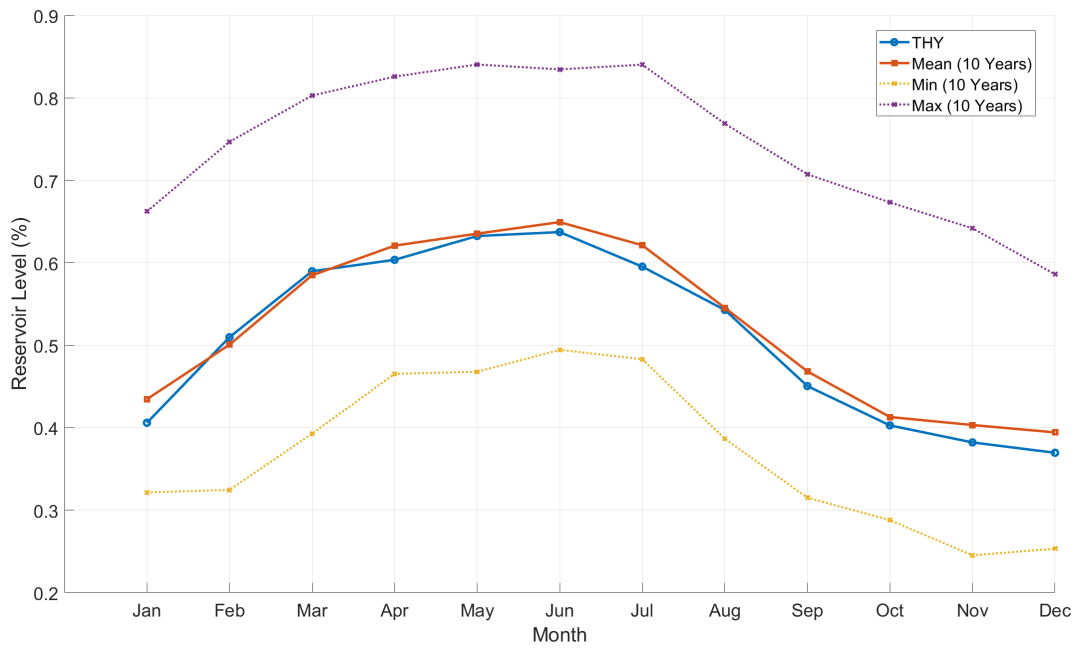


Figure A.4: Monthly reservoir level comparison: TMY vs. Historical min, max, and average.

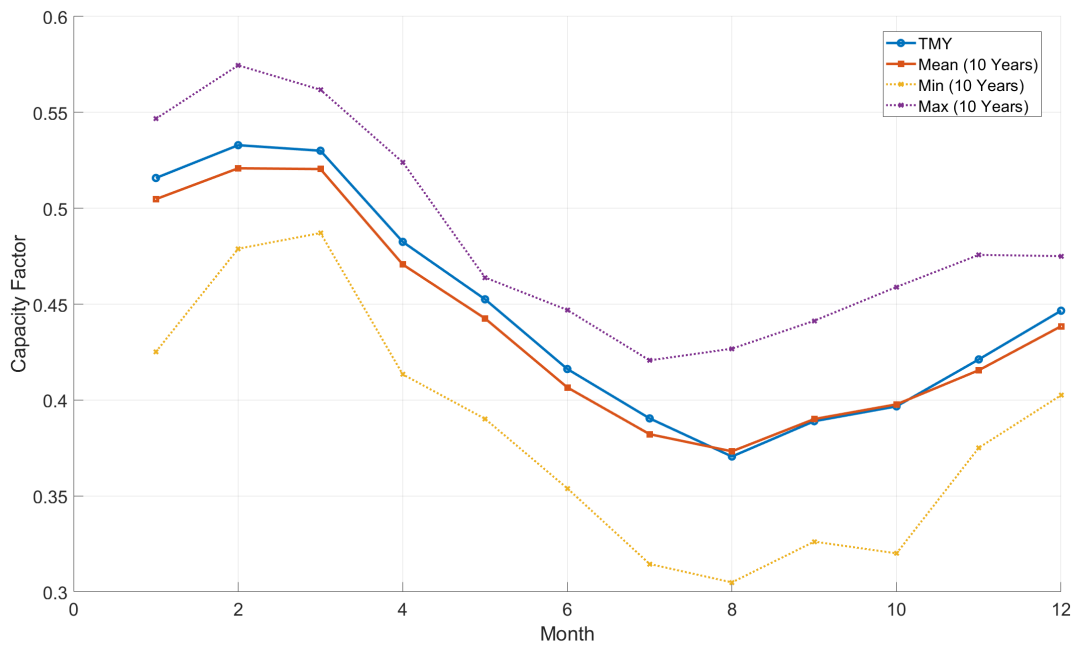


Figure A.5: Monthly capacity factor comparison for ROR Hydro: TMY vs. Historical min, max, and average.

Table A.6: EnergyPLAN simulation input data

Parameter	Value	Curve / Notes
Electricity Demand	1,510.85 TWh/year	Hourly demand profile (2024)
Central Power Plants		
Nuclear Power	3,395 MW	Constant (Correction factor: 0.85)
Reservoir Hydro Capacity	42,450 MW	TMY reservoir inflow
Reservoir Inflow	181 TWh/year	Annual average inflow
Reservoir Storage Capacity	210 GWh	Initial: 37.19%, Final: 36.27%
Pumped Hydro Storage	11,000 MW	Efficiency: 78%
VRES		
Onshore Wind (Centralized)	209,431 MW	TMY wind
Solar PV (Centralized)	80,831 MW	TMY solar
Run-of-River Hydropower	69,265 MW	TMY inflow
Distributed Wind (DG)	998 MW	TMY wind (DG)
Small Hydro (PCH)	16,182 MW	TMY PCH
Distributed Solar PV (DG)	42,904 MW	2024 DG PV profile
Very Small Hydro	1,996 MW	TMY PCH

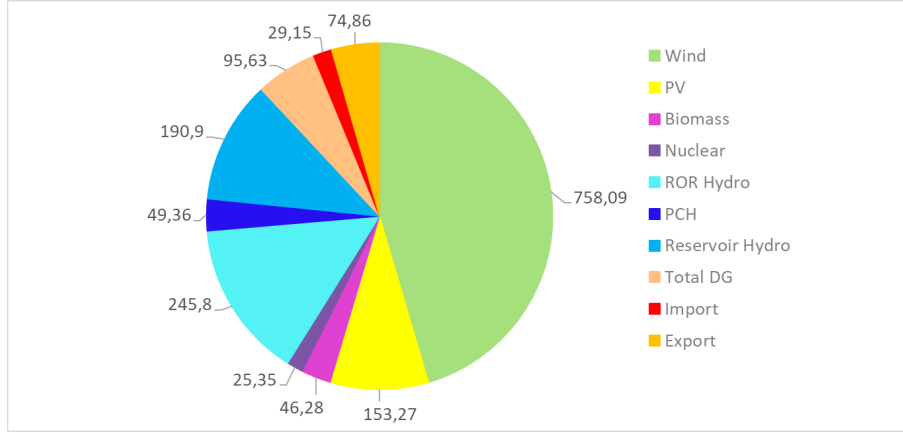


Figure A.6: Share of annual electricity generation by source in the simulation with TMY-Based Capacity Factors and without ESS. All values are expressed in TWh/year.

Table A.7: Gaussian curvature (K) values computed from the avoided electricity import surface $Z(x, y)$. This curvature indicates the inflection region where diminishing returns begin with increasing storage capacity.

Installed capacity (GW)	Energy Storage Capacity (GWh)									
	20	40	60	80	100	125	150	175	200	250
5	-0.594	-0.326	-0.081	-0.038	-0.031	-0.026	-0.008	-0.004	-0.015	-0.020
10	-0.219	0.001	0.144	0.070	0.005	0.016	0.033	-0.006	-0.039	-0.022
15	0.006	0.127	0.187	0.090	0.043	0.062	0.040	-0.012	-0.029	0.005
20	-0.000	0.035	0.074	0.044	0.012	0.025	0.048	0.003	-0.041	-0.010
25	0.000	0.006	0.020	0.018	0.006	0.010	0.028	0.004	-0.027	-0.002
30	0.000	-0.000	0.001	0.005	0.003	0.005	0.012	-0.001	-0.019	-0.007
35	0.000	0.000	0.001	0.001	0.001	0.002	0.005	-0.000	-0.009	0.001
40	0.000	0.000	0.000	0.000	0.000	0.000	0.001	-0.000	-0.004	-0.000
50	0.000	0.000	0.000	0.000	0.000	0.000	0.001	-0.001	-0.001	0.000
75	0.000	0.000	0.000	0.000	0.000	0.000	0.000	0.000	0.000	0.000

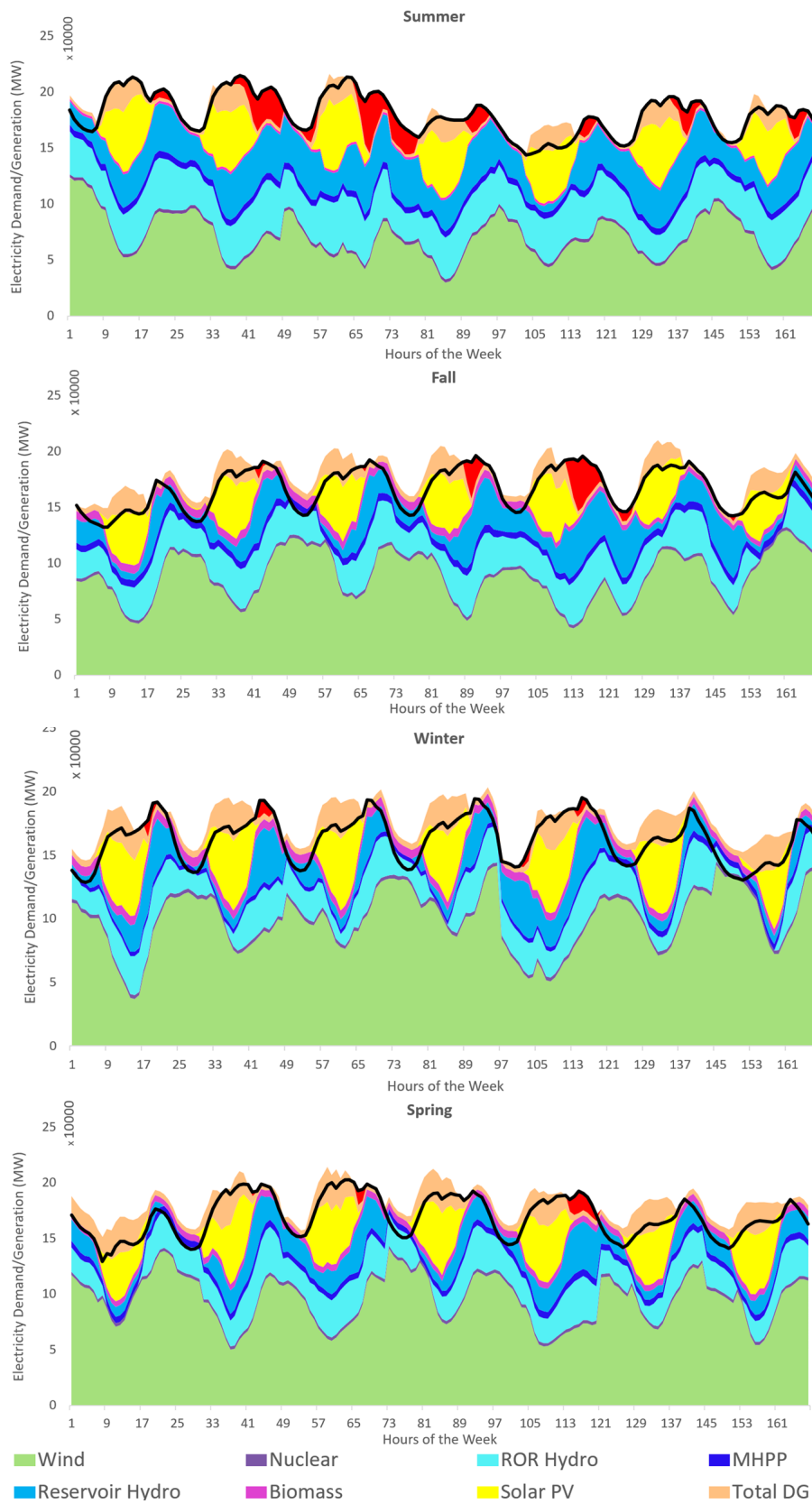


Figure A.7: Hourly electricity generation and demand during a typical operational week for each season in the simulation with TMY-Based Capacity Factors and without ESS.

Table A.8: Hessian determinant (H) values computed from the avoided electricity import surface $Z(x, y)$ for the hydrogen storage system. These values approximate the local curvature and guide the identification of the True Knee Point. Included in Appendix A.8.

E/C Con- figuration (GW/GW)	Energy Storage Capacity (GWh)								
	100	200	300	500	700	900	1200	1500	2000
5/5	-0.001	-0.001	-0.007	-0.006	-0.002	-0.005	-0.007	-0.009	-0.009
5/10	-0.012	-0.006	-0.002	-0.001	-0.000	-0.002	-0.003	-0.004	-0.004
5/15	-0.046	-0.030	-0.008	-0.002	-0.006	0.000	0.007	0.009	0.009
10/10	0.014	0.016	0.012	0.003	0.000	-0.001	-0.004	-0.004	-0.004
10/20	0.031	0.008	-0.007	0.001	0.008	0.003	-0.007	-0.017	-0.017
10/30	-0.116	-0.057	-0.013	-0.004	-0.001	-0.000	-0.001	-0.002	-0.002
15/15	-0.090	-0.014	0.003	0.005	-0.003	0.002	0.003	0.004	0.004
15/30	0.011	0.019	0.005	0.014	0.012	-0.000	-0.004	-0.005	-0.005
15/45	-0.023	-0.027	-0.013	-0.006	-0.004	-0.000	0.001	0.001	0.001
20/20	-0.027	0.016	0.021	0.005	0.003	0.000	-0.001	-0.002	-0.002
20/40	0.002	0.036	0.030	0.027	0.029	0.004	-0.007	-0.009	-0.009
20/60	0.000	0.008	0.013	0.027	0.029	0.004	-0.007	-0.009	-0.009